THE UNIVERSITY OF HULL

Development of microfluidic devices to maintain and interrogate tissue biopsies –biomedical applications

being a Thesis submitted for the Degree of Doctor of Philosophy

in the University of Hull

by

Samantha Margaret Hattersley BSc (Hons)

August 2010

Acknowledgements

I would like to thank Professor John Greenman, Professor Stephen Haswell, and Dr. Charlotte Dyer for their steadfast support. Dr. Peter Docker for his sound advice, Dr. Stephen Clark for manufacturing the microfluidic devices and Mark Tarn with his knowledge of microfluidic procedures. Mrs. Anne Lowry and Mrs. Jenny Foster for their help with the tissue and histology, Mrs. Rhonda Green for being my release valve, my fellow serfs in Chemistry Lab 326 and Wolfson Biomedical Lab for helping me laugh through the hard times. Most importantly, I would like to thank my wonderful husband, Steve, and my equally wonderful children Francesca, Eloise, and Nathaniel for remembering me even though I have been a passing ship in the night for the last three years.

Table of Contents

Table of Figures

Abbreviations

5-FU	5-Fluoro-uracil	CE	Capillary electrophoresis
ABTS	2,2'-azino-bis(3-ethylbenzthiazoline-6-sulphonic acid)	cfDNA	cell free DNA
ADH	Alcohol dehydrogenase	CL	Cross-link
ALD	Alcoholic liver disease	CTC	Circulating tumour cells
BCE	Bovine capillary cells	CYP2E1	Cytochrome P450 2E1
BM	Bone marrow	D5LR	Dextrose lactated Ringers solution
BSA	Bovine serum albumin	DEP	Dielectrophoresis
CAD	Computer assisted design	DFS	Disease-free survival
Calcein AM	Calcein-aceyloxylmethyl ester	DIC	Digital Image Correlation
CCRT	Concurrent chemotherapy and radiotherapy	DMEM	Dulbecco's modified Eagle's medium
CDDP	Cisplatin	DMSO	Dimethyl sulfoxide

DO	Dissolved oxygen	ITC	Isolated tumour cells
DSMC	Direct Simulation Monte Carlo	KC	Kupffer cells
dTMP	thymidine 5'monophosphate	LDH	Lactate dehydrogenase
EBSS	Eagle's Balanced Salt Solution	LGL	Large granular lymphocytes
ECM	Extracellular matrix	LSEC	Liver sinusoidal endothelial cells
EDL	Electric double layer	MACS	Magnetic-activated cell sorting
EDTA	Ethylenediaminetetraacetic acid	MEMS	Microelectromechanical systems
EGFR	Epidermal growth factor receptor	MeOH	Methanol
ELISA	Enzyme-linked immunosorbent assay	MSC	Mesenchymal stem cells
FACS	Fluorescence-activated cell sorting	MTT	3-(4,5-Dimethylthiazol-2-yl)-2,5-diphenyltetrazolium bromide,
FdUMP	5-fluoro-2'-deoxyuridine monophosphate	NAD^+	Nicotinamide adenine dinucleotide
FNAC	Fine needle aspiration cytology	NADPH	(Reduced) nicotinamide adenosine dinucleotide phosphate
GSH	Glutathione	NAPQI	N-acetyl-p-benzo-quinone imine
HCG	Human chorionic gonadotrophin	NHS	National Health Service
H&E	Haematoxylin and Eosin	NK	Natural killer cells
HEPES	4-(2-hydroxyethyl)-1-piperazineethanesulfonic acid	NPC	Nasopharyngeal carcinoma
HIF-1	Hypoxia Inducible Factor-1	OS	Overall survival
HNC	Head and neck cancer	PBPK	Pharmacokinetic/ pharmacodynamic
HNSCC	Head and neck squamous cell carcinoma	PBS	Phosphate buffered saline
HPV	Human papillomavirus	PCR	Polymerase chain reaction
HSC	Hepatic stellate cells	PCLS	Precision cut tissue slices
ICAM-1	Inter-cellular adhesion molecule 1	PDMS	Polydimethylsiloxane

PI	Propidium Iodide	SOD	Superoxide dismutase
PLCA	Poly-lactic-co-glycolic acid	TB	Trypan blue
PMA	Phorbol myristate acetate	TMB	Tetramethyl benzidine
PMC	Paramagnetic capture	TNF-α	Tumour necrosis factor-α
PMMA	Poly methyl methacrylate	TXL	Paclitaxel
PSA	Prostate-specific antigen	UCB	Umbilical cord blood
Re	Reynolds numbers	UV	Ultra-violet
RNS	Reactive nitrogen species	WME	Williams Media E
ROS	Reactive oxygen species	WST-1	(4-[3-[4 - Iodophenyl] - 2 - 4 (4-nitrophenyl)- 2H- 5-tetrazolio-1, 3-benzene disulfonate)
RTDP	Ruthenium tris (2,2'-dipyridyl) dichloride hexahydrate	XTT	2,3-bis- (2-methoxy-4-nitro-5-sulfophenyl)-2H-tetrazolium-5- carboxanilide

Abstract

Currently most cell-based methodologies in microfluidic systems utilize homogeneous or heterogeneous cell populations. However, these systems do not present an accurate representation of *in vivo* dynamics. A microfluidic based experimental methodology has been developed that offers a biomimetic microenvironment in which pseudo *in vivo* tissue studies can be carried out under *in vitro* conditions. Using this innovative technique, which utilizes the inherent advantages of microfluidic technology, liver and cancer tissue have been kept in a viable and functional state for over seven days. Biochemical assays, histological examination, confocal imaging, epi-fluorescent microscopy were all performed to assess the viability of the tissue before and after interrogation by several apoptosis inducing and chemotherapeutic agents. Liver tissue samples were also disaggregated *in situ* on-chip into individual primary cells, using a collagenase digestion procedure, enabling further cell analysis to be carried out off-line. Cancer tissue was probed with chemotherapeutic drugs for the analysis of apoptotic biomarkers such as cytochrome *c*, nucleosomes and DNA that were found to be representative of previous published clinical results. It is anticipated that this methodology will have a wide impact on biological and clinical research in fields such as cancer prognosis and treatment, drug development and toxicity, as well as enabling better fundamental research into tissue/cell processes.

I declare that the work I am submitting for assessment for the PhD degree has been produced wholly by me and not copied, and that any quotations given are appropriately identified and referenced.

1. Introduction

'In the field of observation, fortune favours the prepared mind'

Louis Pasteur 1822-1895

The biological applications of microfluidic technology are expanding rapidly, with recent uses including cell culture, DNA sequencing, and cytokine separation and detection.(1) Microfluidics utilises micron-scale geometric shapes and channels for manipulating pico- to nanolitre volumes of fluid with a high degree of spatial and temporal precision and accuracy.(2) The general benefits of microfluidics are portability, disposability, and short analysis times in relation to conventional testing, lower reagent and sample consumption with associated reduction in costs. The biological benefits are the ability to replicate the *in vivo* environment, which are lost when using traditional macroscopic vessels, such as laminar flow; mass transport driven by diffusion rather than turbulence; and constant removal of waste products whilst maintaining cell-to-cell interactions via paracrine and autocrine signalling molecules. The ability to replicate the *in vivo* dynamics of biological tissue is revolutionary and when applied to tumour biology, provides a unique platform to explore the tumour microenvironment. This technology will permit a better understanding of key biological mechanisms operating within pathological and normal tissues as well as providing a gateway to novel point of care devices. Key parameters needed to achieve this will be discussed in later sections, the first of which is the science of microfluidics.

1.1 Microfluidics

Since the first paper was published in 1977 culturing cells within a microchannel,(3) there has been a growing interest to apply such methodology to cell biology in order to address the difficulties of simulating *in vivo* environments *in vitro*. Current avenues of research in cell biology using microfluidics include; cell culture, cell physiology, extracellular signalling, toxicology, cell separation, cell sorting and manipulation and cell patterning.

Microfluidics is the science of manipulating minute volumes of fluid (10^{-9} to 10^{-18} litres) in small channels (10^{-5} to 10^{-4} metres).(4) The sizes of macro compared with micro are shown in Figure 1. The major benefits of microfluidic technology to cell culture are laminar flows and diffusion-based phenomena, both of which will be discussed in later sections.

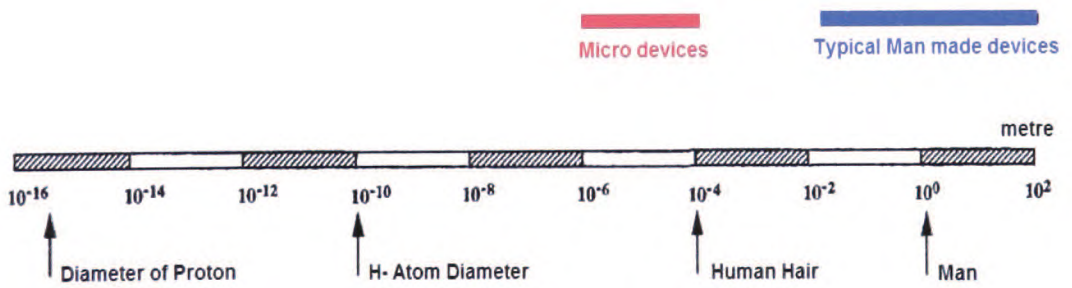

Figure 1. Macroscopic verses microscopic. [Adapted from (5)]

1.1.1 Laminar Flow

Fluid flow characteristics in micro devices differ significantly from macroscopic devices (Figure 2), in that the flow is laminar whereas in macrochannels turbulent flow predominates. Laminar flow occurs when a fluid flows in parallel layers with very little or no disruption between the layers and

mixing is diffusion dependant. It is characterised by low (< 2000) Reynolds numbers (*Re*). Reynolds numbers, named after Osborne Reynolds (1842-1912), are the measure of the ratio of inertial forces ($v_s\rho$) to viscous forces (μ/L) and are dimensionless.(6)

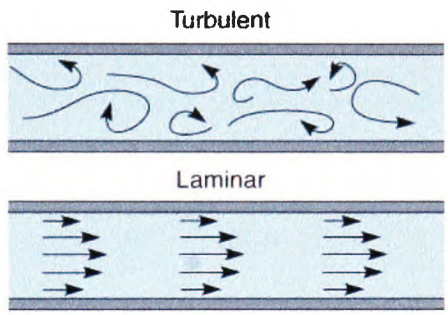

Figure 2. Flow characteristics in channels. Turbulent flow is characterised by Reynolds numbers greater than 4000. Laminar flow is characterised by Reynolds numbers less than 2000 is the principle flow in microfluidic devices.

The Re of a flow can be calculated with the formula:

$$Re = \frac{\rho V D_h}{\mu}$$ Equation 1

where ρ (kg/m^3) is the fluid density, μ is the fluid viscosity, D_h (m) is the hydraulic diameter and V (ms^{-1}) is the characteristic velocity.

Laminar flows are dominated by viscous forces and are characterised by smooth, constant fluid motion. Turbulent flow, which are characterised by high Reynolds numbers (>4000) are dominated by inertial forces, which can produce random eddies, vortices and other flow fluctuations. Transitional flow, which is mixture of laminar and turbulent flow, occurs between 2100-4000 *Re*. Turbulent

flow occurs in the middle of the flow and laminar flow near the channel walls in transitional flow profiles.

Fluid flow within *in vivo* vascular capillaries and tissues is known to have Re <100 and therefore is laminar in nature.(7) Furthermore, gradients in shear stress within blood vessels, caused by turbulent flow, have a strong correlation with the genesis of atherosclerosis with endothelial cells migration and motility increased by twofold when subjected to disturbed flow.(8) This contrasted with a uniform laminar flow field, where the cells showed no migration and continued to rearrange their position within the model of the vessel wall. In addition, cell division increased in the vicinity of turbulent flow whereas cell loss increased both upstream and downstream in regions where the shear stress gradient decreased. Stenotic atherosclerotic plaques are associated with laminar blood flow and high wall shear stress upstream of the stenosis and low shear stress and turbulent flow downstream.(9) It has been shown that plaque growth continues downstream of the plaque and ruptures upstream. Within areas of turbulent flow within blood vessels there has also been shown an upregulation of cell adhesion molecules, which are not present in laminar flow conditions.

The work of Takayama, as shown in Figure 3, has demonstrated the power of multiple laminar flows in which bovine capillary cells (BCE) were adhered in a microfluidic channel. Three laminar flows were then used, one containing Trypsin/tetraacetic acid (EDTA) and the other two had only media. The cells in the Trypsin/EDTA showed removal of cells and disruption of the membrane, while cells in the other two streams were unaffected therefore

demonstrating how two different treatments can occur on one cell sample at the same time.(10)

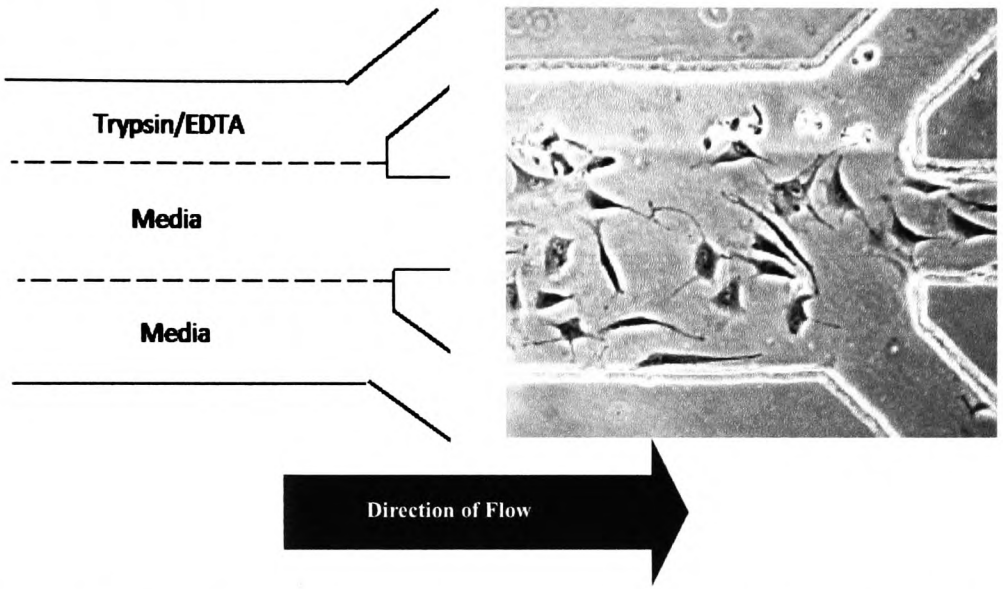

Figure 3. The use of multiple laminar flows to pattern cells. Localised patterned detachment of bovine capillary cells (BCE) by treatment with trypsin/tetraacetic acid (EDTA) with the schematic on the left and the photomicrograph on the right.[11]

Perfusion culture microdevices, in which media flows over adhered cells, have been designed to provide microenvironments suitable for the culture of several mammalian cell types including HepG2/C3A cell lines,(12) oral cancer-2,(13), NIH 3T3 fibroblasts,(14) rat hepatocytes co-cultured with 3T3-J2 fibroblasts,(15) human carcinoma cells (HeLa),(16) and embryonic hepatocytes and kidney cells.(17) Media flow is necessary for cell culture as a means to deliver fresh nutrient and oxygen supplies, to remove waste, and importantly, to deliver material gradients to affect a range of cell responses as shown in Figure 3. Microfluidics replicates *in vivo* laminar flow characteristics, as shown in the previous examples, and allows for greater approximation of the *in vivo* microenvironment for experimentation and analysis.(11)

1.2 Transport Mechanisms

There are two main transport mechanisms in microfluidics, directed transport and statistical transport.(18) Directed transport is controlled by exerted pressure on the fluid and results in bulk flow of the fluid either by mechanical means with pumps called pressure driven flow, or electrically by voltage called electro-osmotic flow (EOF).(19) Statistical transport is an entropy-driven transport and only occurs if, after directed transport, the molecules within the fluid are more disordered than before. (20) An example of statistical transport is diffusion. In microfluidic systems, a combination of the two transport mechanisms can occur. When directed transport meets a gradient, whether it is temperature or concentration, diffusion (statistical transport) occurs.

1.2.1 Pressure Driven Flow

Pressure driven flow has been employed in many microfluidic applications. The reason for this is due to the relative ease and flexibility of operation, insensitivity to surface contamination and no alteration to ionic strength or pH of the fluid. Pumping or drawing of liquids with syringes or peristaltic pumps, achieves hydrodynamic flow in a microfluidic device. The form of the flow is a parabolic shape. This is due to the flow being uniaxial along the principal axis of the channel with the speed of the flow varying over the cross-section of the channel as shown in Figure 4. The rectangular-shaped channel generates additional complexity in the distribution of analytes and indicators because of the parabolic velocity gradient across one or both cross-sectional dimensions.(21)

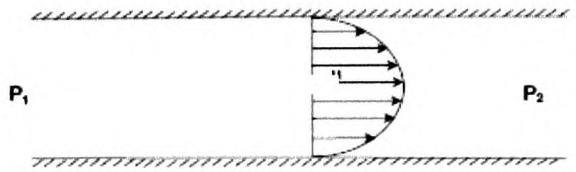

Figure 4. Schematic of pressure driven flow. [From (21)]

Predictions of fluid flow using conventional macroscopic continuum models are embodied in the Navier-Stokes equation

$$\rho \frac{Dv}{Dt} = -\nabla p + \nabla \cdot \mathbf{T} + f$$

Equation 2

Dv is the change in velocity (m/s), Dt is the change in time (s), p is the pressure (Pa), ρ is the fluid density (kg/m^3), f is the body force vector (per unit volume), $\mathbb{T}$ is a tensor that represents the surface forces applied on a fluid particle (Pa) and ∇ is the del operator.

Using these equations, fluid flow in macroscopic channels can accurately be predicted. Within microscopic channels, these equations are not as effective due to the differing conditions found at the channel surface.

Continuum models, such as described above, assume there is zero velocity at the channel walls as shown in Figure 5. The macroscopic model does not take individual particles into account but rather treats them as a

uniform collective, where matter is assumed to be continuous and indefinitely divisible.(22) However, fluid in microchannels can be only a few particles wide, depending on the size of the particle and channel, and interactions between the channel wall and particles distort the flow profile.(23)

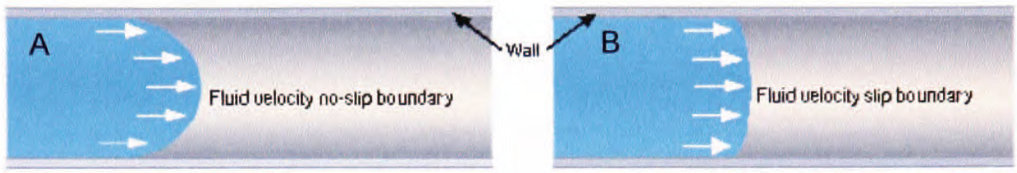

Figure 5. Fluid flow at the microscale (A) A continuum model of fluid velocity treats particles uniformly and assumes that particles travelling near a channel wall have zero velocity, or no slip. (B) A particle-based model can more accurately simulate micrometer-size channels because it allows particles near the wall to exhibit slip and not slow to zero velocity.(24)

This is especially true when the fluid is hydrophilic and the walls hydrophobic and *vice versa*. Therefore, particle-based models based on a class of computational fluid dynamics (CFD) methods for fluid simulation are being investigated. These new models are based on the Lattice Boltzmann Algorithm:

$$\frac{\delta f}{\delta t}+e_i\frac{\delta}{\delta x_i}f=\Omega$$

Equation 3

where f is the particle distribution function, e_i is the discrete set of velocities (m/s) and Ω is the collision operator.

The lattice Boltzmann algorithm(25) is derived from the Boltzmann equation, an equation for the evolution of the particle-velocity distribution, by discretizing the velocity space using a finite set of velocity vectors. New models including the Direct Simulation Monte Carlo (DSMC) method are now being used to simulate the fluid mechanics in microchannels.(5, 26-28) The DSMC

method models fluid flow using simulated molecules that represent a large number of actual molecules in a probable simulations to solve the Boltzmann equation. Molecules are directed through simulated physical space to model flow characteristics. Intermolecular collisions and molecule-surface collisions are determined using probabilistic, phenomenological predictions.(29) This is a new developing model has been used for gas dynamics within microchannels.(30)

1.2.2 Electrokinetic Flow

The current work discussed within this thesis has relied principally on pressure driven flow however, there are now many cell-based microfluidic systems that use electrokinetic flow. Electrokinetics refers to the union between electric currents and fluid flow containing electrolytes as shown in Figure 6. Electrokinetics includes electrophoresis, electrokinesis, dielectrophoresis, electro-osmosis and electroporation.(31) In general terms, electrokinetics describes the conversion of electrical energy into kinetic energy and *vice versa*.

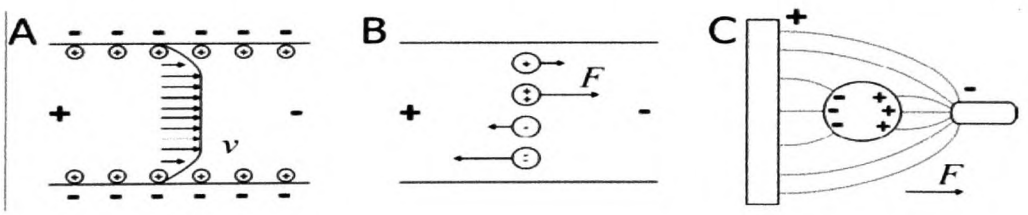

Figure 6. Basic electrokinetic effects. A Electroosmotic flow (EOF) v, planar velocity profile, B Capillary Electrophoresis (CE) *F*, force, C Dielectrophoresis (DEP) [From (32)]

EOF occurs when the solid substrate of the microchannel such as glass, silicon, and polymeric materials acquires a surface charge (zeta potential) when in contact with an electrolyte.(33) The immobile surface charge in turn attracts a

cloud of free ions of the opposite sign creating a thin (1–10 nm under typical conditions) Debye layer of mobile charges next to the surface.

The thickness of this electric double layer (EDL) is determined by a balance between the intensity of thermal (Brownian) fluctuations and the strength of the electrostatic attraction to the substrate. In the presence of an external electric field, which is acting in a tangential (parallel) direction to the double layer (capillary wall), the fluid in this charged Debye layer acquires a momentum, which is then transmitted to adjacent layers of fluid through the effect of viscosity. If the fluid phase is mobile, it causes the fluid to flow (electroosmosis, sometimes also called electroendosmosis).(34)

The electro-migration of a particle under an electrical field is called electrophoresis. A charged particle moves towards the electrode of opposite electrical polarity under the uniform or homogeneous external electric field. This movement is due to Coulombic force, generated by the interaction between the net charge on the particle and the applied electric field.(35) Capillary electrophoresis (CE) is one of the major separation tools used for bio-analysis, based on difference in mobility of analytes in electric field.(36) In such systems a physical matrix or gel (gel capillary electrophoresis) is often used to impair migration of charged species (such as DNA and certain proteins) to enhance the separation process. Dielectrophoresis (DEP) arises from the interaction between a dielectric particle within a medium and a non-uniform electric field.(37) A dielectric particle and the suspending medium become polarized when they are subjected to an electric field. Due to the polarization, electric

charge separation occurs within the dielectric particle as well as in the liquid side of the solid–liquid interface, giving rise to a dipole moment as shown in Figure 6.(38) When a charged dielectric particle moves through a region with non-uniform electric field inside a microchannel, the electrokinetic motion of this particle is the combination effect of EOF, electrophoresis and DEP. (35)

An important advantage of electrokinetic flow over hydrodynamic flow is that it provides a uniform velocity profile, except close to the microchannel wall, when a consistent distribution of charge is applied to walls.(39) In practical terms, microfluidic devices that utilize electrokinetic flow are generally more reliable and less likely to breakdown as the need for moving parts (pumps) is removed.(21)

1.2.3 Diffusion

Diffusion occurs when there is a concentration gradient within a fluid. The control of diffusion-based processes is achieved by utilizing small length scales and/or short distances. Molecules diffuse from areas of higher concentration to areas of lower concentration due to their intrinsic kinetic energy, which can be mathematically modelled using Fick's first law of diffusion:

$$J = -D\frac{dC}{dx} \qquad \text{Equation 4}$$

where J (amount of substance length^{-2} time^{-1}) is the flux of molecule, D is the diffusion coefficient (length^{2} time^{-1}); C (amount of substance length^{-3}) is the concentration, and x (length) is the position.

Transverse diffusion of solutes in pressure-driven flow of two or more miscible or immiscible liquids has been of interest in chemical field. In microfluidic devices, simply T sensors achieve separation of solutes, as shown in Figure 7. T sensors contain two inputs and one output allowing the two flows to come in contact side by side. By adjusting the volumetric flow rates of the two input streams, hydrodynamic spreading and narrowing can be controlled. Typical measurements are achieved by fluorescent detection along the optical axis.

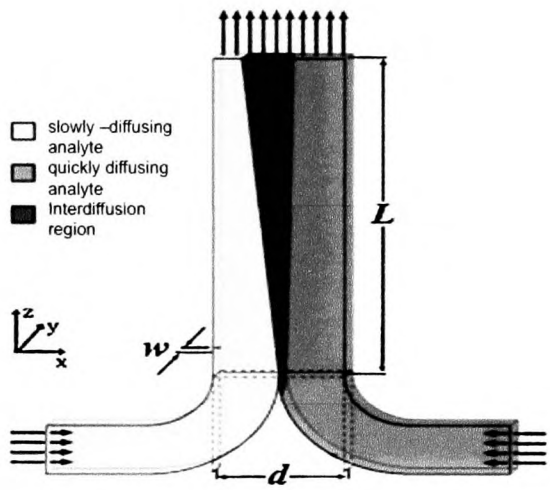

Figure 7. Gradient generation using microfluidics. (A) A schematic representation of a T-sensor with two inputs. Diffusion can be seen between the two laminar flows along the microfluidic channel.(40)

The rate of diffusion between the contacting surfaces at the microscale is very quick (ms^{-1}) depending on the size of the molecule and the distances needed to cross fluid volumes. As the size parameters shrink to microscale, the surface area-to-volume (SAV) ratio also increases. In their review 'Microenvironment design considerations for cellular scale studies' Walker *et al(41)* give the example of a 35 mm tissue dish with 1 ml of medium having a SAV ratio of 11 cm^{-1}. A microchannel with the dimensions of 50 μm x 50 μm x 3 mm (H x W x

L), a volume of 75 nl and a SAV ratio of 800 cm^{-1}. Ratios of this magnitude are advantageous for cell culture due to increased efficiency in mass transport *via* diffusion to and from cells. An increase in SAV ratio limits turbulence and therefore eddies and vortexes, which affects the *in vitro* cell microenvironment. High SAV ratio also limits regional variations in glucose, oxygen and H^+ as large media volumes are decreased, which can affect an individual cell's behaviour such as cell signalling. There is no limitation to diffusion-reaction kinetics such as decreased substrate delivery and metabolite removal from proliferating cells therefore allowing the cells to exhibit more natural behaviour.(42) The driving force of mass transport in microfluidic devices is diffusion the same as *in vivo* microenvironments. The types of diffusion, which occur *in vivo,* are osmosis and facilitated diffusion.

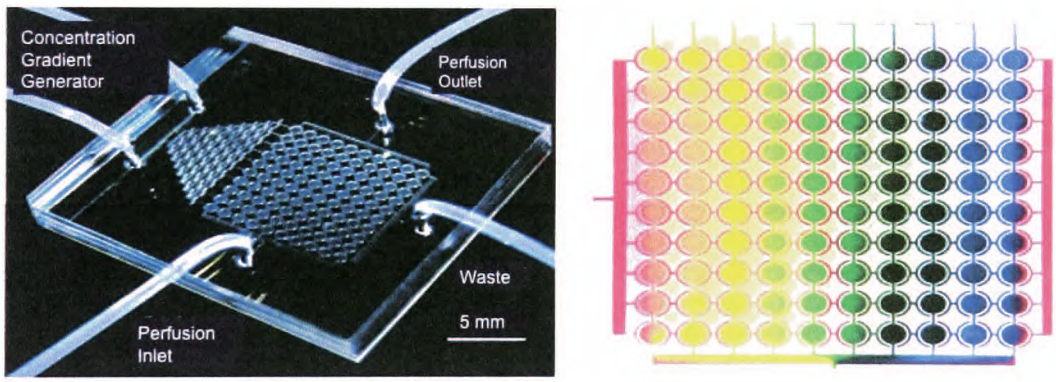

Figure 8. A microfluidic cell culture array containing 100 cell culture chambers and a demonstration of gradient generation using red, yellow and blue dyes.(16)

Microfluidics has become a clearly understood technology by many chemists, engineers and physicists. The new frontier actively researched in the last two decades has been in the field of cell biology. Microfluidic devices with the additional features of miniaturized culturing vessels and highly controllability for operation and on-line monitoring/sensing are becoming increasingly of

interest in cell culturing and cell interrogation techniques. Cell culture has been the cornerstone of many areas of biology in the last and present century. By the application of microfluidics to cell and explant culture models it is hoped that a new methodologies which can create biomimetic microenvironments in which pseudo *in vivo* studies can be carried out under *in vitro* conditions.

1.3 Cell culture

Cells used in *in vitro* models are obtained from either primary tissue samples or from established immortal cell lines. Cells are grown in suspension or in monolayers within flasks of differing sizes. These cells are set in culture flasks from which aliquots are taken and used for analysis. The main advantage to cell culturing is the ability to possess a single well-defined cell type with the ability to work in controlled conditions that allows the manipulation of an individual cell phenotype. Cell culture also provides access to large number of different cells with identical phenotypes in days. Culturing offers an alternative to large-scale animal testing and can be used as initial model systems for the discovery of physiological principles which can later be verified or tested on a relatively smaller number of animals.(43)

The disadvantages of cell culture are biological relevance, the cell will exhibit behaviour that is not representative of the cell dynamics found *in vivo,* and the genotype and phenotype will also alter as an artifact of culturing methodology, as will be discussed.

1.3.1 History of cell culture

The concept of maintaining animal cells *in vitro* was first deliberated in the 19th Century, demonstrated at the turn of the 20th Century and becoming routine from the 1950s as shown in Table 1. Ross Harrison (1870-1959) published the first study on cell culture when he described the *in vitro* growth of frog neurons in 1907.(44)

Table 1. The initial years of cell and tissue culture – an abridged history	
1902	Leo Loeb places embryonic epithelial tissue in agar and coagulated serum and then inserts them in an adult animal. Not strictly cell culture.
1907	Ross Harrison publishes experiments showing frog embryo nerve fibre growth in vitro
1912	Carrel and Burrows cultures connective tissue for extended periods and shows heart muscle tissue contractility over two or three months
1948	Katherine Sanford *et al.* clone L cells for the first time
1952	George Gey *et al.* establishes the first human cell line - HeLa from a cervical carcinoma
1954	Abercrombie and Heaysman begin quantitative cell culture experimentation when they observe contact inhibition between fibroblasts
1955	Harry Eagle and others develop defined media and describe attachment factors and feeder layers
1961	Hayflick and Moorhead describe the finite lifespan of normal human diploid cells
1962	Buonassisi *et al.* publish describe methods for maintaining differentiated tumour cells
1968	David Yaffe studied the differentiation of normal myoblasts in vitro

[Adapted from (45)]

Explants of neural tissue from frog embryos were sealed into a chamber containing coagulable frog lymph that subsequently generated neuron axons. This simple experiment began the technique of cell culture, probably the most important and widely used tool in biological sciences.(46)

The early days of cell culture were dominated by the work of Alexis Carrel (1873-1944) who continued Harrison's work to improve the method of cell cultivation by culturing the tissues of the chick embryos in plasma.(47) The complexity of Carrel's methods coupled with the lack of antibiotics delayed significant progress until the late 1940s.

In 1961, Leonard Hayflick and Paul Moorhead published their seminal work(48) that contradicted Carrel's assertion that diploid cells had infinite potential to replicate and that cells entered a stage of replicative senescence where cells stopped dividing and is discussed in Section 1.3.4. Further major developments in cell culturing methodology were the use of proteolytic enzymes such as trypsin to remove continuously growing cells from culture vessels. By the 1970s, specialized media were being developed for the growth of numerous different cell lines. The defined mixture of supplemental components required for a variety of cell lines come from methods described in this era.(45)

In the 1980s cell culture became an important technology in the establishment of molecular biology.(49-51) Cell culturing remains vitally important when studying pathological states, tissue engineering and manufacturing pharmaceutical products such as monoclonal antibodies, hormones and enzymes.(52-54)

1.3.2 Primary culture

Primary cell culture can be derived from any source of tissue. Tissue can be acquired from normal or tumour, somatic or embryonic tissue and from

virtually any species. Work with animal tissue is governed by the Animals (Scientific Procedures) Act, 1986 and for human tissue; permission must be obtained from the local research ethics committee.(55) Primary cells are grown in culture before subdivision and transfer to a sub culture. The majority of human cell lines are derived from tumour tissue due to the tissue availability and the inherent genetic changes causing unbridled growth, which make culturing relatively simple. Normal somatic cells are superior to tumour cells when studying genetics, molecular biology and cell signalling due to the lack of genetic and phenotypic alterations. However, normal somatic cells will die due to the normal life span of the cell with limited number of cell divisions, (cells from Galapagos tortoise can divide 110 times,(56) murine cells only 15 times(57)) before entering a phase called replicative senescence or Hayflick's limit, making them harder to maintain in culture.(48) In senescent cells growth is arrested in the transition from first growth (G1) phase to synthesis (S) phase of mitosis.(58) Embryonic tissue allows greater potential cell divisions than adult somatic tissue. Nonetheless these tissues, such as the heart, have phenotypic differences between somatic and embryonic material that add inherent difficulties when studying physiological dynamics.(59)(60)

1.3.3 Cell Isolation

Isolating cells from tissue can be achieved by several methods such as enzymatic digestion, perfusion, mechanical disaggregation and explant cultures. All of these have been used successfully and are briefly described:

(i) Enzyme digestion of tissue samples involves enzymes such as trypsin, collagenase, elastase, hyaluronidase, pronase and dispase.(61) Trypsin and pronase were the first enzymes used for this

method however these enzymes can be destructive to cell membranes, giving lower viable cell yields, than later discovered enzymes such as collagenase and dispase.

(ii) Perfusion is an enhancement of enzymatic digestion as proteolytic enzymes are perfused through the tissue and cells collected as they are liberated.(61) This can be used for the disaggregation of tissue and organs where the large blood vessels can be secured at either end with the solution left within the vessels for an extended period of time, for example liver disaggregation.

(iii) Mechanical disaggregation is a method using mechanical measures such as a wire mesh, sieve, or syringe needles to retrieve cells.(62) The advantages for this method are that it is quicker, less expensive than using enzymes and does not suffer from enzyme batch inconsistencies. It can result in more cellular damage and lower viability rates than enzyme digestion.(63)

(iv) Explant uses tissue biopsies and is the slowest method of primary cell recovery. (64) It involves the cutting of tissue into small pieces in a Petri dish and covering with a small amount of medium for several hours to allow attachment of cells to the surface. With the addition of more media, cells can grow out from the tissue pieces and form a monolayer on the surface of the dish. This method is useful if there is a limited amount of tissue available, however this method tends to grow fibroblasts if the media is not supplemented.

1.3.4 Formation and Properties of Immortal Cell Lines

Immortal cell lines have an infinite lifespan. Immortalization occurs when the cell line becomes continuously culturable with limited alteration in the growth phenotype and is the first step to 'transforming' the cells. Transformation occurs when cell lines acquire genotypic and phenotypic changes, which alter growth control such genetic events include point mutations,(65) telomerase reactivation(66) and gene insertions.(67) Cell transformation can be induced chemically; for example with methylcholanthrene and azoxymethane, and virally; for instance by Simian virus 40 and Epstein Barr virus.(68) Spontaneous transformation can also occur after a transient proliferative crisis, such as lack of nutrients, and is usually accompanied by abnormal morphology with a deterioration of cell numbers. This is then followed by the emergence of a fast dividing cell line that overwhelms the culture.(69, 70)

As described by Hayflick and Moorhead cells in culture grow, after an initial lag phase, exponentially in a logarithmic phase until a plateau is reached when cell division and cell death is balanced (stationary phase). This is followed by a death phase when cell death greatly exceeds cell division. Good practice in cell culturing dictates that cells should be kept in the logarithmic phase and therefore subculturing is necessary.

Subculturing or passaging is advantageous when suspension cells reach a density of between 10^6 and 10^7 cells ml^{-1} of culture medium. Tumour cells do not desist from growth in these conditions as they have commonly 'lost' contact inhibition or density-dependent growth inhibition and continue to divide.(71)

Subculturing involves diluting the cells by splitting and aliquoting into several culture flasks or continuing the growth of a proportion of cells in another suitable sized flask. It is standard practice to maintain a continuous supply of cells while experimenting with the remainder. It is vital that the number of subcultures (passages) is chronicled as 'normal' or nontransformed mammalian cells have a limited lifespan in culture, which is approximately 5 cycles.(72)

1.3.5 Explant Culture

Cell and tissue culture has provided invaluable information about cell dynamics. Tissue culture is often used generically or metaphorically to describe all *in vitro* cell techniques. Tissue culture involves a comparatively homogeneous isolation of cells whereas explant/organ culture utilises small samples or tissue slices which contain multiple cell types. Explant/organ culture can be defined as an *in vitro* technique that maintains sections or whole organs in culture using specialized media, vessels and atmosphere.(73) One of the main roles for explant culture is to isolate cells for culture as described in a previous section. However, isolated cells present a limited view of events within *in vivo* microenvironments, due to lack of tissue architecture, cell signalling molecules and cell diversity.(74) A number of lines of evidence indicate that the removal of cells from their usual immediate microenvironment may disturb normal signalling pathways.(75, 76) Removal of thymocytes from interactions with thymic stromal cells, for example, causes spontaneous upregulation of the $\alpha\beta$ T-cell receptor ($\alpha\beta$ TCR) complex occurring simultaneously with the dephosphorylation of the CD3ζ chain.(77) Further studies have shown that activation of protein kinase with phorbol myristate acetate (PMA) induces rapid endocytosis of the CD4 coreceptor on immature thymocytes in suspension

however; this is not evident on those cells within foetal thymus organ cultures.(78) Explant culture enables the normal architecture of the tissues with three-dimensional intercellular relationships to be retained in culture conditions.(73)

Since a review in explant culture in 1991(79) the focus of explant studies have moved from morphology to mainly cell signalling as shown in Table 2 as the value of explant culture has begun to be acknowledged by more and more research groups. In the beginning of research into explant culture, studies limit the culture period to only two hours to avoid the effects of tissue cell death, now studies using explant culture for longer periods, over seven days, have been successfully undertaken.(80, 81)

Human tissue can be acquired for explant studies from diagnostic biopsies obtained from surgery, autopsy or organ donation. When using human material, several factors need to be considered for improving the viability of the tissue. Factors that can affect explant viability include original health status of the patient, temperature and hydration of the material.(82)

Most, if not all, pathological episodes occur in organs that involve more than a single tissue or cell type (e.g. cancer, diabetes, etc.). Pathological and toxicological investigations are particularly appropriate for study within organ culture models. A well-preserved and viable explant with an appropriate dosage of the toxicant or carcinogen placed in culture can be used to characterize the morphological response,(83) cell injury/toxicity(84), metabolism(85) and cellular

or molecular biological alterations. Many types of tissue have been studied, as shown Table 2, these are mainly neuronal tissue,(86) however more diverse tissues are now being studied such as cancer ((81) foetal (87) and cartilage.(88)

Table 2 Different types of explant culture studies

Tissue	Focus/Assay	Reference
Adipose	Immune response, cell signalling, protein synthesis/RNA extraction, cDNA synthesis, rt-PCR, radioimmunoassay	(80, 89)
Neurons	Cell signalling, morphology, homostasis, cell growth/bioluminescence, rt-PCR, immunohistochemistry, biochemical	(86, 90-98)
Hormonal glands	Protein synthesis, cell signalling/bioluminescence, radioimmunoassay, rt-PCR	*(86, 89, 99, 100)*
Lungs	Cell Signalling/bioluminescence	*(86)*
Kidneys	Cell Signalling/bioluminescence	*(86)*
Cancer	Apoptosis, cell signalling, therapy design, protein synthesis/RNA, western blot, immunohistochemistry	(81, 101, 102)
Cartilage	Cell signalling, morphology/ biochemical	(88, 103)
Tendons	Cell growth dynamics, cell signalling/migration, western blot	(104)
Foetal Tissue	Tissue development, regeneration, differentiation/gene expression, histology, immunohistochemistry, western blots, rt-PCR	(85, 87, 105, 106)

Traditional assays of cell viability are often not directly applicable to organ culture models and require careful consideration and sometimes modification. The most common viability tests include Trypan Blue (TB) and lactate dehydrogenase (LDH) release. The former utilizes attached cells or single cells in suspension and determines viability by the percentage of nonviable cells on the basis of diffusion of the dye into cells with non-viable membrane pumps.(107) TB viability measurements are dependant on physical factors such as dye concentration, media osmolality and incubation temperature. LDH is a cytosolic enzyme that is released from the cytoplasm of injured or dead cells

and the media concentrations can be used to assess the percentage of cell death. Explant cultures by definition are not single cell suspensions and therefore are difficult to evaluate by TB alone. LDH is more applicable but consideration must be given to the total of potential LDH release since absolute values are not necessarily predictive of injury. As an example, a quickly growing culture will have a significant number of cells; a certain percentage of cells will terminally differentiate and die. Although the LDH value in the media from these cultures could be high, the relative value may be low. Ordinarily, morphology is the technique of choice to evaluate viability of explant cultures(108, 109) yet, once the explants are prepared for histological analysis, they are fixed and no longer viable and available for further study.

Traditionally explants are set in culture vessels submersed with media with a rocking chambers, platforms or roller bottle equipment to improve diffusion of nutrients into the tissue.(79) Plastic Petri dishes are the most widely used labware for explant culture; some with spacers for mesh supports. The supports facilitate the attachment of explants to the culture vessel as well as promoting the maintenance of tissue differentiation through the continuance of cell junction and signalling cohesion with the surrounding cells and the extracellular matrix (ECM) which is secreted by the cells themselves.(79) Mesh substrates like collagen, fibronectin and laminin have positive effects on cell growth and differentiation as they mimic the ECM found *in vivo*.(110, 111) The typical explant response to organ culture is comparable to the wound response found *in vivo* such as increased DNA synthesis and mitosis after 7-20 hours after culture, and cell migration.(112-114) Studies have shown perfusions and washes of cultures with media have improved viability of cultures as compared

with static culture, for example cartilage explant culture remains viable for up to 14 days in static culture this increases to 56 days with perfusion conditions.(115, 116) The function of the explant is also modified depending upon the flow conditions of the culture. Placental explants exposed to various embryonic tissues modified human chorionic gonadotrophin (HCG) secretion in static cultures however, co-perfusion with embryonic tissue increased HCG secretion to levels comparable to those obtained from patients.(117)

The number of studies using explant tissue is increasing year upon year however; the numbers are still dwarfed by the number of cell-based studies as shown in Figure 9.

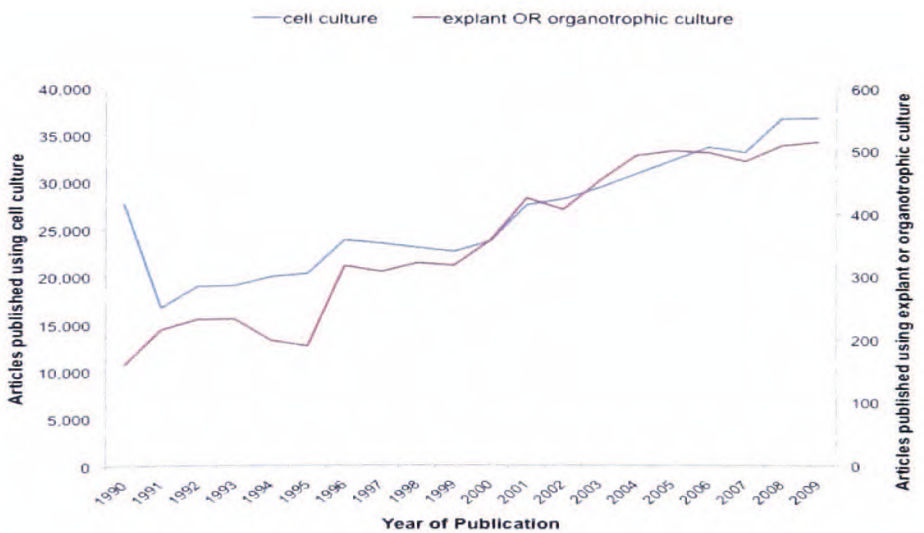

Figure 9. Scientific articles published utilizing cell culture* or explant/organotrophic culture* in title, abstract or keywords from Scopus search engine.

1.4 Current microfluidic applications within cell biology

The responses of defined cell types to specific physiological stimuli can be manipulated within the microfluidic cell culture environment to provide greater knowledge of key cellular responses. The high degree of fluidic control within a microsystem can make it possible to pinpoint different environmental conditions to a particular cell or groups of cells.(11) Conventional cell analysis is usually based on bulk averages of multiple cellular responses where it is impossible to isolate a single cell and analyse its output.(118) This is due to the fact that vessels used to culture, store, interrogate and analyse cell responses are considerably larger than the individual cell. The microfluidic environment can facilitate the continuous perfusion of fresh media at a scale that enables the contents of the microchannels to be continually replaced and analysed without disturbing individual cell dynamics.(119, 120) With these advantages, microfluidic devices have the potential to revolutionize the field of cell biology and open new avenues of research which were inaccessible such as for example; pinpointing individual signalling pathways in response to a single stimulus or the response of different cells to extracellular matrices.(11, 121) Growth in the use of microscale systems in the field of cell biology has been rapid over the past few years, as shown in Figure 7, largely due to the many practical advantages offered by such methodology.

In addition to the fundamental fluidic properties further advantages such as; portability, reusability or disposability of equipment, reduced costs and low cell number requirement make microfluidic devices superior to conventional cell culture in many assays. Whilst the main thrust of this study has not focussed on

cell-based techniques, it is appropriate to review briefly the recent advances in cell-based methodology, as these are highly relevant to the effective development of tissue-based applications in the future.

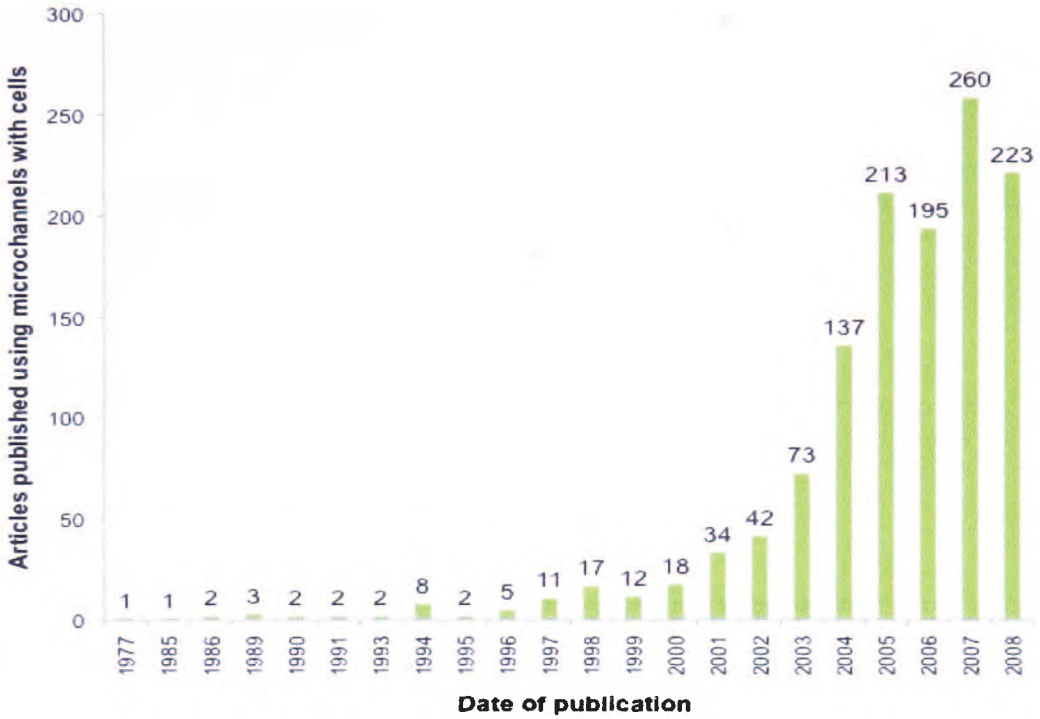

Figure 10. Scientific articles published using keywords microchannel* AND cell biology in the title, abstract or keywords from Scopus search engine.

1.4.1 Cell culture and viability using microfluidics

It is vital that any proposed methodology based on microfluidics will need to maintain the viability, and possibly growth, of cells or tissue in an environment as close to *in vivo* conditions as possible. After this has been established, then manipulation of their phenotypic and functional responses can be reliably evaluated. Traditional cell culture models use cells grown in batches within large culture vessels with the volume of 12.5 ml to 370 ml. Some of these vessels are coated to initiate cell adhesion that increases viability and

proliferation.(122, 123) Perfusion culture microdevices, in which media flows over adhered cells in microchannels, have been designed to provide microenvironments suitable for the culture of several mammalian cell lines as described earlier.

In the past few years there has been a move to perfusion of cells in traditional cell cultures, which is also present in microfluidic systems. However, the problems still remain in traditional cell culture with fluid stress, irregular temperature distribution, solute and dissolved gas concentrations together with less than one cell volume/medium volume ratios which can all contribute to undesirable artefacts to current cell culture methodology.(41) After understanding the need to perfuse cells to improve viability within microenvironments was achieved, the next progression in microfluidic research was to understand how cells react physiologically.

1.4.2 Microfluidic approaches to cell physiology research

Understanding the physiological norms of morphology and phenotypic cell behaviour *in vitro* is critical before endeavouring to understand *in vivo* physiological conditions. The functional characterization and evaluation of cellular responses to chemicals in microdevices has been demonstrated using a variety of cell types, including the application of glutamate to rat cortical neurons(124) and embryonic hippocampal neurons,(125) nerve growth factor (NGF) to adrenal pheochromocytoma (PC12 cells),(126) and caffeine to cardiomyocytes(127). While the cellular response shown in these studies has been demonstrated previously using traditional methodologies,(128-130) the

use of microfluidic technology could be employed in the future to evaluate the effect of newly manufactured drugs on cells in culture.

Micro-scale models of vascular systems are required because vascular diseases often occur in arterioles or capillaries. Microchannel systems, constructed to mimic blood capillaries, are directly comparable with an *in vivo* microcirculation. Such systems have been used to evaluate deformation of erythrocytes in order to understand the effect on microvasular perfusion. This can be used in the future to study many blood-associated diseases such as sickle cell anaemia, diabetes and malaria. This study has shown that network perfusion with deformed erythrocytes, after graded exposure to glutaraldehyde (0-0.08%) erythrocytes exhibit a higher sensitivity to small changes in deformability causing blockages in microchannels.(131) Conventional methods, such as filtration, to measure erythrocyte deformability does provide invaluable information on the cell's rheological property however, it delivers sparse knowledge on the effect on microvasular perfusion.

Another study on vascular cell behaviour used microelectromechanical systems (MEMS) sensors to link real-time shear stress with monocyte/ECM interactions in an oscillatory flow environment to understand leukocyte rolling, adhesion, and transmigration.(132) It demonstrated that monocytes in oscillatory flow conditions compared with pulsatile flow, significantly upregulated P-selectin, inter-cellular adhesion molecule 1 (ICAM-1) and monocyte chemotactic protein-1 (MCP-1) mRNA expression. Also presented was the increased probability of monocytes binding to epithelial cells, found on the base

of the microfluidic channel under these conditions. Traditional methods of researching monocyte behaviour using histological cell culture techniques does not give insight in the binding kinetics found *in vivo* in response to oscillatory shear stress, adhesion molecules and chemokine gradients. Microvascular models *in vitro* in microdevices also include cultured human vascular endothelial cells which have been evaluated for high shear (25 dyn/cm^2), response to inflammatory cytokine, tumour necrosis factor-α (TNF-α),(133) and depletion of erythrocytes from whole blood at high volume flow rates mimicking blood flow phenomena previously observed and characterized in the *in vivo* mammalian microvascular system.(134) These studies have shown that cells cultured in microchannels exhibit the same properties as those found *in vivo* with comparative microenvironments, such as arterial shear stress. Microfluidic analysis using assays for adhesion molecules can be undertaken in the same microchannel with detailed kinetic studies of cell activation and adhesion to chemotactic molecules revealed in seconds at concentrations in the picoMolar range. (134)

1.4.3 Extracellular signalling within microfluidic cell culture

The need to understand and control extracellular signalling under *in vitro* conditions has become a growing research trend in the last few years. Generally, cells found *in vivo* are located in a three dimensional structures with other cells of possibly different phenotypes, which affect surrounding cell behaviour by cell-cell (or cell-matrix) contact, and/or by secreting paracrine, endocrine, and autocrine signalling molecules. The microfluidic environment, also described in an earlier section, with its diffusion-dominant principal

provides an ideal methodology for studying cell behaviour by incorporating, for example, different cytokines, hormones and antibodies.

Real-time monitoring in microsystems for cellular secretion phenomena has been investigated. The secretions examined include murine IgG from B cells using time-resolved luminescence analysis,(135) insulin secretion from islets of Langerhans, albumin secretion by the cultured primary rat adult hepatocytes,(136) both using serial immunoassays,(137) reactive oxygen or reactive nitrogen species (ROS) or (RNS) respectively from macrophages using electrochemical detection.(138) These studies have shown the detection of released extracellular molecules at higher sensitivity than those found using conventional enzyme-linked immunosorbent assay (ELISA) and this can be accomplished in real time, using cell populations numbering in the 100s rather than 1000s as used in standard cell analysis systems.

A number of groups have investigated the biological effects of concentration gradients of different molecules on cells. These include O_2 gradients on murine C2C12 myoblasts to understand the effect of tissue oxygenation on intercellular mechanisms that play critical roles in many human diseases including cancer, heart disease and stroke.(139) Areas of hyperoxygenation (20% O_2) were created using water electrolysis by noble metal microelectrodes to manufacture an effect on the C2C12 myoblasts. Using microscopy, it was reported that the cells took on a spherical shape and contracted away from the surface of the electrode. Although there were no signs of ruptured cell membranes through microscopic examination, use of a

LIVE/DEAD assay indicated the initiation of apoptosis in the areas of hyperoxygenation as shown in Figure 11.

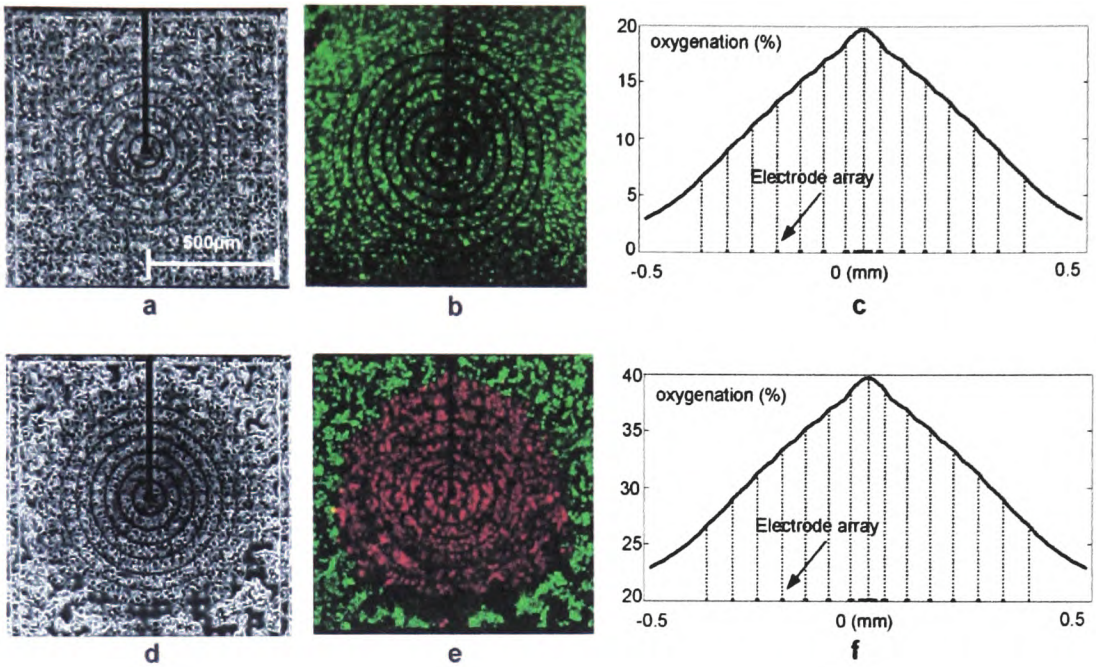

Figure 11. Hyperoxia-induced apoptosis in C2C12 myoblasts. a) 2 h after seeding (without oxygen input from OMA) b) LIVE/DEAD1 image of myoblasts after 72 h in anaerobic chamber (95% N2 : 5% CO_2), with constant current density of 10 mA mm^{-2}. c) Oxygen concentration plot of b); this axi-symmetric array makes a linear, cone-shaped concentration profile. d) 2 h after applying current density of 10 mA mm^{-2}. e) Fluorescent image of d) with LIVE/DEAD stain. f) Oxygen concentration plot for hyperoxic condition; this oxygen profile was applied to d) and e).(139)

Another study examined the effects of chemokine gradients on T-cell chemotaxis which has been previously limited to studies in 3D matrices or under agarose assays, which does not allow precise control or variation in conditions.(140) Using single and competing chemokine gradients of 100 nM CCL19 and 100 nM CXCL12 showed that the chemotactic index and the speed in response to CCL19 in the competing gradients are similar to those seen with the single CCL19 gradient. A high percentage of the cells migrated toward the CCL19 gradient in both single CCL19 gradient and the competing gradients. In contrast, the chemotactic index and the speed in response to the CXCL12

gradient in the competing gradients are significantly lower than those in the CXCL12 gradient alone. The advantage of microfluidic technology is the precise gradient control coupled with the lack of the previous techniques to study T cell chemotaxis in real-time, which may provide new biological insights into this important process. In addition, since only a small number of cells are required for seeding in the microfluidic system, chemotaxis of rare cell populations can be studied.

1.4.4. Measuring toxicological effects in cell populations using microfluidics

Microfluidic systems have also been used to analyse the toxicological effects of different stimuli on a diverse number of cells. The importance of 3-D cell cultures when recording the cytotoxicity results have included studies into the effects of three anticancer drugs (Cisplatin, CDDP; 5-Fluoro-uracil, 5-FU; paclitaxel, TXL) on human breast cancer (MCF-7).(141) The cells were embedded in a collagen-gel matrix and entrapped in a pyramidal-shaped silicon hole. By comparing microfluidic 3D culture to the standard 2D culture using scanning electrochemical microscopy analysis and colorimetric assays it was found that cells proliferation was lower compared with the 2D culture, and the results from the chemotherapy test showed little effect on the cells from CDDP, moderate effect from the 5-FU and the greatest effect from the TXL. This resulting difference is thought to reflect more accurately the *in vivo* dynamics of chemotherapy as proliferation rate is slower than in 2D culture, which is important when validating the effects of drugs which effect cell cycles. Continuous monitoring of chemosensitivity is important in drug screening, as the kinetics of anticancer drugs differ, depending on the agent's mechanism. These studies are advantageous due to the ability to continuously monitor cell

response by using different drugs and/or different cancer cells, with the normal cellular activity as a control.

Microfluidic technological development in the field of hepatotoxicity has progressed towards the merging of tissue engineering, transport phenomena and biomaterial applications. Kane *et al*(142) for example have demonstrated the ability to support metabolic and synthetic function with micropatterned primary rat hepatocytes and 3T3-J2 fibroblasts within a perfused, microfluidic array. Using this approach the capability of long-term synthetic and detoxification functions using albumin and urea synthesis was illustrated. The functions of the hepatocytes were compared to 'control' microfluidic devices which were kept in an 'open configuration', however it is not exactly clear from the article what this actually meant. There was no comparable data with other studies to determine whether the hepatocytes were functioning in parameters, which reflect previous *in vitro* or *in vivo* studies. However it was, to the author's knowledge, the first paper to cultivate hepatocytes with another cell type in a microfluidic system.

In a separate study, a heterogeneous-cell patterning microfluidic chip was described which facilitates the assembly of liver tissue *in vitro* using dielectrophoresis, with parallel manipulation, stable control, high cell viability, and cell modulation.(143) Later studies have continued to create 3D microenvironments for primary rat hepatocyte cultures to assess the heptocytotoxicity of drugs such as paracetamal and diclofenac, in dose-dependant manner.(144) These studies however, do not mimic the complex

cellular and extracellular composition of the liver organ that has been shown, using traditional methodology, as invaluable when understanding how the liver manages and removes toxic drugs as will be shown in Chapter 3. Refinements of microfluidic liver analogues need to include connective tissue, satellite cells and other cell types.

1.4.5 Microfluidic separation and sorting of different cell populations

Separating in microfluidic-based devices offers the advantages of fully automated processing, portable instrumentation for field and point-of-care use, and small input sample volume (µl or less of blood) along with corresponding reagent volumes. Separating target cells from other cells or biological fluids prior to characterisation represents the first step in many bioanalytical procedures. Cells range in sizes from 130 µm to 8 µm, and exist in dense populations therefore; sophisticated separation methods are needed as shown in Figure 12.(145)

There have been over 250 articles published detailing the use of microchannels for the separation of blood and blood cell populations. These include, for example, the use of a simple array of microchannels to separate blood cells and blood plasma using high and low flow rates within the different channels.(146) The plasma separation volume percentage collected varied from 15% to 25% with increasing 10% to 35% inlet hematocrit. Whole blood consists of 55% plasma and 45% cells. The traditional method of preparing blood plasma is by centrifugation of fresh blood with an anti-coagulant and the resulting plasma poured or drawn off.

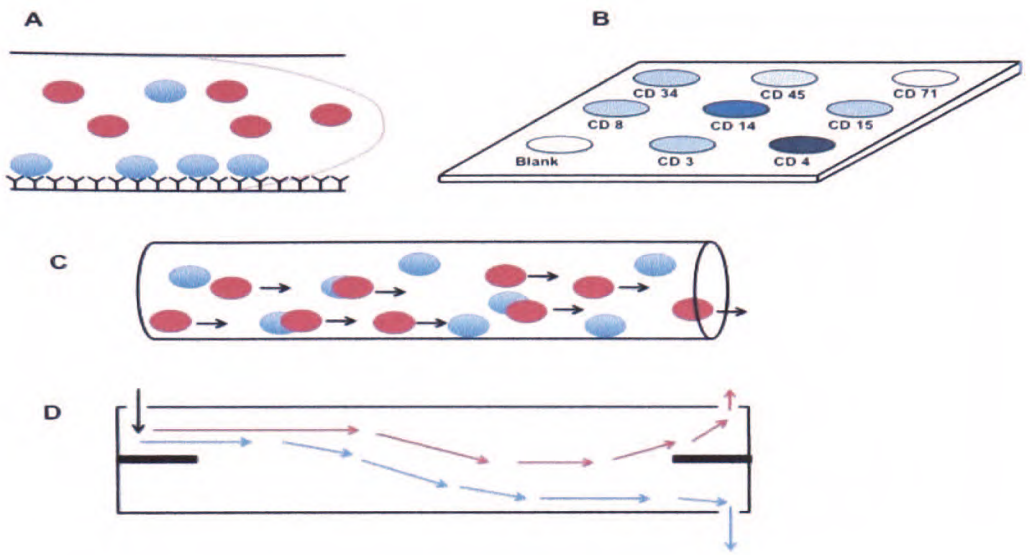

Figure 12. Overview of common cell separation strategies.(145) Affinity capture separations rely on the adhesion of cells to an immobilized, specific antibody (A). Unretained cells are washed to waste. The affinity format can be applied to array formats (B), where more than one capture molecule is attached to a surface. Here, antibodies corresponding to different cell surface antigens are used to separate blood cells. Affinity separations can occur in a column (C), facilitating elution and collection. Cells can also be separated by mechanical methods. (D).

This proposed microfluidic method seems cumbersome compared to the conventional method with the blood needing to be diluted before flowing onto the device and the collection of plasma seemingly inefficient compared to the volume of plasma in the initial blood sample.

Another area of study for separating and sorting blood cells uses magnetophoretic microseparators for the separation of erythrocytes and leucocytes from diluted blood based on their native magnetic properties. For example, experimental results for the single-stage paramagnetic capture (PMC) microseparator show that 91.1% of erythrocytes were continuously separated from the sample at a flow rate of 5 ml h^{-1}. In addition, the three-stage cascade PMC microseparator continuously separated 93.5% of erythrocytes and 97.4% of leucocytes from whole blood at the same flow rate.(147) The authors

acknowledge that the methodology needs refinement as the flow rate required (2.5–20 ml h^{-1}) is relatively low for efficient enrichment of rare cells, such as circulating tumour cells and hematopoietic stem cells. This method however, allows the ability of separating different cell populations for further use downstream.

Another example of a blood cell separation and sorting technique currently being studied uses a hydrophoretic method to isolate leucocytes from erythrocytes in a 1:20 diluted blood sample with 13 mm high slanted obstacles and 4 mm filtration obstacles to focus them to a sidewall.(148) This was achieved by employing successive structures on the top and bottom of the microchannel with the height and gap of the pores set between the diameters of small and large cells, which defined the critical separation diameter. Erythrocytes have a biconcave disk shape, and their diameters are 6.2–7.9 mm, a similar size to that of leukocytes. Therefore, it can be difficult to separate two cell types based on their sizes. The thickness and deformability of the erythrocytes (1.7–2.6 mm) allowed them to pass through the 4 mm filtration obstacles while the leukocytes could not. Accordingly, the cells smaller than the criterion freely pass through the gap and kept their focused position. The device was also used to separate neutrophils and lymphocytes from a 1:10 diluted blood sample. After the hydrophoretic filtration, neutrophils and lymphocytes were recovered up to 75 and 70%, respectively. The most commonly used methods for the differential separation of leukocyte subpopulations are magnetic-activated cell sorting (MACS) and fluorescence-activated cell sorting (FACS). In these methods, monoclonal antibodies tagged with magnetic or fluorescent compounds are used to separate cells based on

their specific antigenic determinants. Refinements to this microfluidic method for example incorporating MACS and FACS could allow the separation, detection and analysis of whole samples on a single platform which at present is not available.

Investigations into blood cell separation and sorting are continuing and the techniques highlighted here are just some of the methods being examined. It is hoped by the various research groups that the range of on-chip stationary filtrations of blood cells could be used for further cell selections, manipulation, and possible point-of-care clinical diagnostics.

1.5 Tissue-based microfluidic applications

The rapid development of bioanalytical applications in microfluidic systems of cell culturing has shown many fallibilities of the current conventional methodology. Microfluidic literature over the last ten years has focused largely on tissue engineering with devices being described that create tissue-like micro-architectures for subsequent interrogation or transplantation. These include a microfluidic bioreactor for culturing high-density hepatocyte arrays in order to mimic physiological liver mass transport,(149) an engineered cardiac tissue-like structure with anisotropic properties,(150) a microfluidic analog of the alveolo-pulmonary barrier of the lung.(151) Also reported are polydimethylsiloxane (PDMS) gel modules which contain 10^8 – 10^9 cells cm^{-3} in a microfluidic chamber to combine microfluidics and soft-lithographic moulding(152) and the encapsulation of AML-12 murine hepatocytes within microfluidic channels

formed from agarose hydrogel.(153) Whilst these models have made progress in providing *in vivo* microenvironmental phenomena such as diffusion and laminar flow, as previously discussed, they still lack the complexity of *in vivo* dynamics. The microenvironment cells occupy, can dramatically alter the genotype and consequently the phenotype of the cells, such as the addition of serum to fibroblast culture can alter the gene expression of the cell.(154) The chemical composition of the microenvironment is rigidly controlled by the release of signals from different cells, which may or may not be in close proximity. Therefore, a number of different cells are needed within an experimental model in order to give a greater approximation of typical cellular responses to external stimuli. Cell patterning of different cell types in microfluidic systems has only been achieved using two cell types(155, 156) whereas *in vivo*, organs are composites of several cell types such as exocrine cells (ceruminous cells), endocrine cells (pinealocytes), epithelial cells (squamous epithelium), neurons, and contractile cells (cardiomyocytes).

Many of the cell lines used in cell culturing both in traditional and microfluidic systems have been immortalized or are tumour-derived, which are genetically unstable, have intrinsic changes in gene expression, loss of proliferative regulation and signaling transduction pathways as described in Section 1.3.5. These cells therefore are not a replicate of the typical *in vivo* cell.(157) It has also been shown lately the importance of the ECM and its components. ECM is composed of structural proteins such as collagen and elastin, specialized proteins such as fibrillin, fibronectin, and laminin and proteoglycans. In their review article 'The extracellular matrix: At the center of it all' Bowers *et al* has compiled research into the relationships between cardiac

myocytes, fibroblasts, endothelial cells and the surrounding ECM, which highlights the importance of particular cardiac cell populations and extracellular matrix factors that are critical to the development and regulation of heart function. These include the differences in ECM in conditions such as hypertrophy and aortic valve stenosis, increased fibronectin and collagens I, III, IV, compared with physiological hypertrophy where there is no increase in ECM factor expression.(158) There are at least 19 different vertebrate collagens with tissue-specific distributions and unique functional properties.(159) Proteoglycans, for example, are a diverse multifunctional component of the ECM, playing roles in regulating matrix organization, growth factor activity, cell proliferation, and differentiation.(160) The ECM used in both traditional and microfluidic 3D cell culture lacks these *in vivo* complexities.(161, 162)

Direct cell-cell contacts have also been shown to promote growth, transfer of soluble factors and differentiation. A recent tissue engineering article has demonstrated, for example, the impact of cellular interactions between umbilical cord blood (UCB) hematopoietic cells and bone marrow (BM)-derived mesenchymal stem cells (MSC) on the *ex vivo* expansion and differentiative potential of UCB CD34 enriched cells.(163) UCB cells were cultured in contact, non-contact, or non-stroma conditions. After 18 days of culture, cell expansion was significantly higher in contact (fold increase of 280 ± 37) compared with non-contact (85 ± 25) environment. Direct cell interaction with BM MSC significantly enhanced the expansion of early lymphoid CD7+ cells, yielding considerably higher (x3-10) progenitor numbers compared with non-contact conditions.

It is also widely acknowledged that there is a need for preclinical models of human disease which better reflect the *in vivo* environment incorporating all components of the tissue in their *in vivo* configurations(164). However, tissue-based microfluidic applications are still in their infancy. The first article published, which could be said to use 'tissue', involved the culture of murine embryos in microchannels.(165) The objective of this study was to determine if static microchannels permitted the culture of murine embryos to the blastocyst stage. The embryos cultured in the microchannel exhibited a lower degenerated index (embryos at 8-cell stage and earlier stage) than the control. It should be recognized that the embryos at this stage of development are not yet differentiated and the phenotype of the cells are different from adult somatic cells. This is the first culture, using microfluidics however, that retains the native ECM with the cells instead of an attempt to replicate the environment using synthetic materials, as in the field of tissue engineering. Further research has used microfluidics to culture and study *Drosophila* and zebrafish embryos. *Drosophila* embryos are extensively used to examine genetic and phenotype changes in molecular biology. It has been demonstrated using traditional methodology that local temperature can have an effect on the signalling pathways of the developing embryo.(166) Using two laminar flow streams with different temperatures, signalling pathways have been manipulated in developing *Drosophila* embryos.(167) Intervention of developing organisms is highly appealing as it can give invaluable information into how physiology evolves and how different tissues develop. This type of research could be employed to study how gene therapy can be used to correct genetic disorders with pinpoint accuracy.(168) It show be noted however, that the simultaneous

delivery of different compounds by microinjection is standard procedure in molecular biological research and was first published in 1988.(169)

The first microfluidic studies using tissue slices were the culture of *ex vivo* brain tissue employing either a hollow SU-8 microneedles on 2.7 mm circular disks within a microfluidic system(170) to perfuse 400 µm thick hippocampal rat brain tissue at 40 µl min^{-1} or a three-layer PDMS device incorporating 530 - 700 µm thick medullary brain slices from neonatal rats perfused at 1 ml min^{-1}.(171) Using these approaches cell viability was found to be lost after 4 hrs at 36°C in the case of the microneedle device and 3 hrs in the PDMS system, this is a shorter viability period than traditional methods as shown in a earlier section. Liver explant culture is the latest development in microfluidic tissue studies. The first is detailed in this thesis; the second study used precision cut tissue slices (PCLS), in a 10 layer PDMS microfluidic device. The PCLS had 4 mm diameter and were 100 µm thick and perfused at 10 µl min^{-1}, and maintained viability for 24 hours. The PCLS were subsequently interrogated with 7-ethoxycoumarin (7-EC) and exhibited results comparable to PCLS cultured in 1.3 ml well plates.(172) The difficulties of using PCLS for testing novel drugs are described in depth in Chapter 3. Within this thesis two different types of tissue have been studied within a microfluidic system; liver and head and neck cancer tissue.

1.6 The liver

The liver is the largest visceral and most versatile organ of the mammalian body. It is essentially an exocrine gland, which secretes bile into the digestive tract but is also important as an endocrine gland and blood filter.

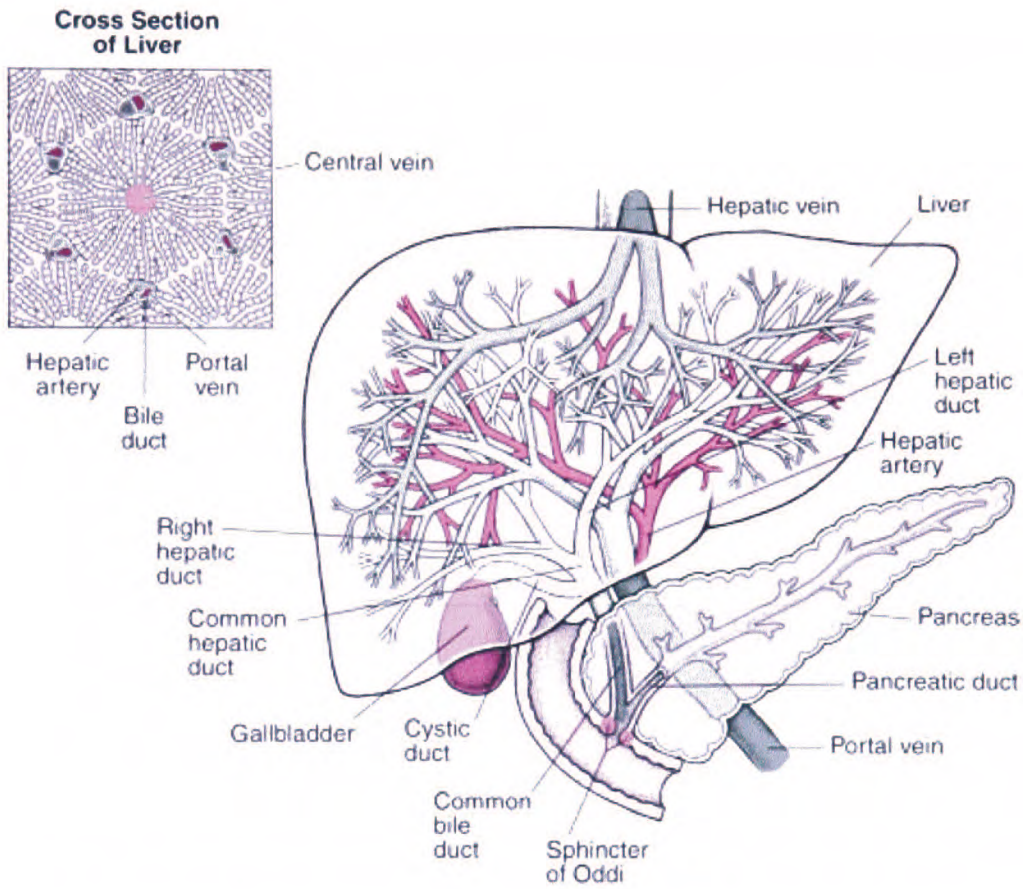

Figure 13. The liver and gall bladder with detailed structure of the liver highlighted.(173)

The liver as well as being a major physiological organ is also the major target of toxicity for a number of xenobiotics, chemicals and byproducts such as N-acetyl-p-benzo-quinone imine (NAPQI) produced during paracetamal metabolism.(174) This is due to its pivotal role in intermediary and energetic metabolism and in biotransformation processes such as glycogenesis, triglyceride oxidation and protein deamination.(175) Surrogate methodologies

and approaches for *in vitro* hepatotoxicity testing are necessary, and these must be robust, reliable and truly reflect *in vivo* dynamics. An almost impossible problem arises however, when attempting to replicate the highly specialized organization and complexity of the liver within a laboratory setting using traditional methodologies.

1.6.1 Histology of the liver

There are several different cell types found in the liver. These include hepatocytes, sinusoidal endothelial cells, stellate cells, cholangiocytes, Kupffer cells, pit cells and hepatic stem cells. Hepatocytes are the major parenchymal cell of the liver and constitute 70-80% of the overall cytoplasmic mass of the liver.(176) The average life span of a hepatocyte is five months.(177) Hepatocytes are relatively large compared with other somatic cells, approximately 6800 μm^3 in volume, with a diameter of 10-30 μm.(178)

Hepatocytes are complex and unique epithelial cells, which undertake important biological processes. They are involved in protein synthesis manufacturing albumin, fibrinogen, and the prothrombin group of clotting factors lipoproteins, ceruloplasmin, transferrin, complement components and a variety of glycoproteins.(179) Hepatocytes are also involved in carbohydrate and lipid metabolism synthesizing the former through gluconeogenesis and the latter from components supplied by the systematic circulation.(180) Hepatocytes synthesize bile salts(181) and importantly in toxicological studies metabolize, detoxify and inactivate both exogenous and endogenous compounds, for example, drugs and steroids.(182, 183)

Histological organization of the lobes of the liver is controlled by connective tissue. The functional units of the liver, liver lobules, can number up to 100,000 and are separated by an interlobular septum as shown in Figure 14. The hepatocytes in the liver lobule form asymmetrical plates of only one cell depth (Remak's plates) with the exposed hepatocyte surfaces, top and bottom, are covered with short (0.5μm) microvilli. A characteristic cross section of a liver lobule has a hexagonal shape. Within lobule sinusoids, the capillaries are lined with fenestrated (gaps between cells) endothelial cells with no basement membrane, allowing the free exchange of water and solutes under 200 nm in size between blood and interstitial fluid.(184)

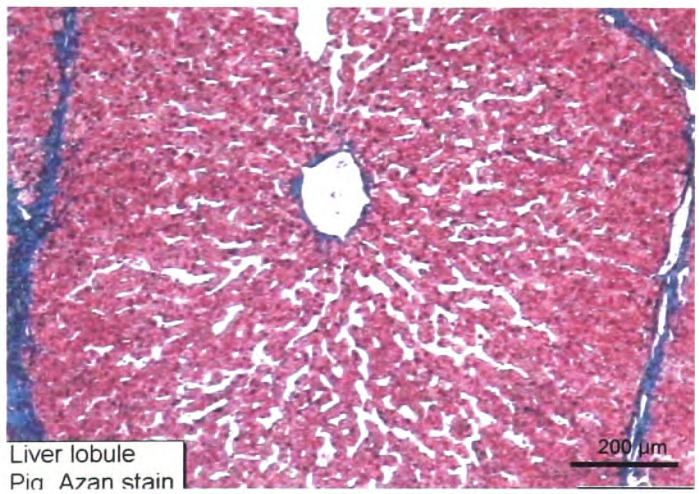

Figure 14. Image of porcine liver lobule stained with Azan stain(185)

The diameter of the fenestrae can be transformed by several factors such as the neurotransmitter, serotonin (5-hydroxytryptamine), toxic compounds for example carbon tetrachloride (CCl_4), alcohol, nicotine and high pressure.(186-188) The liver lobules are surrounded by a highly specialized layer of cells known as liver sinusoidal endothelial cells (LSEC) which act as a mechanical filter and are involved in multiple physiological and pathological processes such as liver organogenesis, regeneration, chronic inflammatory

disease and heptatocarcinogenesis.(189) LSEC are the second most abundant cells after hepatocytes and constitute 20% or 1 x 10^8 of the cells found in the liver. LSEC are the foundation of angiogenesis and vasulogenesis of the liver.

The area in between the hepatocytes and the sinusoids, as shown in Figure 15, is known as the perisinusoidal space or the space of Disse named after its discoverer, Joseph Disse (1852-1912).

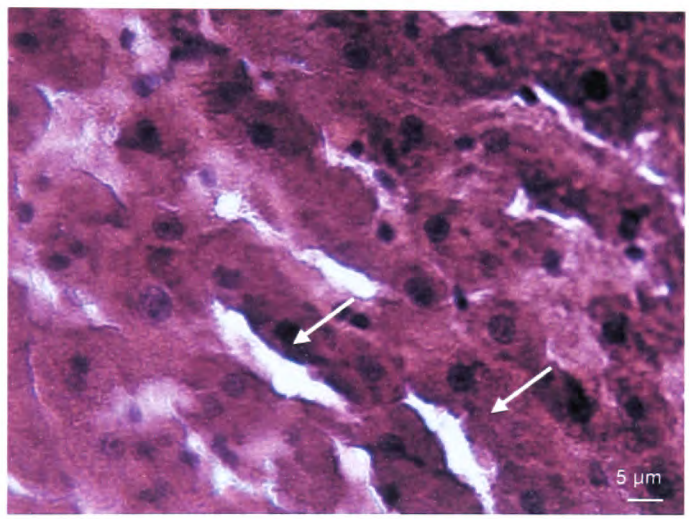

Figure 15. Histological image of liver tissue showing the space of Disse, indicated by the arrows

Blood flows through the space of Disse and hepatocytes can be described as existing in direct contact with blood. Exo- and endocytosis takes place in the space of Disse and is a function of the sinusoidal plasma membrane. The space of Disse is principally made of connective tissue with reticular (collagen) fibres and is where the hepatic stellate cells (HSC) or Ito cells can be found. (190)

Hepatic stellate cells are star-shaped phagocytes that have a three-dimensional structure consisting of a cell body with several long, branching cytoplasmic processes.(191) They constitute 5-8% of liver cell population and their structure and spatial augmentation in the liver lobule make them sufficient to envelop the entire hepatic sinusoidal microcirculatory network. The importance of this cell type within the liver was only recognized two decades ago and their significance within the liver is still being investigated.(192) HSC play a key role in the metabolism and storage of retinoids.(193) Nerve endings are localized in the Disse space and are oriented towards HSC and there is evidence of interplay with the autonomic nervous system.(194)

In a normal liver, ECM represents 0.5% of the wet weight.(195) Interstitial matrix structures, the ECM and basement membranes, support epithelial, endothelial and mesenchymal cells. The space of Disse is constructed from a network of collagen III and IV and non-collagenous laminin and nidogen.(196) Collagen I is associated with reinforcing the architecture of the perisinusoidal space in the form of large diameter fibre bundles. ECM in addition to collagen is made up of small amounts of several non-collagenous components, which include glycoproteins such as: fibronectin, laminin, nidogen, tenascin and undulin, sulphurated proteoglycans such as proteodermatan sulphate and hyaluronic acid, a carbohydrate polymer.(196) This non-fibrillar complex establishes optimal diffusion between hepatocytes and bloodstream.

Another group of cells found in the liver are the biliary epithelial cells or cholangiocytes, which envelop the biliary tree. These cells make up 3-5% of the

liver mass. Bile manufactured by hepatocytes and secreted into a network of canaliculi, which progressively increase in size into bile ducts that empty into extrahepatic duct and is stored in the gall bladder. Cholangiocytes are polarized with one side facing the lumen (apical) of the bile canaliculi and the other side (basolateral) facing the sinusoidal space.(197) The apical membrane secretes water and electrolytes such as bicarbonate (HCO^{-3}) through the driving force of Cl^- ions through the cystic fibrosis transmembrane regulator (CFTR).(198) Cholangiocytes also reabsorb bile components such as bile salts, glucose monomers and drugs through the apical membrane which are then subsequently effluxed into the peribiliary plexus via the basolateral membrane.(197)

Another important cell type found in the liver is the Kupffer cell (KC). Kupffer cells are the largest population of somatic fixed tissue macrophages. KC represent 30% of non-parenchymal cells and 15 % of all hepatic cells.(199) They are found in the hepatic sinusoids attached to the lumen of the sinusoidal endothelial cells and as a result of the fenestrae can contact the stellate and parenchymal cells.(200) Due to their position, KC are in continual contact with the blood where their main function is to remove all foreign bodies from the blood by phagocytosis or pinocytosis. These are then eradicated by lysosomal degradation and consequently have lysosomal enzymes and superoxide.(201)

Kupffer cells have a pathophysiological role in several liver diseases. These include hepatic ischaemia-reperfusion injury,(202) drug induced liver failure(203) and alcohol-induced liver disease. In alcohol-induced liver disease,

acute and chronic exposure to ethanol causes activation of KC, which leads to enhanced cytokine and chemokine release with an increase in ROS manufacture.(204)

Additional populations of cells located in the liver, which also have a role in the immune system are Pit cells. These cells are unique natural killer (NK) cells, resident in the liver that have the ability to kill certain tumour cells and virus-infected cells without prior sensitization.(205) Pit cells were named by Wisse *et al*,(206) due to their characteristic cytoplasmic granules, called pits in the Dutch language. Although morphologically resembling large granular lymphocytes (LGL), pit cells are immunophenotypical and functional characteristics are different from blood NK cells. Pit cells exist in the liver sinusoids where they are frequently found adhered to endothelial cells but are sometimes found in combination with Kupffer cells. Pit cells produce IFN-γ, TNF-α, IL-5, IL-10, and IL-13 cytokines,(207) and compared with blood NK cells they have be shown to be four to eight times more cytotoxic against syngeneic rat colon adenocarcinoma cell line (DHD-K12).(208)

The final group of cells found in the liver are the hepatic stem cells or Oval cells. This group of cells has only been recognized in the last few years by animal experimentation.(209) These cells are thought to reside in the terminal bile ducts (canals of Hering). While hepatocyte mitosis is responsible for the bulk of liver regeneration after the majority of hepatic injuries, stem cells are also thought to contribute to hepatocyte regeneration and in severe cases of injury, may take over this role.(210, 211) Hepatic stem cells are found to

differentiate into cholangiocytes or hepatocytes during *in vitro* and *in vivo* animal studies.(212, 213) These cells have also been implicated in the development of dysplastic nodules, hepatocellular carcinoma and cholangiocarcinoma.(214-216)

1.7 Cancer

Cancer is the second biggest killer in United Kingdom after cardiovascular disease. Almost 1 in 3 of the population will develop cancer in their lifetime and almost 75% of those will die directly or the cancer contributing to their deaths.(217) Cancer cells disrupt the ordered series of events that lead to normal cell division and exploit all opportunities to multiply.(218) Dysplasia is the disordered development of cells that result in modification in their size, phenotype and organization. This can be reversible however; dysplasia commonly precedes neoplasia, the process of tumour growth. A tumour is an abnormal mass of tissue and is the result of autonomous disordered growth that continues after the initial growth signal(s) have dissipated. Tumours are categorized as benign or malignant: benign tumours are localized, slow growing but can compress the surrounding tissue. Malignant or cancerous tumours invade and destroy adjacent tissue, metastasize, grow rapidly and are usually poorly differentiated.(219)

The treatment of cancer requires a comprehension of the principles of cancer evolution, multiplication and metastasis.(218) In brief, cell proliferation and division, is usually, kept in tight control by two opposing sets of critical genes, proto-oncogenes and tumour suppressor genes respectively. Loss of

function in the tumour suppressor genes and the gain of function in the proto-oncogenes remove the cell's ability to control growth. Accumulations of mutations result in cells that are genetically different from each other. Eventually, fast-growing, less differentiated cells take over often begin invading surrounding tissue and proliferate in foreign sites, i.e. metastasis.

A solid mass of cancer cells can be removed surgically, destroyed by radiation and toxic chemicals as the latter agents preferentially kill rapidly dividing cells.(220) It is extremely difficult to remove every cell and there is always the possibility that tumours, through their ability to rapidly mutate, can become resistant to the reagent used to destroy them, or worse still the treatment itself causes further cancerous growths or cell damage.(221, 222) Nevertheless, effective cures have been found for many formally lethal cancers such as Hodgkin's lymphoma, testicular cancer and many childhood malignancies.(223, 224) Some cancers however, have proved more difficult to treat due to the stage of progression on detection such as locoregional spread and distant metastasis to secondary sites. One of these cancers is head and neck cancer.

1.7.1 Head and neck cancer

The majority of head and neck cancer (HNC) begin in cells that cover the mucosal surfaces of this anatomical region.(225) These malignancies include cancers of the buccal cavity, larynx, pharynx, thyroid, salivary glands and nose/nasal cavities as shown in Figure 16, and the majority are head and neck squamous cell carcinomas (HNSCC).

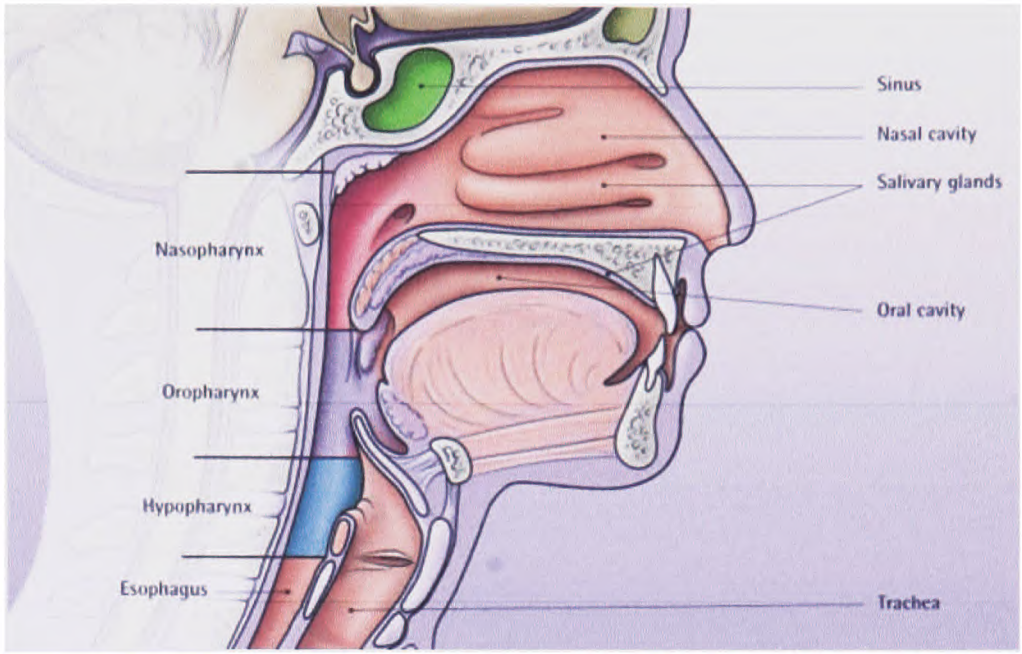

Figure 16. Anatomy of the head and neck highlighting areas where HNSCC occurs. (226)

In the United Kingdom, HNC constituted only 3% of all the reported cancers in 2007 but is the 6th most common worldwide due to the high incidence in South East Asia and the Mediterranean area.(227-229) These cancers are more frequent in men and people over the age of 50,(230) in the UK however, evidence suggests that the incidence in the younger population is increasing.(231)

The major risk factors of HNC are tobacco (including smokeless tobacco, also known as 'chewing tobacco' and 'snuff') and alcohol.(232-234) Eighty-five percent of HNC are tobacco-related.(235) People who use a combination of both these major risk factors are significantly more likely to develop cancer, than those who just use either tobacco or alcohol; showing synergistic effects of these agents.(234) Other major risk factors recognized in the last decade include sun exposure (lips),(236) human papillomavirus (HPV) which alters the

DNA of the cells (oropharynx),(237) industrial exposure from wood and nickel dust inhalation,(238) Epstein-Barr virus infection, which again alters the DNA of the cells (nasopharynx)(239) and Plummer-Vinson syndrome (hypopharynx).(240)

Diagnosis of HNC is achieved through medical history evaluation, clinical examination by an experienced clinician, fine needle aspiration cytology (FNAC) and ultimately biopsy of tissue.(241, 242)

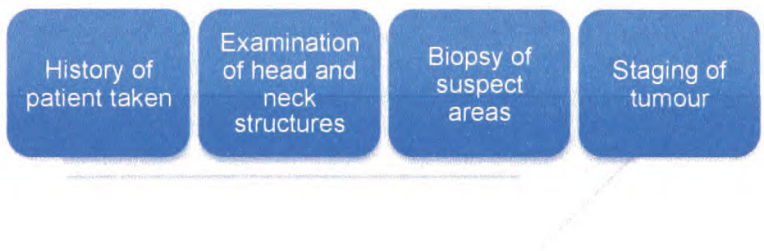

Figure 17. Diagnostic procedure of HNC

If the diagnosis of HNC is verified as show in Figure 17, then the clinician will want to know the stage (or extent) of the disease. Staging is an attempt to determine the spread of the cancer and if so, what other parts of the body are affected. Primary tumour is first described by site, and then graded on depth of invasion, tumour type, pattern of infiltration, excision margins, vascular and perineural infiltration.(243, 244) Nodal involvement through metastatic disease affects prognosis adversely. In a recent study, it was demonstrated that isolated tumour cells (ITC) were detected in 12 of 146 patients (8%), and 24 of 1694

(1%) lymph nodes. After a median follow-up time of 28 months, ITC in pathological node-negative lymph nodes was associated with poorer outcomes compared with true node negative disease.(245) Public awareness of HNC is generally low and therefore many patients present with advanced cancerous growths that have a relatively poor prognosis.(231, 246)

The treatment plan of each individual patient depends on a number of factors, including the exact location of the tumour, its stage, and the age and general health of the patient.(247) Surgery may be the treatment of choice if the primary tumour can be excised with an appropriate margin of normal tissue without resulting in major function compromise. Surgical treatment through neck dissection can remove both the affected soft tissue and the lymph nodes, to avoid further spread.(247) Resections in the neck are small, most often ~0.5cm^3 in size but can be up to 10 cm^3, compared with larger resections on other cancerous tumours like the liver and lung (>20 cm^3).

Treatment after surgery is radiotherapy and/or chemotherapy.(248) Radiotherapy uses ionizing radiation to treat the malignancy. Ionizing radiation is delivered by external beam radiotherapy or by brachytherapy (implantation of radioactive source within the tumour). Radiotherapy can be delivered as radical radiotherapy with curative intent or as palliative to provide symptomatic relief only.(249) After locoregional therapy, HNC patients are treated with chemotherapy. No evidence has identified the approach of chemotherapy alone as a curative treatment for HNSCC.(250) Chemotherapy can be given as

neoadjuvant, delivered in the weeks before locoregional therapy, adjuvant, delivered after locoregional therapy, or concurrent with radiotherapy.(251)

CDDP and 5-FU (Figure 18) are widely used in the treatment of human cancer. In HNC chemotherapy, current regimens use radiotherapy with a combination of 5-FU and a platinum based agent, usually CDDP.(252) The survival rates at 1 and 2 years were 81% and 76%, respectively. The progression-free survival rates at 1 and 2 years were 69% and 66%, respectively.(253)

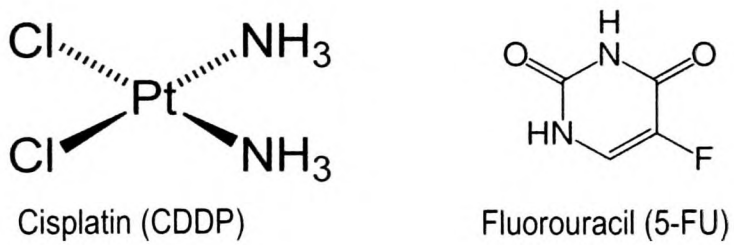

Figure 18. The chemical structures of the commonest chemotherapeutic agents.

The cytotoxic effects of 5-FU are described in Table 3. 5-FU is an analogue of uracil and quickly penetrates into cells using the same non-facilitated diffusion and facilitated transport mechanism as uracil.(254) Inside the cell, 5-FU is converted intracellularly to several active metabolites including 5-fluoro-2'-deoxyuridine monophosphate (FdUMP). The foremost mechanism of 5 –FU cytotoxicity is theorized to be the inhibition of thymidylate synthase (TS) by FdUMP, although as yet the exact molecular mechanisms of TS inhibition are unknown. Inhibition of TS causes the depletion of thymidine

5'monophosphate (dTMP) leading to the inhibition of DNA synthesis and interference with DNA repair.

Table 3 DNA-directed cytotoxic effects of 5-FU

Biochemical consequences of thymidylate synthase inhibition	*Direct and indirect effects on DNA synthesis and integrity*
Deoxyribonucleotide imbalance	Inhibition of net DNA synthesis
Depletion of thymidine monophosphate and thymidine triphosphate	'Uracil' misincorporation (fluoro- and deoxyuridine triphosphate)
Accumulation of deoxyuridine monophosphate	Interference with nascent DNA chain elongation
Elevation of extracellular deoxyuridine	Altered stability of nascent DNA
Formation of deoxyuridine triphosphate	Induction of DNA single-strand breaks in nascent DNA repair
Accumulation of deoxyadenosine triphosphate	Interference with DNA repair
	Induction of single-strand and double-strand breaks in parental DNA

[Adapted from (254)]

CDDP or cis-Diamminedichloroplatinum (II) is among the most active antitumour regents used in human chemotherapy.(255) It was the first platinum based drug introduced to the clinic after its medicinal effects were published in 1969.(256) There is an extensive body of research that the success of platinum complexes in destroying tumour cells is mainly due to its ability to form various types of adducts on DNA.(257, 258) Bifunctional cisplatin contains two non-leaving ammonia ligands and two reactive chloride groups as shown in Figure 19.

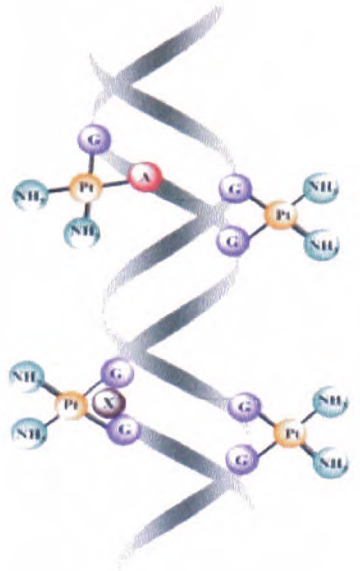

Figure 19. DNA adduct formation with cisplatin leaving two amino groups coordinated on the platinum atom(259)

The major DNA adduct of cisplatin is the intrastrand cross-link (CL) formed between two neighbouring purine bases (1,2-GG or AG intrastrand CL) with CDDP coordinated to the N7 atom of the purine bases as shown in Figure 49.(259) The full details of the underlying antitumour mechanisms are not entirely understood despite extensive study. One theory is that adducts are formed by CDDP that distort DNA conformation, inhibit replication and transcription.(260) Another hypothesis proposed is that a number of proteins exhibit an increased affinity for CDDP-modified DNA, for example transcription factors, effectively high jacking these proteins from their regular binding sites and disrupting fundamental cellular processes.(261)

Chemotherapy results in a small statistically non-significant (2%) overall survival benefit at five years if given neoadjuvantly (before treatment) and no survival benefit if given adjuvantly. The supplementation of chemotherapy to

locoregional treatment with non-metastatic stage III and IV HNSCC significantly increases survival by 5% at two and five years.(251) Standard practice in the UK is the use of neoadjuvant chemotherapy using CDDP or 5-FU to treat HNC cancer. These chemotherapy agents give significant survival benefit compared with locoregional treatment alone. Other chemotherapy drugs are also being employed to treat HNC these include docetaxel, capecitabine, and cetuximab.(262, 263) When chemotherapy is dispensed concurrently with radiotherapy in HNSCC there is an overall survival benefit of 8% at five years.(250) The absolute survival benefit for concurrent single agent CDDP, compared to all other drugs, is 11% at five years. The reduction of death has been calculated for each subsite as these in many ways can be considered as distinct entities, shown in Table 4, the benefit of all types of concurrent chemoradiotherapy is also age-dependant, with greatest benefit seen in patients' aged 60 and below, as demonstrated in Table 5.

The survival benefits connected with concurrent chemotherapy are at the detriment of increased acute toxicity (mucosal and haematological) and dental problems relating to late toxicity however, these are usually considered acceptable. Single agent CDDP is recommended, by the National Health Service (NHS), as the chemotherapeutic agent of choice in concurrent chemoradiotherapy.(250) HNC is affecting a growing number of people in the population and public awareness is still low, and although treatment is available, mortality rates have not significantly improved, over the past thirty years despite improvements in clinical strategies.

Table 4 Reduction of mortality rates after concurrent chemoradiotherapy compared to no chemotherapy

Subsite	Percentage reduction in risk of death
Oropharynx	23%
Larynx	22%
Buccal cavity	17%
Hypopharynx	16%

[From (250)]

Table 5 Mortality reduction of death after concurrent chemotherapy by age

Age	Percentage reduction in risk of death
60 or below	22-24%
60-70	12%
Over 70	3%

[From (250)]

As described in this chapter, cell culture has provided invaluable information on cell dynamics. Microfluidics has the ability to provide the *in vivo* microenvironment that is lacking in current *in vitro* cell based methodologies and allows an opportunity to increase our current knowledge. Cell based microfluidic applications have been continually evolving over the last 20 years with one of the latest developments being the maintenance of *ex vivo* explant biopsies in microfluidic systems. The following experiments describe the maintenance and interrogation of liver and cancer tissue in the microfluidic system for pharmacological, toxicological and fundamental studies in cell biology.

2. Aims

The global aim of this thesis was to develop and validate a microfluidic system for the monitoring of cellular functions within an explant/organ biopsy. This was to be achieved by manipulating the microenvironment of a tissue biopsy to ensure the viability of the explant while also maintaining the extracellular architecture. Subsequently, the tissue will be interrogated to invoke an intracellular or extracellular response that mimics the same response found in previous *in vitro* and *in vivo* models. In reaching this aim the following objectives were met:

- Development and validation of microfluidic systems for the maintenance of highly metabolically active biopsies, e.g. liver and head and neck cancer. This was achieved through epi-fluorescent and confocal microscopy, viability and functional biochemical assays and histological analysis of individual cells within prepared tissue sections.

- Establishment of suitable methodology to stimulate and probe explant samples to mimic organ and/or cellular responses found within *in vivo* followed by analysis of cells in tissue and at the single cell level.

- Detection and analysis of individual biomarkers from cancer biopsies after interrogation with chemotherapeutic drugs

3. Development and validation of microfluidic devices for tissue-based methodologies

'No amount of experimentation can ever prove me right; a single experiment can prove me wrong.'

Albert Einstein 1879-1955

The concept of a 'system biology' platform, which would be more relevant than current cell-based applications and more appropriate than animal models in its representation of human organ functions is an ideal that has been alluded to by many researchers and practitioners in recent years.(1, 264) Bridging the gap between cell and *in vivo* models, removing the need for extraneous animal experimentation whilst allowing tissues and organs to be probed and monitored at the molecular and cellular level, has been of increasing interest to the biological, clinical and microfluidic communities. Research is commonly hampered by the lack of sophisticated pre-clinical *in vitro* models to replicate effectively the *in vivo* dynamics involving multiple cell types, complex ECM interactions and mechanical forces. These are vital in pharmacokinetic / pharmacodynamic (PBPK) models, where the lack of suitable preclinical models can ultimately lead to drug withdrawal with possibly useful drugs never getting to the clinical setting or some drugs reaching patients that cause deleterious effects and have to be withdrawn.

Tissue is maintained *in vivo* within a highly regulated environment with cell signalling acting via paracrine, autocrine and endocrine pathways. In order to

replicate the microenvironment of the cells and tissue, retention of these pathways is essential. Therefore to ensure that the tissue is successfully maintained, the microfluidic system has to be designed and optimized with viability, functionality and maintenance of the signal pathways being the paramount consideration. This chapter describes the design and fabrication of the microfluidic system and how this aims to maintain tissue and cell viability and function.

3.1 Fabrication of microfluidic device

In order to maintain and interrogate the tissue, the microfluidic device needs to have the following properties. It must be able to hold an appropriate sized tissue sample, to comprise all the different specialized cell types, connective tissue, stroma and cell products that perform the relevant functions within the tissue. This must be achieved whilst maintaining the viability, functionality and the architectural structure of the tissue. The design of the chamber should allow efficient perfusion of the tissue across its entire surface with nutrients and oxygen while preserving the laminar flow. Efficient perfusion is essential to ensure all the cells are experiencing the same conditions within the tissue therefore avoiding erroneous artefacts. The channels in the device have to be large enough to permit adequate flow and the flow rate must allow the accumulation of signalling molecules while removing waste products but not be too large to disrupt paracrine and autocrine signalling by removing excess fluid from the tissue microenvironment; in effect creating a effective culture volume. The device must be transparent, with the base being thin enough to allow the analysis of the tissue morphology and functionality through optical

means including epi-fluorescent and/or confocal microscopy. It also needs to be dismantled sufficiently to allow cleaning and sterilization to be performed or be made of inexpensive materials to allow single use.

The material from which the microfluidic device is fabricated in is also important; it must be biocompatible, chemically and thermally stable. Glass has been extensively used in biology for cell culture and has all of the properties mentioned. The surface properties of glass were also well characterized allowing these devices to easily be tailored to several applications.(265) However there is a significant problem associated with using glass, principally that it is gas impermeable and further mechanisms are needed to ensure oxygenation. Over the last ten years theirs been a steady progression from glass to several different polymers that are gas permeable, with the principal elastomer being PDMS.(266) PDMS is a polymeric organosilicon compound that has applications ranging from contact lenses and medical devices to shampoos and lubricating oils. PDMS has been widely used, with other polymers also being explored such as poly methyl methacrylate (PMMA) and poly-lactic-co-glycolic acid (PLCA). The benefits of both glass and polymers are summarized in Table 6. However, due to the previous in house experience of micromachining glass microdevices, only the bung, which sealed the chamber, was manufactured from PDMS and the main body of the device from standard glass.

The microfluidic device is to be used to facilitate the study of cells within a tissue environment therefore the recreation of the *in vivo* microenvironment is

essential. Cells in macroscale culture vessels confront the problem of mechanical forces from fluid motion and bubbles.(267)

Table 6. A comparison between polymers and glass properties with respect to their use for microfluidic applications

	Polymers	Glass
Manufacturing costs	Relatively low in cost compared with glass, especially for mass-production.	High in cost, especially for relatively large-area substrates. Higher costs are also associated with clean-room facilities.
Fabrication	Fabrication steps are simpler than glass, and no wet chemistry is needed.	Time consuming and expensive, and wet chemistry is used.
Clean room facilities	Clean-room facilities are necessary for aseptic techniques. In certain cases, particles may become pressed into the polymer during processing without having an effect on device functionality.	Clean-room facilities are needed to avoid contamination.
Properties	Wide selection of polymers, hence mechanical, optical, chemical and biological properties can be tailored.	Less variability.
Operation temperature	Limited for polymers because of relatively low vitrification temperature (Tg) compared to glass.	Wider range of operation temperatures
Optical properties and fluorescence detection	Optical transparency is lower than glass. Except for special grades, polymers also have higher auto fluorescence relative to glass.	Excellent optical properties; auto fluorescence levels do not affect detection capabilities.
Bonding	Different bonding options are available, e.g. adhesives, thermal fusion, ultrasonic welding and mechanical clamping.	Time consuming. Bonding options include thermal, adhesive and anodic bonding.
Surface treatment	Surface treatment methods are available for polymers, but routine, well-established derivatization techniques are not available.	Established chemical modification procedures for glass are available using organosilanes.
Compatibility with organic solvents or strong acids	Except for some special grades, polymers are generally not compatible with most organic solvents nor in some cases, strong bases or acids.	Good resistance to organic solvents and acids.
Joule heating	Subject to significant Joule heating because of low thermal conductivity.	Relatively resistant to Joule heating relative to polymers.
Electro osmotic flow (EOF)	Smaller EOF produced relative to glass, because of lack of ionisable functional groups.	Higher EOF relative to polymers.
Geometrical flexibility	Polymer processing techniques offer more flexibility for geometrical designs, including for example different cross- section (curved, vertical or V-groove), high aspect ratio square channels, channels with a defined but arbitrary wall angle, or channels with different heights.	Due to the isotropic nature of the etching process, only shallow, low aspect ratio, mainly semicircular channel cross-sections possible.
Permeability to gasses	High gas permeability.	Impermeable

[Adapted from (268)]

Stirring and rocking is standard procedure for explant culture within biological laboratories though the fluid motion can cause cell damage through shear forces. Bubbles, which are essential for aeration, can cause damage to cell membranes especially when they rupture.(269) Bubbles can arise through low air pressure created by the fluid flow. Bubbles can be minimized if the media is filtered before flowing through the device. Media replacement is necessary to meet the nutritional requirements of the cells, but can also be responsible for the creation of shear stress on the tissue, especially for the cells on the periphery of the tissue. Shear stress is felt by an entity when a force is applied to its surface.(41) In liquids, the shear stress present throughout a channel can be represented mathematically using Newton's law of viscosity:

$$\tau = -\mu (dv/dx) \qquad \text{Equation 5}$$

Where τ is the shear stress, μ is the viscosity, υ is the velocity, and x is the position within the channel.

When tissue is placed in a microchannel, intercellular space plays an important role on determining the effect of shear stress on individual cells. A mathematical model has been developed to determine the influence of cell spacing within a microchannel(41) however, this is not relevant to tissue mechanics as the model is too ordered and less complex compared with *in vivo* tissue. Extensive studies into the mechanical properties of soft tissue such as the liver have focused on compression (pushing force), indentation (hardness of a material to deformation), uniaxial tension (stretching in one direction) and

aspiration (drawing or suction motion).(270) Experiments into the shear properties under finite deformation have been limited. A study used 130 *ex vivo* porcine liver tissue samples conducted two types of pure shear test, unconfined compression and uniaxial tension.(271) A Digital Image Correlation (DIC) technique was used to measure the deformation field. The most important facet of the pure shear (or planar tension) test used was that the specimen was much shorter in the direction of stretching than in its width dimension. The specimen was constrained in the lateral direction such that all specimen thinning occurs in the thickness direction. Due to gravity, the deformation field was not uniform in the vertical direction and the authors proposed two new constitutive models to describe the full range of deformation for both compression and tension, and also good for representing tissue deformation in pure shear. There have however, been no results published about the effect of shear stress on soft tissue in a microenvironment.

Other factors that are of consequence in tissue culture are SAV ratio and effective culture volume. Cells that are cultured in the macroscale have extremely low SAV ratios. This is contrary to *in vivo* dynamics, which have high SAV ratios that allow the efficient transport of gases and nutrients to the tissue. Effective culture volume is an indicator of the cell's ability to control its environment. In macroscale vessels, cells are cultured in relatively large volumes and therefore the biomolecules secreted by the cells are diluted into the relatively vast quantity (> 5 ml) of media or buffer. In the microscale, like *in vivo*, cells are bathed in small volumes (< 20 µl) allowing the accumulation of signalling molecules allowing effective communication between the cells.

3.1.1 Fabrication of glass devices

Dr. Stephen Clark produced all the glass microfluidic devices used in this thesis. The first step in constructing the glass microdevices was to draw the channel structure using AutoCAD LT software computer assisted design (CAD) software package. The drawing was transferred to a mask or thin film with the channels left blank on a black background; this allows light to penetrate through to expose the channel design on to glass wafers (Telic, Valencia, USA) during the procedure to produce the devices.

The B-270 glass wafers, 1mm thick, used to manufacture the devices were coated with a chromium layer and a photoresist layer, which was required for photolithography as illustrated in Figure 20. Photolithography is a process to remove selectively either the channel or the bulk of a substrate. This was achieved by placing the mask on a ultra-violet (UV) exposure unit with glass wafers placed on top of the channel design. This was called contact printing and was used for small volume (10s) production. The exposed plate was immersed in developer solution (Chestech Ltd., Rugby, UK) for 60 s. The plate was then rinsed under running water and dried it by blowing N_2 over it. The plate was then placed into a small basin containing Chrome Etch MS8 solution (Chestech Ltd., Rugby, Warwickshire, UK) for 60 s, or until the pattern is fully exposed on the glass. The plate is then rinsed with deionised water and blown dry with N_2. The glass was then wet etched using hydrofluoric acid (48 %), ammonium fluoride (40 %), hydrochloric acid (38 %) and deionised water. Etching time depended on the depth of the channel required. For this study, the channel dimensions were 190 µm width and 70 µm depth. The depth was subsequently

verified using light microscopy. Due to the nature of the etching process, etching occurs both widthways as well as downwards, creating channels with a cross section that is approximately trapezoidal.

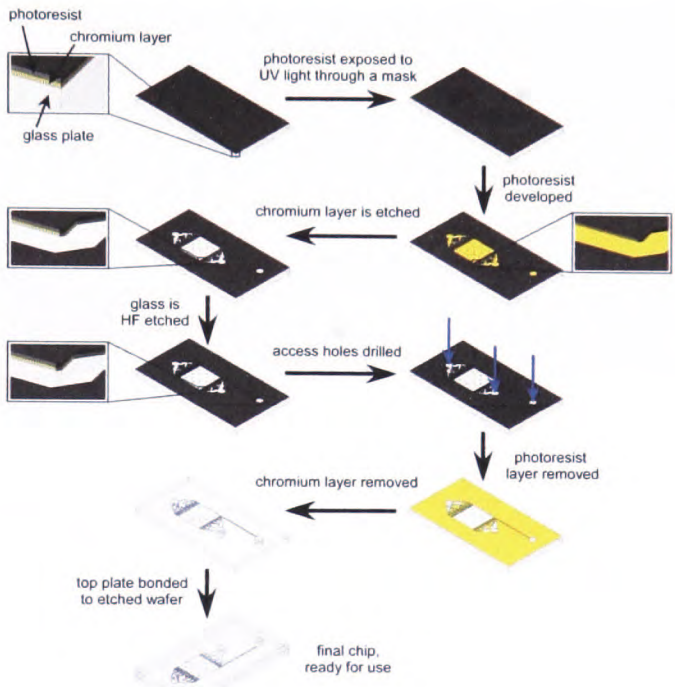

Figure 20. The photolithography and wet etching method of microfluidic chip fabrication.(272)

The glass underneath the photoresist and chrome layers was etched whilst the top two layers remain intact. The etched plates were then immersed in a small basin of acetone for several minutes until all of the photoresist was removed, rinsed with water and dried them with N_2. At the next stage the chrome layer was removed using a chromium etchant, Chrome Etch MS8, for several minutes removed then allowed to dry. Access holes were drilled in the 3 mm thick top plate, using 1.5 mm drill bits by standard drilling techniques as shown in the schematic in Figure 21.

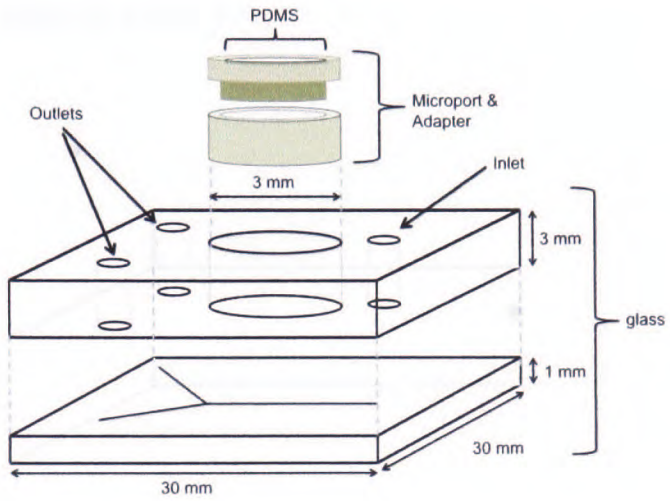

Figure 21. Schematic of microfluidic device used for these studies.

A central hole with a diameter of 3mm was drilled into the top plate to provide a chamber for the tissue. The tissue chamber is cylindrical with an internal volume of 21 μl. The top plate with the drilled holes was then thermally bonded onto the etched bottom plate in a furnace at 590 °C for 3 h. The bonding temperature for B-270 must be above the transition (or transformation) temperature of 520 degrees, but below the softening point of 710 degrees. Above the transition temp the glass starts to become "rubbery", allowing two plates to be bonded, as they will be soft enough to press into each other slightly (hence the fact two distinct layers in a bonded chip). Above the softening temperature, the glass is essentially molten and therefore is not suitable for bonding.

The microfluidic system used during the study comprised of the glass device, Teflon tubing, incubator and hydrodynamic pumps. The microfluidic device was fitted with a microport fitting (Anachem, UK) that was attached to the surface of the top 3 mm glass layer. This was in order to seal the circular tissue cavity using an English threaded adapter (Anachem, UK). The adapter was

filled with PDMS (Dow Corning, UK) to allow gaseous exchange to occur as shown in Figure 22.(142)

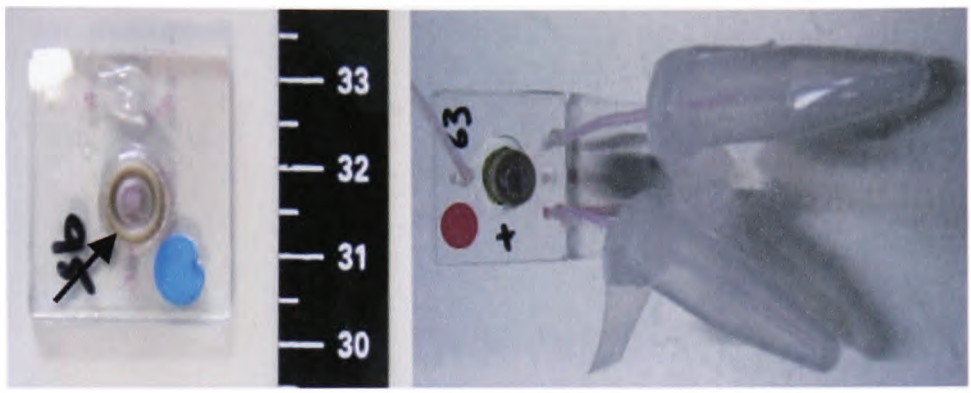

Figure 22. Images of the microfluidic devices with and without the bungs. In the image on the left, tissue can be seen in the tissue chamber, as indicated by the arrow. In the image on the right, media is collected in two individual 1.5 ml microcentrifuge tubes for later analysis.

A Baby Bee syringe pump (Bioanalytical Systems Inc., UK) was connected to the device *via* 1/16" Tefzel tubing (Anachem, UK), this was subsequently upgraded to a Harvard PhD 2000 syringe pump (Harvard, UK) for more precise measurements with the tubing changed to 0.8 mm ID x 1.58 OD TFE Teflon® tubing due to the latter's greater flexibility. The length of the tubing from 1-20 ml syringe (BD™, UK) to the device was 30 cm and outlet tubing was 8 cm long as shown in Figure 22. In between the syringe and the tubing, a 0.22 μm filter was fitted; this reduced the possibility of bacterial and particulate contamination as well as minimising the occurrence of bubbles into the device. A 1.5 ml polypropylene centrifuge tube, with a hole in the lid covered with parafilm to stop contamination and leakage, was placed on the end of each outlet tubing to collect eluent as shown in Figure 23. The entire system, except the pumps, was placed in an egg incubator at 37^0C.

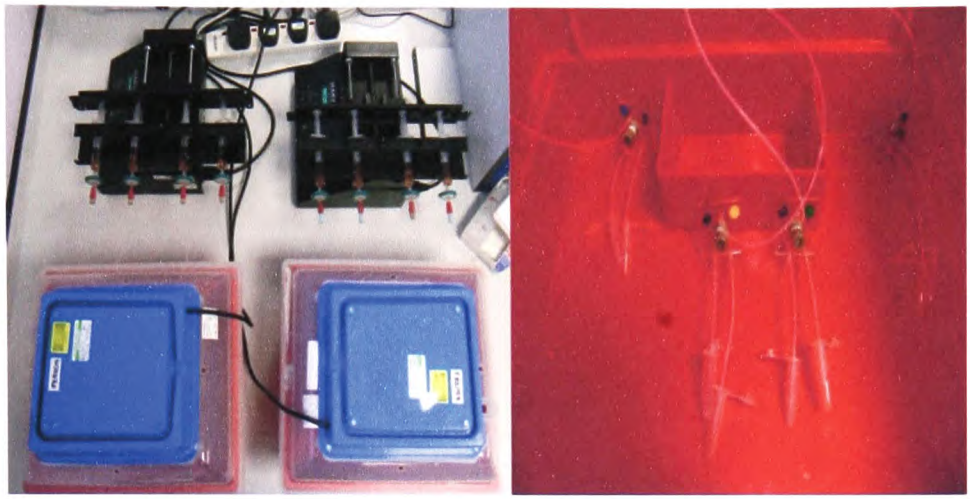

Figure 23. Images of the microfluidic systems. Left: each pump connected to four different individual devices; Right, inside one incubator.

3.2 Tissue Harvesting

Wistar Rats, obtained from B&K Universal Ltd, were used for all experiments. All animals had free access to food and water until being anaesthetized. The animals killed using Schedule 1 of the Animals (Scientific Procedures) Act 1986 and were anaesthetized (10 ml kg^{-1} of 10mM sodium thiopentone, intraperitaneal) before undergoing a total hepatectomy. Liver biopsies were used immediately or frozen as described below.

3.3 Materials

All chemicals and reagents were supplied from Sigma, UK and were of tissue culture or molecular grade as appropriate unless otherwise attributed.

3.4 Preparation and cryopreservation of tissue samples

Due to the inherent wastage from using fresh samples for every experiment, cryopreservation for subsequent use was imperative. Two methods of cryopreservation were tested. The first approach was rapid freezing without cryoprotectant, where the sections were rapidly placed into 1 ml cryovials (Alpha Laboratories, Hampshire) that were immediately plunged into a Dewar of liquid nitrogen for 2 minutes before being transferred into a -80°C freezer for long term storage. The second approach was vitrification.

Vitrification is the solidification of a liquid not produced by crystallization but by a radical increase in viscosity, so the solution becomes glassy and cell damage by ice crystal formation is impeded.(273) A fluid can be effectively vitrified during this process if the cooling rates employed are higher than the critical cooling rate (v_{crc}); the formation of ice-crystals has been shown to be low.(274) Prevention of devitrification by using warming rates above the critical warming rate of the fluid (v_{crw}) stops ice-growth formation in the nuclei of the cells on thawing. In order to achieve vitrification, a high concentration of cryoprotectant (18% (v/v)) Dimethyl sulfoxide (DMSO), $(CH_3)_2SO$, was used.

Williams Media E (WME) was set on ice and 18% (v/v) DMSO was added and left for 10 minutes. Into individual cryovials, 1 ml of the solution was added and the vials were set into crushed ice, subsequently the liver was cut into samples of approximately 1 cm^3 dimensions and a single sample placed into each of the vials. The vials and tissue were left a further 10 minutes on ice

before being sealed and the vials plunged into liquid nitrogen for approximately 5 minutes after which they were stored at -80 °C until required.

3.4.1 Rewarming and DMSO removal

Liver sections cryopreserved by either method were returned to physiological temperatures by placing the cryovials in an incubator at 37°C until ice crystals were no longer visible in the vial (approximately 1 min). The sections were then removed from the cryogenic media, set in fresh WME in 1.5 ml centrifuge tubes and incubated at 37°C until required. All thawed tissue was used within 60 minutes of being removed from storage. To investigate the action of disaggregation enzymes in a later experiment however, the tissue was cut frozen into 3 mm^3 before being allowed to thaw, in order to visualise the edges of the tissue in Section 3.12.

3.4.2 Morphology Analysis

To visualize cell architecture within the tissue, it was first embedded on a cork tile covered with Tissue-Tek® (Sakura, Netherlands) and plunged immediately in liquid nitrogen cooled 2-methyl butane solution. Frozen sections (12 µm thick) were then cut using a Microm HM505E cryostat. Sections were selected from the centre of the sample and these were stained with Haematoxylin and Eosin (H&E). The sections were then fixed with 10% (v/v) formalin for 10 minutes in a fume cupboard, stained with Delafield's Haematoxylin for 5 minutes before rinsing with running cold tap water. After rinsing for 10 minutes the tissue was dehydrated with sequentially higher concentrations of 25%, 50%, 75%, 85% and 95% (v/v) ethanol over 8 minutes. The tissue was then stained with 100% Eosin for 1 minute before being quickly dipped with 95% (v/v) and absolute

ethanol. The tissue was finally placed in Histoclear for five minutes to remove any excess stain and non-specific stain and then mounted in Depex using a coverslip. The tissue was imaged by light microscopy.

3.4.3 Cryopreservation Results

The aim of this experiment was to determine which method of cryopreservation was appropriate for the banking of liver tissue that would otherwise be lost. Eight liver samples were removed from -80°C after 2 weeks and stained with H&E. Representative results of the different cryopreservation methods are shown in Figure 23. Both images show little effect on cell and tissue morphology. The cords of hepatocytes have remained intact in both procedures with little loss of cytoplasm through shrinkage or ice crystal damage. The cell membranes can be seen in several places, with the hepatocytes preserving their original hexagonal shape. In addition there is minimal to moderate heptocellular dissociation, indicative of disruption of intercellular junctions.(275) Minimal apoptosis was randomly distributed within the parenchyma. Three independent liver biopsies were frozen using the two different methods with twelve sections taken and stained from each biopsy. This gave a total 72 sections that were imaged and analyzed. There have been inconsistent findings regarding hepatocyte viability following storage time. Some researchers state a significant loss of viability and functionality of hepatocytes after cryopreservation. In one study, hepatocyte viability was investigated for the possible transplantation into patients as an alternative to whole liver transplants and the aim was to assess cryopreserved hepatocyte proliferation capacity.(276)

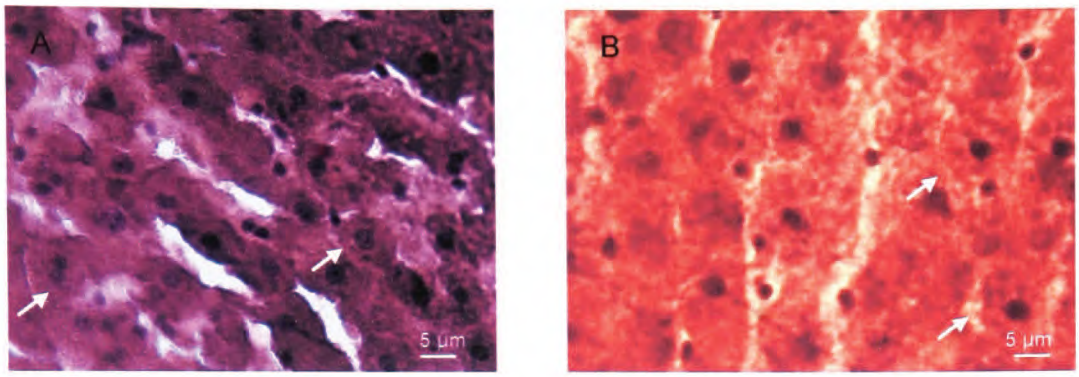

Figure 24. Images of rat liver tissue with H&E staining. The tissue was frozen using two different methods (A) vitrification by incorporating a high percentage of cryoprotectant, 18% (v/v) DMSO, in the storage media. (B) Snap frozen in liquid nitrogen with no cryoprotectant. The tissue was stored at -80°C for 2 weeks before staining and imaging. Arrows indicate cells that still retained the hexagonal shape with membranes intact. There is minimal to moderate heptocellular dissociation. Magnification 40x.

Fresh and frozen/thawed mouse hepatocytes were transferred separately into the livers of recipient mice with transgene-induced liver disease. It showed that after storage for 32 months in liquid nitrogen, cryopreservation decreased hepatocyte viability. The study proved that individual viable frozen/thawed hepatocytes demonstrated clonal replicative potential identical to that of fresh hepatocytes. In a later study, human hepatocytes derived from unused liver segments from transplants showed that after cryopreservation, viability, attachment efficiency, enzyme activity, and albumin production of hepatocytes were all significantly decreased, with lactate dehydrogenase (LDH) leakage significantly increased.(277) The viability and attachment efficiency of cryopreserved hepatocytes isolated from liver resections for tumours were significantly higher, and the LDH leakage significantly lower, than those isolated from all donor tissue. The viability and attachment efficiency of cryopreserved hepatocytes isolated from liver resections for tumours were significantly higher, and the LDH leakage significantly lower, than those isolated from all donor tissue.

Another group also reported that in general, hepatocyte viability decreased appreciably within 60 minutes of thawing.(278) Cells suspended in 5% dextrose lactated Ringers solution (D5LR) however, maintained greater cell viability. Hepatocytes from normal liver donors showed less LDH enzyme leak in comparison with cells from fatty liver donors. Mild hypothermic temperature (32°C) inhibited cellular damage that otherwise significantly increased at 60 min. Hepatocytes did not proliferate until 12 h from thaw, regardless of supernatant or conditions of suspension.

There have been many assertions about the correct method of freezing rates and protocols with equally as many claim for a particular protocol as against it. This can be seen from the number of articles published on different methodologies, which has been accelerating in the last ten years as the push for tissue engineering increases. In the experiments that follow all the tissue used were cryopreserved using snap freezing as it was easy and less time consuming. In some cases, the tissue was over six months old when used in the microfluidic device. Throughout the study there was little variation in the results between the different experiments.

3.5 Determination of tissue viability on cavity slides

To analyse tissue viability and concentration of fluorescent probe before placing in a microfluidic device, liver samples were analyzed on cavity slides.

The tissue biopsies were cut into approximately 3 mm^3 sections. The samples were placed on separate cavity slides and covered with 20 µl of WME. Cell viability was evaluated using Calcein-aceyloxylmethyl ester (Calcein AM) and Propidium Iodide (PI). Calcein AM is modified carboxylic acid with an additional ester group that allows entry through the plasma membrane of a cell, when hydrolyzed within a viable cell, it becomes a membrane impermeant carboxylate which fluoresces as shown in Figure 25.(279)

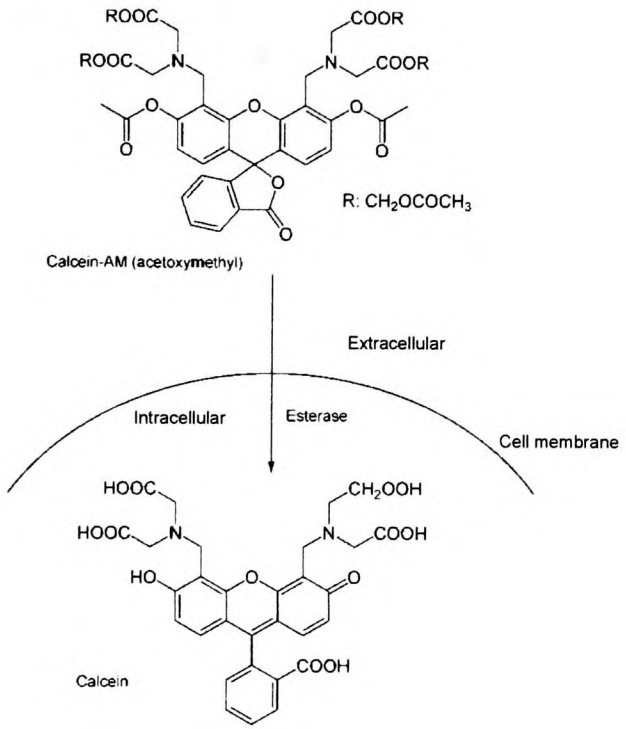

Figure 25. Image of Calcein AM metabolism in the cell. Calcein AM is a non-fluorescent, electrically neutral, non-polar analogue of fluorescein diacetate, which passively crosses cell membranes and is cleaved to a fluorescent derivative by non-specific intracellular esterases. Once cleaved in viable cells, the resultant fluorescent salts are retained by intact cell membranes. Image taken from Molecular Probes.

PI enters cells with disrupted plasma membranes and intercalates with the DNA making non-viable cells fluorescent.(280) The structure of PI is shown in Figure 26. PI is impermeant to viable cells; fluorescence is therefore inversely correlated with cell viability. Consequently, both probes are useful for measuring parameters of cell viability *via* complementary mechanisms.

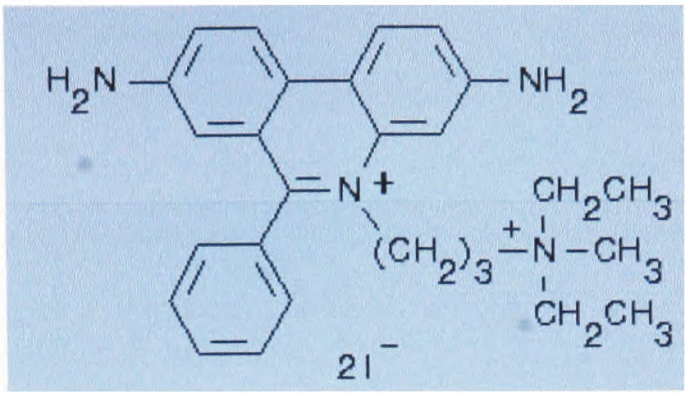

Figure 26. The structure of Propidium Iodide from Molecular Probes

Each tissue biopsy was first incubated with 50 µL of 10 µM Calcein AM (Invitrogen, UK) in phosphate buffered saline (PBS) for forty minutes. This time period allows for the cells in the tissue to take up and cleave relatively large amounts of calcein probe. The liquid was subsequently removed by pipette and replaced with PBS to remove any excess probe; this was repeated thrice. The tissue was subsequently incubated with 50 µL of 3.75 mM PI in PBS for ten minutes. The PI stain was removed and the tissue washed thrice with PBS. Finally, the tissue was visualised an epi-fluorescent Nikon Eclipse 80i microscope (Nikon, Japan) employing 10x Plan Fluor (0.30 NA) objective and 4x Plan Fluor (0.13 NA) objectives. The following excitation and emission wavelengths were used: for Calcein (λex = 494, λem = 517nm) and for PI (λex = 536, λem = 617nm). Images of the tissue samples were recorded using Hamamatsu orca ER camera and analysed using Metaview 6.1 image processing computer software.

3.5.1 Analysis of tissue viability on cavity slides

On examination of the tissue under epi-fluorescent microscopy, the native tissue was verified to be non-fluorescent. The liver tissue was incubated with

Calcein AM and PI separately and consecutively to verify areas of live/dead liver cells. Higher incidence of fluorescence from the calcein indicates the viability of the cells; i.e. healthy cells actively metabolize more probe than cells, which are dying as shown in Figure 27.

Figure 27. Image taken of the periphery of the liver tissue on a cavity slide using epi-fluorescent microscopy. The fluorescence of the tissue is caused by the retention of fluorescent probe, calcein, in the cytosol of the individual cells. Some of the structual organisation of the tissue can be observed, as indicated by arrows, known as Space of Disse. Focus is blurred due to the undulations of the tissue. Magnification 10x

The primary area of dead cells stained with PI was determined to be around the periphery of the tissue where the area was cut to allow the placement of the tissue on the cavity slides, as shown in Figure 28. This experiment was repeated ten times on ten different liver samples.

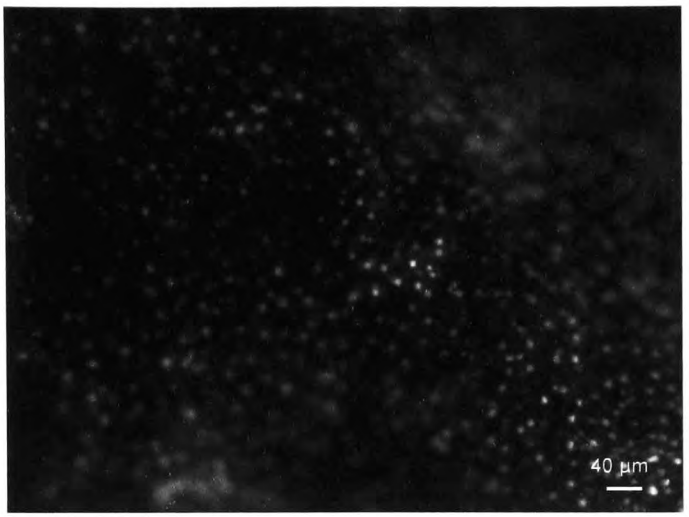

Figure 28. Epi-fluorescent image of cells on the surface of rat liver sample exhibiting nuclei staining from propidium iodide (PI) on a cavity slide. The spots of fluoresence are from PI intercalating with DNA in the nuclei of dead cells. Cells are in and out of focus due to the morphology of the liver surface. Magnification 10x

3.6 Determination of cell death in liver tissue on cavity slides using fluorescent probes and hydrogen peroxide

To determine cell death in the liver tissue and the time frame for cell death to occur, hydrogen peroxide was used. This analysis would specify the parameters required to envoke cell death when interrogating the tissue in the microfluidic device. Hydrogen peroxide (H_2O_2) is a ROS, which induces apoptosis via several cell signalling pathways as shown in Figure 29.(281) H_2O_2 is the first product from the conversion of the superoxide anion radical ($O_2^{\cdot-}$) by superoxide dismutase enzyme or by spontaneous disproportionation. H_2O_2 damages cells through the production of the extraordinarily powerful oxidant, hydroxyl ($^{\cdot}OH$) radical. Free radicals are atoms, molecules, or ions with unpaired elections in an open shell configuration. An oxidant is a chemical that readily transfers oxygen atoms or a substance that gains an electron(s) in a redox reaction. An antioxidant is a molecule capable of inhibiting the oxidation of other molecules.

In hepatocytes, this production is enhanced by the metal cation Fe (II) that is stored within the cell from erythropoiesis.(282) These free radicals cause extensive damage to cellular membranes leading to cell dysfunction and death. Therefore, the disposal of H_2O_2 by peroxidases and catalase-catalyzed reactions to O_2 and $2H_2O$, is critical to prevent the accumulation of such radicals. Liver tissue, approximately 3 mm^3 was set in cavity slides and was treated with the probes as indicated in previous section to highlight cell viability and death before interrogation.

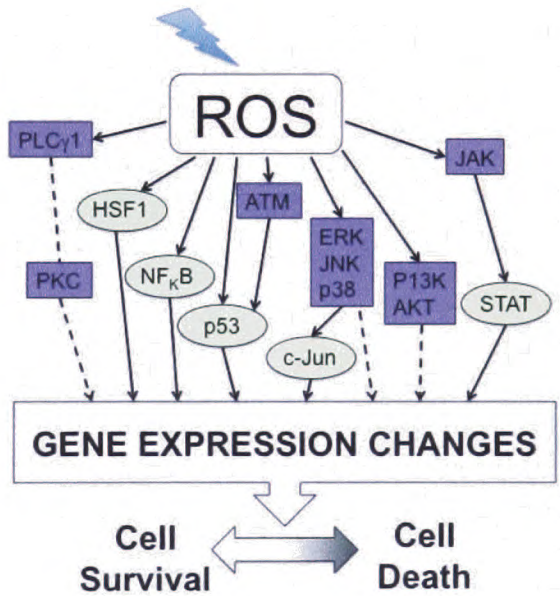

Figure 29. Oxidative stress activates numerous signalling pathways. Reactive oxygen species (ROS) are highly reactive and can directly or indirectly modulate the functions of many enzymes (boxes) and transcription factors (ovals) through a multitude of signalling cascades. Ultimately these signals result in changes in gene expression, which influences apoptosis mechanisms. The magnitude and duration of the stress in combination with the cell type involved are significant factors in the determination of which pathways are activated and the ultimate cellular outcome. ATM, ataxia-telangectasia mutated; ERK, extracellular signal-regulated kinases; HSF1, heat shock transcription factor 1; JAK, Janus protein kinase; JNK, c-Jun N-terminal kinases; NF_KB, nuclear factor $_KB$, P13K, phosphoninositide 3-kinase; PKC, protein kinase C, PLC-γ1, phospholipase C-γ1; STAT, signal transducers and activators of transcription.

The tissue was then interrogated with 50 µl aliquots of H_2O_2 in concentrations of

50 μM, 0.5 mM, and 10 mM in distilled water for 5, 10, 20, 30, 60 minutes. These concentrations were chosen because they had been used by other groups(283, 284) investigating apoptosis in various cell types and would allow the comparison of results when applied to tissue. The tissue was washed three times with PBS to remove any residual reagent as described earlier. The tissue was examined via epi-fluorescent microscopy with 10 x magnification then subsequently 'reinterrogated' with Calcein AM and PI probes, as described earlier, and re-examined with epi-fluorescent microscopy. All concentrations were duplicated on separate cavity slides with individual liver samples. This experiment was repeated three times.

3.6.1 Cell death within liver tissue on cavity slides after interrogation with H_2O_2

The aim of these experiments was to determine the concentration of H_2O_2 needed to kill liver cells in the tissue sample. A series of H_2O_2 concentrations were used to induce apoptosis in the cells of the tissue, as indicated in the methodology. Cell death was determined by the loss of calcein fluorescence in the cytosol and the increase of PI fluorescence in the nuclei of dead cells as determined by epi-fluorescent microscopy. After five minutes, oxygen bubbles began to form on the tissue surface, which increased in size and number with time and H_2O_2 concentration. It is most likely that oxygen formation was due to the cells' antioxidant enzyme, catalase, decomposing the H_2O_2 to O_2 and H_2O. Catalase is ubiquitously found in all mammalian cells with its highest activity found in liver and kidney cells.(285) After incubation with H_2O_2 but before the addition of the fluorescent probes, the tissue was examined visually and epi-fluorescent microscopy. Under visual examination the tissue appeared

bleached. The tissue was imaged before the addition of further probe and depletion of the calcein fluorescence, with no discernible change of the PI fluorescence was noted within all tissue specimens. This was true for all the H_2O_2 concentrations in the initial inspection by epi-fluorescence microscopy. However, there was a total cessation of fluorescence from calcein in the tissue treated with 10 mM H_2O_2 indicating cell death in the sample. Following the reapplication of calcein AM and PI however the calcein fluorescence was returned. This was a problem when distinguishing areas of cell death after the reapplication of the probes. This was thought to be due to the retained probe in the viable cells underneath the dead cells. Cells on the surface of the tissue were the first to be exposed to H_2O_2 and underwent oxidative stress and subsequent cell death. Cells beneath the surface layer of cells were only exposed to H_2O_2 after it flowed through the gaps in the tissue through diffusion. The H_2O_2 concentration determined the depth of cell death in the sample as cells on the periphery would come in contact first and use catalase to neutralize the chemical prior to any contact with underlying cells.

Epi-fluorescent microscopy did not allow the discrimination between cell layers in the tissue. It was impossible to determine the effectiveness of the H_2O_2 concentration and the length of time needed to cause apoptosis or necrosis due to the underlying fluorescence from the cells underneath those that were subjected to the interrogation.

3.7 Determination of oxygen within microfluidic system using ruthenium tris (2,2'-dipyridyl) dichloride hexahydrate

Before studying the responses of the *ex vivo* explants under a simulated physiological microenvironment, it was necessary to investigate the chamber environment to ensure that there is sufficient distribution of nutrients, oxygen and temperature. Dissolved oxygen (DO) is a paramount concern when culturing cells and tissue. Solubility of oxygen in the media is relatively low (7 mg/l at 37°C) making it vital that fresh supplies are maintained and supplied.(286) PDMS at 25°C has a relatively high diffusivity D = 3.55 x 10^{-5} cm^2 /s, which is advantageous for cell-based applications.(287) Thus the passive gas exchange of oxygen through PDMS is adequate for supplying the required amounts of oxygen for mammalian cell cultures that have moderate oxygen uptake rates.(288) Through the uptake of oxygen by the cells, DO levels drop leading to the formation of oxygen concentration gradients and hypoxia. When this occurs within tissue the cells in the centre, where oxygen is relatively low, they produce paracrine signals to the surrounding cells such as Hypoxia Inducible Factor-1 (HIF-1), which is a key regulator of cellular adjustment to oxygen deprivation. This signal acts as a survival factor of hypoxic cells, primarily by activating transcription of genes involved in angiogenesis, glycolytic metabolism and oxygen consumption.(289) If critically low oxygen concentrations at the centre of the tissue persist, cell proliferation rate decreases and ultimately, these interior cells die off creating a necrotic core.(290) To study the issue of oxygen supply in the microfluidic environment, an optical-based method was used. Fluorescent probes are suitable for the small geometries and volumes associated with these devices, as they do not

expend oxygen during measurement, are relatively non-harmful to cell functions and are suitable for temporal studies.

Oxygen fluorescent imaging studies on cell-based microfluidic applications using ruthenium tris (2,2'-dipyridyl) dichloride hexahydrate (RTDP) have been documented.(291, 292) RTDP relies on fluorescence quenching; this is a physical mechanism resulting in a decrease of fluorescence from a fluorophore. Collisional quenching of fluorescence relates to a process whereupon an excited fluorophore is de-excited, non-radioactively, to its ground state due to physical contact (collisions) with an agent (quencher). Oxygen has been found to be an effective collisional quencher of nearly all fluorophores.(293) Collisional quenching decreases the fluorophore quantum yield (the ratio of emitted fluorescence photons to adsorbed excitation photons) causing a reduction in emitted fluorescence intensity, in addition to the fluorophore excited-state lifetime.

The relationship between fluorescence intensity (or lifetime) and dissolved oxygen concentration is described by the Stern-Volmer equation(291):

$$I_o / I = 1 + K_q [O_2] \text{ or } \tau_o / \tau = 1 + K_q [O_2]$$

Equation 6

where I_o or τ_o is the uninhibited sensor dye intensity or lifetime (i.e. 0% oxygen), I or τ is the sensor dye intensity or lifetime at oxygen level $[O_2]$ and K_q is the Stern-Volmer quenching constant.

To determine the maximum and minimum fluorescent signals from deoxygenated and oxygenated media two bungs were used in the device, one filled with epoxy resin, which is gas impermeable, and one containing gas permeable PDMS. Polypropylene tubes were filled with 1.5 ml WME media containing 1 mg ml^{-1} RTDP were sonicated for 15 minutes. To ensure that no oxygen was remaining, nitrogen gas was bubbled through for 5 minutes. Conversely, oxygen gas was bubbled through a second sample of WME for 10 minutes to give positive oxygenated sample of media. A 1 ml syringe was filled with either the oxygenated or deoxygenated media and put on the microfluidic system. The device was sealed with a resin filled bung and the media pumped through at 20 µl min^{-1} until media had flowed through the outlets. The speed of the media was then decreased to 2 µl min^{-1} and left to flow for 10 minutes before images were taken.

To determine the amount of dissolved oxygen in the media sample under different flow conditions, a 1 ml syringe was filled with ungassed WME with 1 mg ml^{-1} RTDP and put on the microfluidic system. The microfluidic device was sealed with the PDMS bung with the media pumped through at 20 µl min^{-1} until it had flowed through the outlets. The speed of the media was then decreased to 2 µl min^{-1} and left to flow for ten minutes before imaging. The device was then flushed using deionised water to remove all media traces for the next sample. This procedure was repeated for 5 and 10 µl min^{-1} flow rates. These flow rates were chosen as they closely replicate *in vivo* flow rates found in interstitial fluid.(294, 295)

A Zeiss Axiovert S100 inverted Epi-florescent microscope fitted with 4x objective was used to measure the intensity of the RTDP dye in the tissue chamber. Images were recorded using a CCD camera and subsequently analysed using Image J computer imaging analysis software (National Institutes of Health, US). The fluorescent images were taken at an exposure time of 0.1 s for each observation and the chamber was imaged three times in rapid succession for each condition.

3.7.1 Analysis of dissolved oxygen in microfluidic tissue chamber

After testing a range of concentrations of the RTDP from 0.1 mg ml^{-1} to 1.0 mg ml^{-1} in a deoxygenated media, it was found that 1.0 mg ml^{-1} give the best fluorescent image within the channels and the chamber. Consequently, all experiments were carried out using this concentration. The intensity and lifetime of the fluorescent signal was observed in the chamber and the channels leading to and from it for the intensity at zero oxygen content, as shown in Figure 30. The positive control, used media perfused with oxygen for the observed intensity at the three different locations at high oxygen content. The observed average intensities of the chamber deoxygenated samples were 238 ± 20 AU and the oxygenated samples were 83 ± 14 AU. These were calculated from three experimental repeats for each sample. By using the Stern-Volmer equation, this corresponds to 708 μM of dissolved oxygen in the oxygenated media in the microfluidic device, as demonstrated in previous fluorescent oxygen detection studies.(296) It was determined by visual and graphically analysis, as shown in Figures 30 and 31, that oxygen was diffusing through the PDMS bung into the untreated media in the tissue chamber at the experimental flow conditions. DO levels in the whole chamber at 2 μL min^{-1} were 279 μM; at 5

$\mu L\ min^{-1}$ were 187 μM; and at 10 $\mu L\ min^{-1}$ were 118 μM. These DO levels are within the venous to arterial range (90 - 260 μM) found *in vivo*.(296) The media in all the flow experiments was not pre-oxygenated and the device was placed within an egg incubator, which while maintaining the temperature did not have any additional gaseous support. Indeed the movement of air achieved in the incubator was by means of vents and fans allowing fresh atmospheric air to be continuously circulated into and around the incubator and the microfluidic devices. Usual cell based methodology grow culture in incubators that provide 5% carbon dioxide (CO_2) into a humidified atmosphere of the interior of the incubator. This is because most media contain buffers that require a CO_2 atmosphere. Severe pH shifts, media becomes acidic, can occur if adequate CO_2 levels are not maintained.

The media used in the current studies were WME and Dulbecco's modified Eagle's medium (DMEM). WME and DMEM use phenol red as a pH indicator. The colour of phenol red gradually changes from yellow to red over the pH range of 6.8 to 8.2 and is routinely used in cell culture. When cells are necrotic, cell products will cause a pH change, which is due to the acidification of the media, turning this from pink to yellow.(297) A similar colour change can also occur when the culture is overgrown with a bacterial contamination. Cell biologists use the indicator within media as an expedient way to quickly confirm the health of tissue culture. In addition, waste products produced by mammalian cells will slowly decrease the pH if accumulation occurs.(298) In this study, no changes of pH from the media indicators by eye were recorded in any of the experiments.

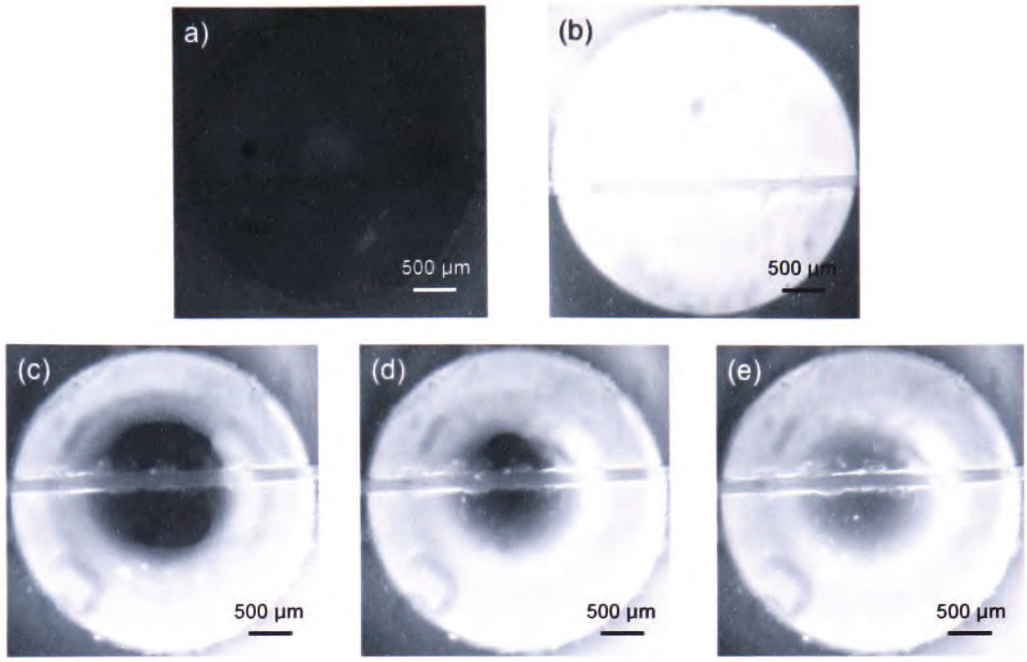

Figure 30. Epi-fluorescent images of microfluidic tissue chamber showing oxygenation of the media using RTDP probe (A-E). Using the oxygen reactive fluorescent probe ruthenium tris (2,2'-dipyridyl) dichloride hexahydrate (RTDP) images were taken of the 3 mm diameter tissue chamber to determine dissolved oxygen content within different flow conditions. Images show the chamber filled with Williams Media E (WME) incorporating 1 mg ml^{-1} RTDP (A) oxygenated sample (no fluorescent signal) (B) deoxygenated sample (C) ungassed WME media flowing at 2 ml min^{-1} (D) ungassed WME media flowing at 5 ml min^{-1} (E) ungassed WME media flowing at 10 ml min^{-1}.

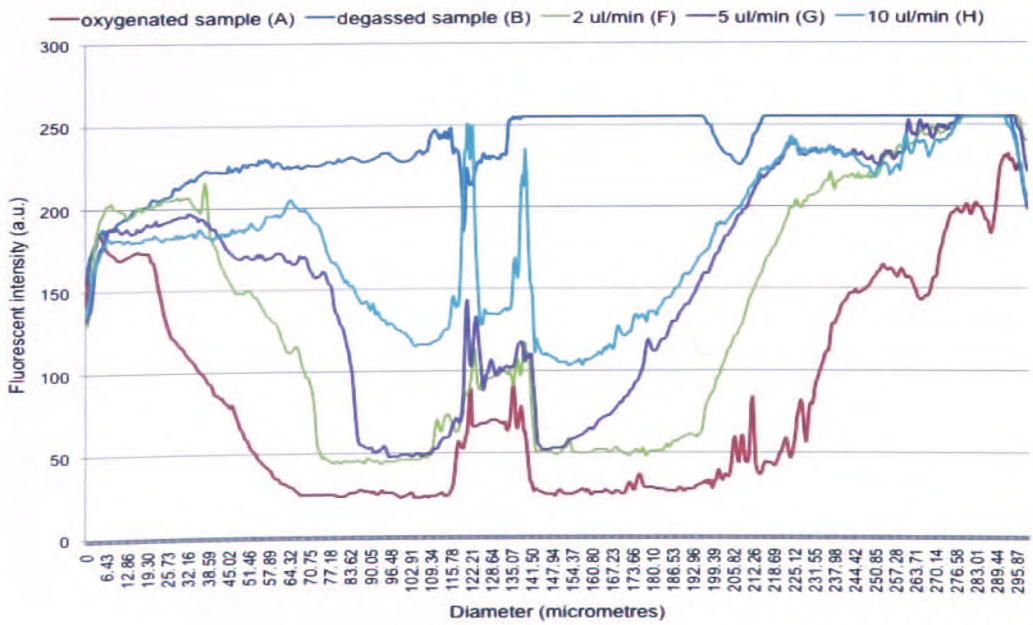

Figure 31. Comparisons of the fluorescent intensities of the oxygenated sample and untreated media in the tissue chamber shown in Figure 29 presented graphically from which all the calculations and analysis were drawn.

3.8 Determination of flow profiles in channels and chamber

The first stage in investigating the use of microfluidics to interrogate tissue was to determine the flow profiles within the microfluidic device. Two parallel laminar flows allow the modification of the microenvironment of a single tissue sample within the same experiment. When using multiple laminar flows for interrogation, it is important to determine flow within the chamber to establish the position of the interface between two or more flows over a tissue specimen. The interface in these microfluidic experiments needs to be aligned approximately over the middle of the tissue to allow for a reagent to be effectively measured against its equivalent control section. If the reagent containing stream covers too much of the specimen, it will be difficult to analyse the impact on the cells as there will be insufficient native tissue to compare it with and *vice versa*. In these experiments, the two split microchannels were used as inlets as illustrated in Figure 21 and the single channel was used as the outlet. To visualise the different flows, one stream contained only PBS and the other PBS and 10 mM rhodamine solution. A range of flow rates, 2 - 20 $\mu l\ min^{-1}$, were investigated to analyse the flow profile in the chamber. The rates of both flows were independently controllable.

3.8.1 Analysis of flow regimes within the microfluidic device

To determine the position of the interface of the two laminar flows, images were taken of the microfluidic channels and chamber as shown in Figure 32. Determining flow within the chamber is important for establishing the position of the interface between two or more flows over a tissue specimen. Laminar flow was achieved in the main channel as shown in Figures 32A and 32B. However, problems became evident when the flows entered the chamber. The fluorescent

probe seemed to pool near the entry point as demonstrated in Figure 32C and 32D. Changes in flow rate in one stream had no effect on the phenomena as shown in Figure 32D. The experiments were repeated using different flow rates over a period of a month and the problems with the probe pooling in the chamber were repeated with every experiment. These problems where thought to be from backpressure caused by the outlet microchannel having the same dimensions as the two-inlet channels.

3.9 Determination of tissue viability in microfluidic device using fluorescent probes

Before the tissue was placed in the system, the system was sterilized by the passage of 70% (v/v) ethanol for twenty minutes at 10 μl min^{-1}. Autoclaved for 5 minutes before the experiment was commenced. The PDMS bung was removed and the flow rate was then raised to 20 μl min^{-1} in order to quickly fill the tissue chamber before the addition of the tissue. When the chamber was full, the flow rate was reduced to 10 μl min^{-1}. During this preparation time, the tissue was cut into approximately 3 mm^3 sections and weighed on a four place analytical balance. Tissue samples between 5 and 10 mg were selected for experimental use and placed in the tissue chamber. The chamber was then sealed using the PDMS bung. Two 1 ml syringes containing 10 µM calcein AM in WME were fitted to the outlets of the device and the flow continued at 2 µl min^{-1} for increasing amounts of time up to one hour, recommended by the manufactures, to determine diffusion profile into the tissue. This flow rate was chosen as it displays had the highest concentration of DO entering the media

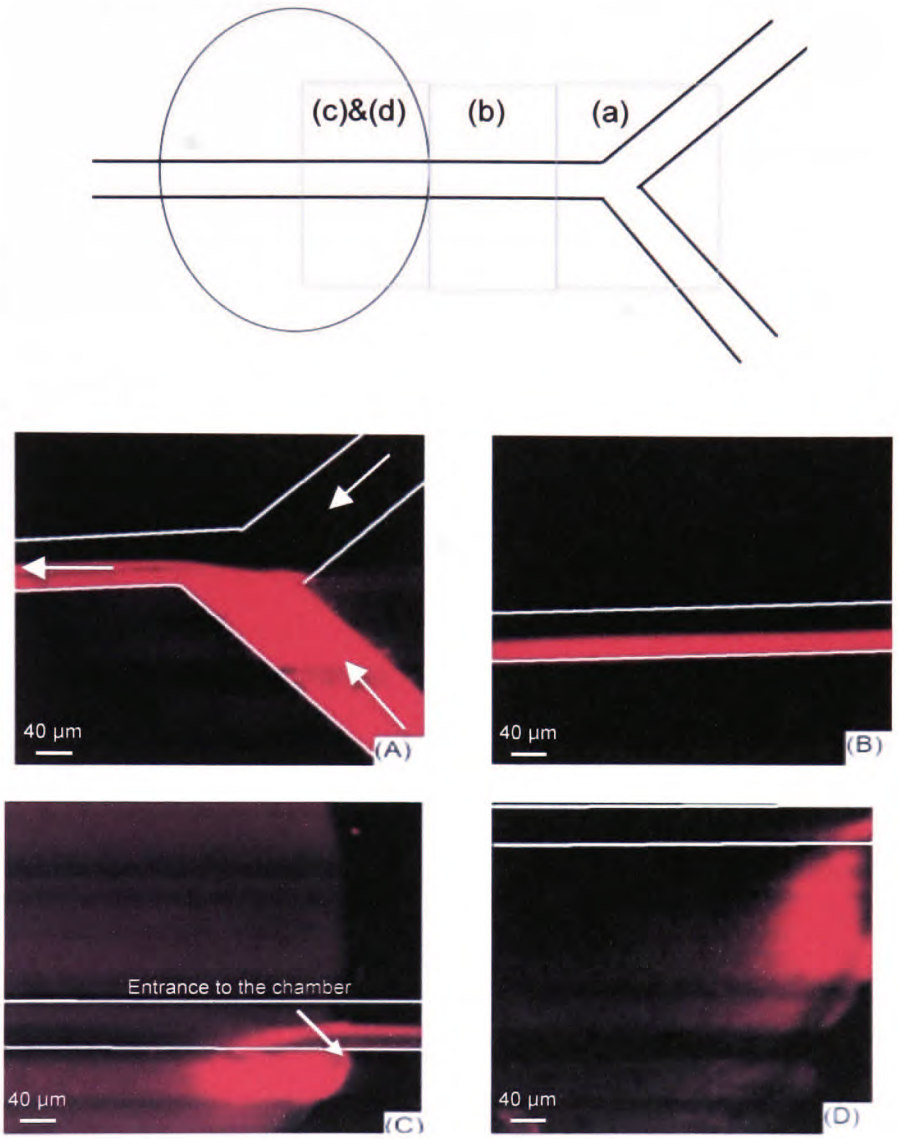

Figure 32. Flow dynamics in the microchannels and the chamber. (A) The intersection of the two inlet microchannels into the main channel. 10 mM rhodamine solution is in the bottom channel and PBS is flowing in the top channel at 10 µl min^{-1}. (B) Laminar flow in the main channel before entrance of the chamber. Both flow rates are equal and the interface between the two streams is in the centre of the channel. (C) Shows the entrance of the chamber with the main channel. The flow rates of both streams are 10 µl min^{-1}. The two flow rates in (D) are as follows; 10 mM rhodamine solution flow is at 3 µl min^{-1} and PBS flow is at 15 µl min^{-1}. Magnification 10 x, (n=30)

through the bung as described in a Section 3.7.1. After this time period, the flow was stopped and the syringes containing PBS were refitted on the system and flow reinstated for increasing amounts of time up to twenty minutes, recommended by the manufactures. A syringe containing 3.75 mM PI was then

installed on to the system and left for twenty minutes to run at 2 µl min^{-1}. A PBS wash of the tissue followed in the same manner as described after the addition of calcein AM. The tissue containing microfluidic chamber was analysed using confocal microscopy, as epi-fluorescent microscopy would not give sufficient detail for analysis due to its inability to 'analyse fluorescence in focal planes within the tissue. The PBS was replaced with WME overnight with the flow rate unchanged. The media was collected overnight, approximately 18 hours, outside the incubator in 15 ml tubes sealed with cling film with a hole inserted to allow the passage of the tubing into the tube. Imaging of the tissue was then repeated after twenty-two hours, after leaving overnight, to determine any changes in tissue viability over time.

3.9.1 Confocal imaging

To understand the complex interactions between cells and their environment it is important to be able to examine cells free of possible damaging or inaccurate artefacts. However, the main problem is to achieve this without causing significant disturbance to the cells or tissue by the experimentation and analysis methods. The optical sectioning facility of the confocal microscope allows visualization of thin sections of intact cells, microns (<200 nm) below the surface the sample.(299) In doing so, possible surface contaminants can be optically removed and the underlying cells can be examined.

The confocal imaging techniques used in this study were: Time-Lapse fluorescence imaging, multi-channel time-lapse imaging, three dimensional time-lapse (4D) imaging, three dimensional multi-channel (5D) and time-lapse

fluorescence imaging. These techniques were achieved by the use of a spectral laser-scanning confocal microscope Nikon Eclipse TE2000-E (Nikon, Japan) equipped with Helium/Neon and Argon laser and images were visualised using Lazershop 2000 software. Scanning resolution was 1024 x 1024; 4x and 10x objectives were used for visualisation.

Time-lapse fluorescence imaging entails repeated imaging of fluorescently labelled samples at specific time instances.(300, 301) This procedure can involve different spatial dimensions: repeated line scans, repeated imaging of a single focal plane, and repeated imaging in multiple focal planes within a 200 nm thick specimen. Multi-channel time-lapse fluorescence imaging includes all of the time-lapse fluorescent imaging with the additional use of different probes with different spectral properties. This attribute allows for multi-labelling of cellular structures simultaneously.(302) Three-dimensional time-lapse (4D) imaging involves the repetitive compilation of *z*-series stacks of images over time. This allows the researcher to analyse how far a probe has penetrated a cell or tissue specimen over time,(303) three dimensional multi-channel (5D) time-lapse fluorescence imaging is when this is done over time.

3.9.2 Confocal microscopy analysis of the viability of liver tissue in microfluidic device

The objective of these experiments was to verify the viability of the tissue in the microfluidic device using fluorescent probes and confocal microscopy and whether viability is sustained over time. As with the cavity slides and epi-fluorescent microscopy experiments, the tissue was incubated with calcein AM

and PI separately and consecutively to verify areas of live/dead liver cells in the liver tissue. Calcein fluorescence can be seen across the tissue as well as the periphery after one hour of probing as seen with the previous experiment with the tissue on the cavity slides indicating cells are actively metabolizing the probe as shown in Figure 33A.

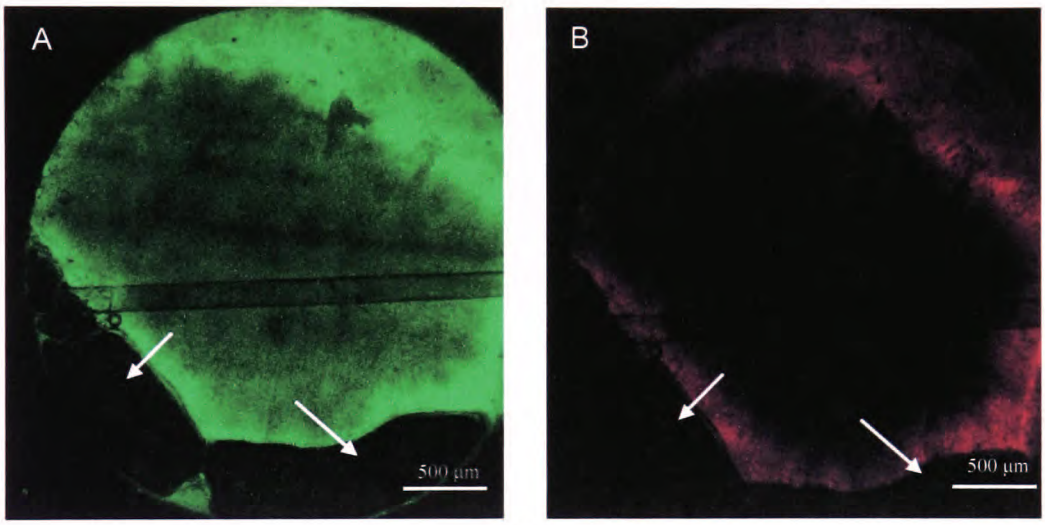

Figure 33. Confocal images of rat liver tissue in microfluidic chamber after incubation with (A) calcein AM for over 1 hour, there is a high incidence of fluorescence in the tissue which demonstrates viability. The tissue has filled the entire chamber however, as evident from this image there are small bubbles trapped with the tissue (illustrated by arrows). (B) PI for over 20 minutes, there is a high incidence of fluorescence around the periphery of the tissue indicating cell death in these areas. The images were taken from below the tissue chamber through the 1 mm base plate and taken approximately 200 nm into the tissue. Magnification 4 x and the resolution was 1048 X 1048. Representative of over 200 images.

The primary area of dead cells, where PI had entered and intercalated with the DNA, was determined to be around the periphery of the tissue where the area had been cut to allow the placement of the tissue in the microfluidic device as shown in Figure 33B. These experiments were repeated 120 times over six months and these images are representative of those results. No PI was seen in any of the centres of the samples in any of the experiments even

after lengthening the exposure time to up to an hour, this was further verified when the samples were sectioned and stained in Section 3.10.1

The system was removed from the confocal platform and the tissue returned to physiological temperatures and left for twenty-two hours with WME flowing through the system overnight and collected. No evidence of contamination or pH change was seen in the collected media.

The tissue was then reimaged after the re-application of fresh probe to distinguish areas of viability and cell death. As seen by the image shown in Figure 34A, the tissue had remained viable during the incubation period of twenty-two hours. However, as seen in Figure 34B, although some PI fluorescence can be determined, cell death once again is limited to the edges of the tissue. This experiment was repeated three times.

These images show that liver tissue can be probed with different probes to visualize areas of cell viability and death. It has also been proved that by using fluorescent probes it is possible to verify viability of the tissue after twenty-two hours. However, it should be noted that the probes used in these experiments are transported by diffusion and that areas of little or no fluorescence could be due to limited penetration of probes to those areas of the tissue, which is 3 mm thick as stated earlier.

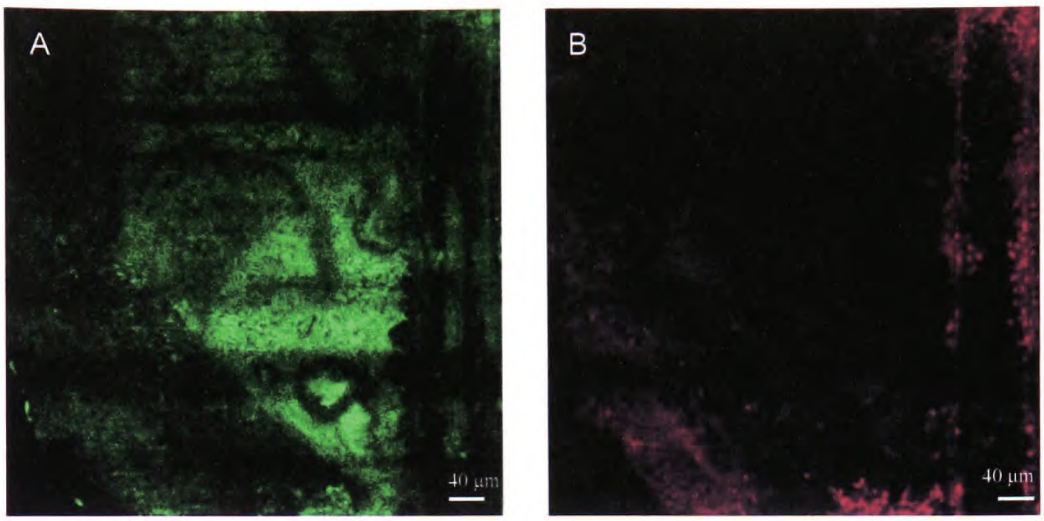

Figure 34. Images of rat liver tissue after twenty-two hours in the microfluidic system. (A)The tissue was reprobed with calcein AM for 1 hour before the image was taken. Due to the diffuse green fluorescence, the tissue is viable and healthy. (B) The tissue shows areas of cell death still around the periphery of the tissue but areas are showing no fluorescent signal indicating no cell death. Magnification 10 x and the resolution was 1048 X 1048. Representative of 50 images.

3.10 Morphological examination of tissue after microfluidic maintenance

It is important that the morphology and architecture of the liver tissue and the ECM is not destroyed during culture within the microfluidic system. The tissue was analyzed using epi-fluorescence and histology. In these sets of experiments, the calcein AM was replaced with LavaCell™ because of reasons explained in Section 4.3.2. Firstly, the tissue was probed with LavaCell™ (Active Motif, UK) to determine areas of viability. LavaCell™ is a naturally occurring compound from the fungus *Epicoccum nigrum* that has be used to fluorescently stain cells.(304) LavaCell™ is a neutral azaphilone (fungal metabolite) molecule that diffuses into live and dead cells staining cell membranes and lipophilic organelles within 2-15 minutes. Unbound probe is non-fluorescent. Limiting the concentration of the probe with the cells determines whether the cells are alive or dead as viable cells are able to store increased amounts of probe more effectively and quicker than non-viable cells.

The tissue was maintained within the microfluidic system as described earlier in Section 3.9. After 70 hours, the WME was removed and replaced with WME containing 10 μM of LavaCell for 30 minutes. The length of time was increased from the recommended amount as the probe is usually used for cell-based methods and time was extended to allow diffusion into the liver tissue. The microfluidic device was then disconnected from the pumps and set on the stage of a Zeiss Axiovert S100 inverted epi-florescent microscope fitted with 10x objective which was used to capture the image of the liver tissue in the tissue chamber. Images were recorded using a Hamamatsu orca ER CCD camera (Hamamatsu Photonics Ltd, UK) and subsequently analysed using HC imaging software (Hamamatsu Photonics Ltd, UK). The following excitation and emission wavelengths were used for LavaCell (λex = 488, λem = 610 nm).

Using the methodology previously described in Section 3.4.2, the tissue was also sectioned and stained using H&E to determine whether any histological changes could be detected.

3.10.1 Morphology analysis of liver tissue

The aim of these experiments was to determine whether liver tissue retained viability after seventy hours of maintenance in the microfluidic device with imaging using Lavacell™ and whether the liver tissue retained the normal *in vivo* architecture using H&E staining. Histomorphology was analyzed before and after liver tissue culture in the microfluidic device as shown in Figure 35. Tissue sections taken through the full depth of samples were analyzed for structural changes. The cell nuclei of the hepatocytes have maintained their

rounded appearance, with little or no shrinkage after 70 hours of culture in a microfluidic device.

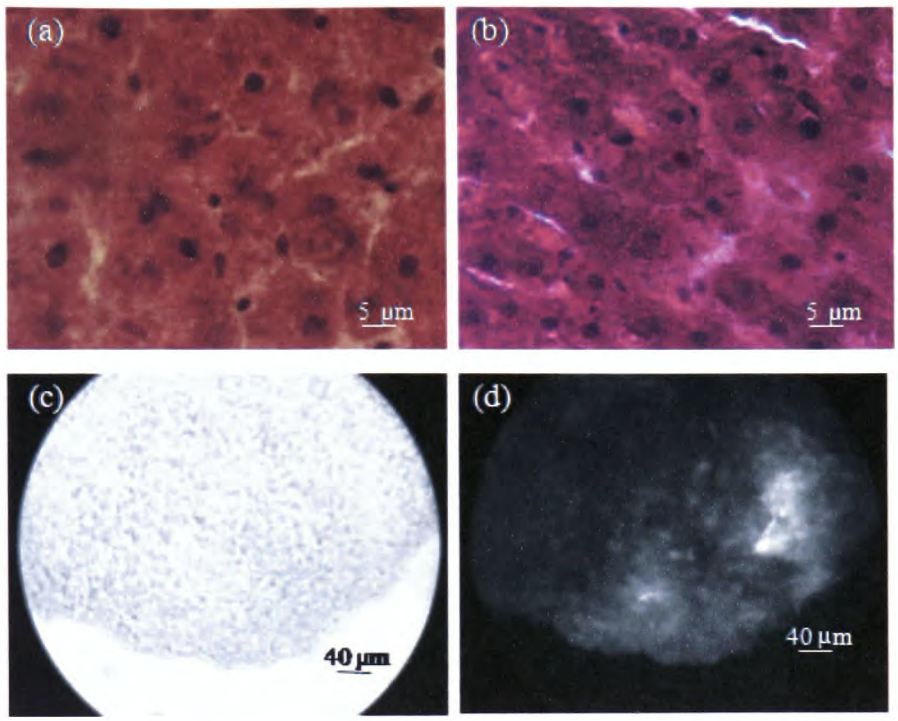

Figure 35. H&E stained cryostat section of tissue before culture in the microfluidic device (a) and after 71 hours (b) using x 40 magnification. Brightfield (c) and epi-fluorescence images (d) of rat liver tissue, after incubation with LavaCell™, following maintenance in a microfluidic device for 53 hours; showing the edge of the tissue distinguished from background. A 40 x objective was used for the histology and 10 x was used for the brightfield and epi-fluorescence microscopy. Representative of nine experiments

The cell membranes can be seen in several places, with the hepatocytes preserving their original hexagonal shape. In addition there is no discernible loss of the ECM between the cells. These results show that the cells within the tissue have retained their *in vivo* morphology with the surrounding ECM remaining intact and indicate that the microenvironment provided in the microfluidic system is sufficient to maintain tissue structural and cellular properties. The experiment was repeated nine times with ~30 sections taken from each sample and 10 slides were analysed with H&E for every experiment.

3.11 Determination of bacterial contamination within the eluent samples

Bacterial contamination of the samples can give results, which reflect the bacterial growth rather than the tissue viability. In order to establish whether the samples were contaminated, eluent was collected for a further hour at the end of every completed experiment before the addition of lysis buffer, when used, and plated on individual antibiotic-free agar plates. Bacterial growth medium (TYG agar) was made in 1.5 L flasks, which had been washed and autoclaved before use. 5 g of yeast extract (OXOID, UK), 10 g tryptone (OXOID, UK), 8 g sodium chloride (Melford Laboratories, UK), 15 g bacterialogical agar were added to the flask and made up to one litre using distilled water. The flask was then stoppered with cotton wool covered with foil and secured in place with autoclave tape. The mixture was stirred using a magnetic stirrer for ten minutes, then autoclaved at 121°C for twenty minutes. The growth medium was allowed to cool to approximately 50°C before being poured into bacterial plates, in the confines of a Level 2 laminar flow cabinet, with enough added (>10 ml) to cover the bottom of the plate with 5 mm thick agar. After the agar was set, the lidded plates were turned upside down to stop condensation and sealed with tape and placed in a 4 °C refrigerator for the maximum of 24 hours before use due to possible contamination from microbes in the refrigerator. The collected media was divided into two and spread on two individual agar plates using a glass spreader within a laminar flow cabinet. Aseptic techniques were used throughout the experiment. These plates were then placed in an incubator and checked at 12 and 24 hours after inoculation for any bacterial growth.

3.11.1 Bacterial contamination analysis of collected eluent

Media that had previously flowed through the microfluidic device was checked at the end of each experiment. Eluent was collected from over 100 microfluidic devices in the study and showed no bacterial contamination at any point. It must be noted that only aerobic bacteria, not anaerobes, were actively screened for, this was because the environment was aerobic by design and the possibility of anaerobe contamination was considered low.

3.12 Disaggregation of tissue to individual cells in microfluidic environment

To analyze individual primary cells isolated from tissue held within the microfluidic device, the tissue was enzymatically disaggregated. The perfusion method, which was modified from Bayliss and Skett,(305) used Eagle's Balanced Salt Solution (EBSS) (Gibco, UK) in place of WME. The disaggregation of cells from the liver explant involved many refinements in enzyme such as collagenase IV varied between 10 - 48 U ml^{-1} and DNase I varied between 10 - 40 µg ml^{-1}. Chemical concentration, such as of ethylene glycol bis- (β-aminoethyl ether) *N, N, N', N'*-tetra acetic acid (EGTA) was varied between 4 - 8.3 mM solution, time of exposure of reagents, such as thirty minutes to two hours for the second collagenase stage, temperatures of the device and solutions (4 - 36 °C) at different stages, and flow rates before the preceding method was found to achieve results.

The liver sample was first perfused at 2 µl min^{-1} for 20 minutes with an 8.3 mM solution of EGTA, to chelate extracellular calcium. After EGTA treatment the tissue was perfused with EBSS at 2 µl min^{-1} for a further 10 minutes to remove any chelator, as EGTA is known to inhibit collagenase action. Collagenase IV (48 U ml^{-1}) was dissolved in EBSS (pH 7.4) (2 ml) with the addition of 0.4 mg trypsin inhibitor and 2 mM calcium chloride ($CaCl_2$). The tissue was then perfused with this collagenase solution for 2 hours at 2 µl min^{-1}. The perfusate was allowed to drain to waste.

Following collagenase treatment the microfluidic device was removed from the incubator while still connected to the perfusate system and set on an ice pack. Ice-cold dispersal buffer containing 10 mM 4-(2-hydroxyethyl)-1-piperazineethanesulfonic acid (HEPES), 142 mM sodium chloride (NaCl), 7 mM potassium chloride (KCl), 5% (w/v) bovine serum albumin (BSA) in water adjusted to pH 7.4, supplemented with 40 µg ml^{-1} DNase I and 5 mM magnesium chloride ($MgCl_2$) was then perfused through the tissue sample at 500 µl min^{-1} for 2 minutes. The enzymatically-disaggregated cells in the eluent were collected in 1.5 ml micro centrifuge tubes and centrifuged at 100*g* for 5 minutes. The supernatant containing cell debris was removed by aspiration. The cells were resuspended in the dispersal buffer containing 40 µg ml^{-1} DNase I and 5 mM $MgCl_2$, and equal volumes of 2% (w/v) TB and cell solution were mixed and the cell count enumerated using a haemocytometer. Counts were measured in duplicate and the percentage viability determined.

The disaggregation method was then repeated three times using the above method however, the tissue probed first with Calcein AM and PI and imaged using confocal microscopy as described in Section 3.9. After disaggregation, the liver tissue was again probed with the fluorescent probes and reimaged to distinguish areas of disaggregation. At the end of the experiment, an aliquot of the cells collected in the eluent was pipetted onto a microscope slide and imaged using epi-fluorescence microscopy as described in Section 3.6.

3.12.1 Analysis of liver tissue and single cells after disaggregation

Individual cell analysis is advantageous when detecting minute differences between individual cells and could improve medical tests and treatments. Parameters based upon averages of large cell populations are frequently deceptive.(306) Cellular heterogeneity *in vivo* is widespread as described in Chapter 1. Therefore, analyzing cells individually with high spatiotemporal resolutions will lead to a more precise portrayal of cell-to-cell variations instead of the stochastic average shrouded by bulk measurements.

Following *in situ* collagenase disaggregation of primary cells from the tissue, viability was determined using TB exclusion. The results indicated that 78% ±2.4 (n=3) of cells were alive which is comparable to values expected from traditional disaggregation methods, these are between 60-90%.(305) A two hour collagenase disaggregation treatment, which offered a relatively gentle method of cell removal, resulted in a total of approximately 30,000 cells being released from a 3 mm^3 biopsy; based on haemocytometer measurements.

Fluorescent images of tissue, before and after collagenase disaggregation, were obtained using calcein and PI probes as shown in Figure 36. The images confirm that both live and dead cells are removed using this procedure and indicate that the 'new' tissue surface generated has a greater proportion of live to apoptotic/necrotic cells. The disaggregated cells were also imaged after collection to verify the viability of the cells and to detect whether the cells were single cells or clusters of cells. Ten images were taken of each sample in all three experiments.

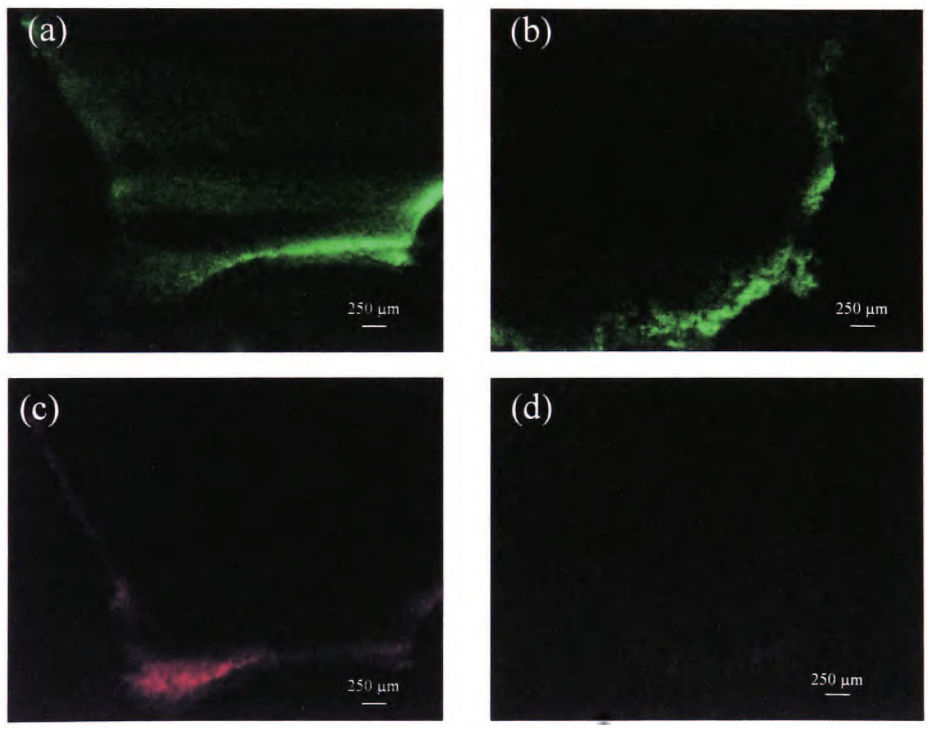

Figure 36. Confocal images of liver tissue after staining with calcein and propidium iodide (PI). Tissue pre- (a) (c) and post- disaggregation (b) (d) was probed with calcein and PI. Changes in the tissue edge shape are evident after enzymatic treatment. Data shown are representative of four independent experiments. Scanning resolution was 1024 x 1024 using a 4 x objective.

As shown in Figure 37, the cells collected were both live and dead however, the viabile cells fluoresced brightly indicating that the cells had metabolized relatively large amount of the probe. The cells themselves were individual

with no clusters occuring in any of the samples indicating they would be suitable in further downstream analysis of single cell characteristics and function.

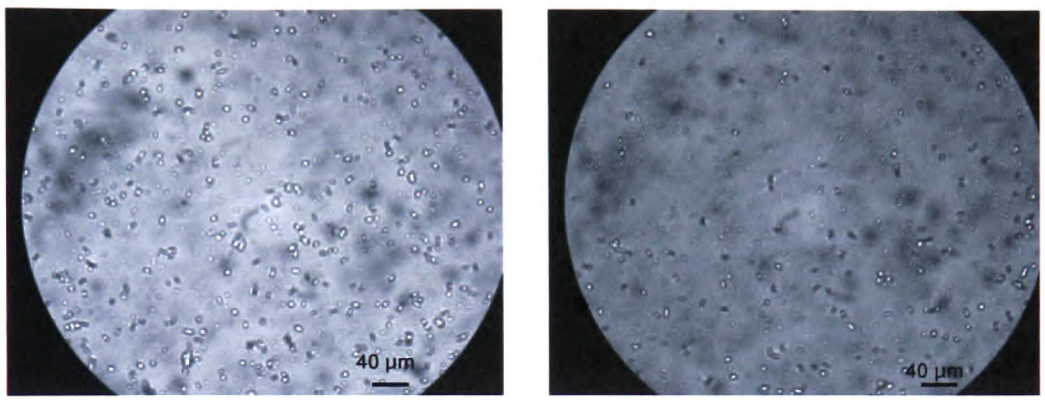

Figure 37. Fluorescent images of disaggregated cells collected from microfluidic system. (A) calcein probed cells and (B) PI probed cells. Magnification 10 x, representative of three experiments.

3.13 Interrogation of tissue within a microfluidic system using lysis buffer

To determine whether the previous results were valid and not just an artefact of the experiment, the tissue was probed using lysis buffer. Lysis buffer is usually used to envoke cell death by rupturing the cell membranes releasing LDH, DNA and other cell contents into the surrounding media. This is usually utilized as a positive control, as it should give the maximum death within a sample.

3.13.1 Viability analysis

To quantify cell viability and cell death within the tissue sample, a colorimetric cytotoxicity assay (Cytotoxicity Detection Kit Plus, LDH, Roche, UK)

4.3.3 Analysis of the use of multiple laminar flows to pattern tissue

This experiment was repeated on twenty separate occasions but only once was it successful in achieving a defined interface over the middle of the sample. Adjusting the individual flow rates at each inlet to control the position of the interface, as described in Section 3.8.1, was attempted to repeat this achievement however, was ultimately unsuccessful. In the single experiment, where there was an interface between the MeOH and PBS, a line of fluorescence defining the interface can be seen in the tissue, as shown in Figure 42.

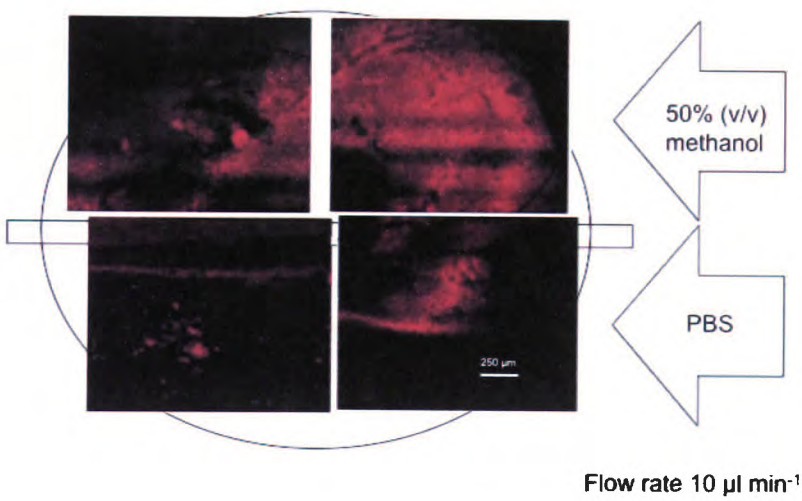

Figure 42. Composite of 4 confocal images of the rat tissue in the microfluidic device over the schematic of the tissue chamber showing cell death in the upper half of the tissue chamber and the interface between the two different solution streams using Propidium iodide (PI). The tissue was interrogated with 50% (v/v) methanol in the upper stream and PBS in the lower stream (n=20). The flow rate for both flows was 10µl min^{-1}. PI was applied after the 2 interrogation streams and these confocal images taken at the same tissue depth (120 µm). The interface between the two streams can clearly be seen in the lower two quadrants. Small areas of naturally apoptotic cells are shown in the lower left quadrant.

Whilst cell death was seemingly universal on the half of tissue, which was treated with methanol by the incidence of PI fluorescence, the other half treated with only with buffer showed little cell death. This was demonstrated by an increase of PI in the cells in this area as shown in the upper two quadrants of

Figure 38. There was also an increase in cell death in the region treated with PBS near the entry to the chamber as shown by a slight drop in the interface in the lower right quadrant. This was due to the geometry of the chamber and the difference in pressure within this region compared with the microchannel. There was also an area (upper left quadrant), where there is a deformation of the interrogation profile. This was due to a bubble residing in this area diverting the MeOH flow away from the cells. When analysing the images recording the instance of calcein fluorescence, the interface is not so clearly defined, as shown in Figure 43.

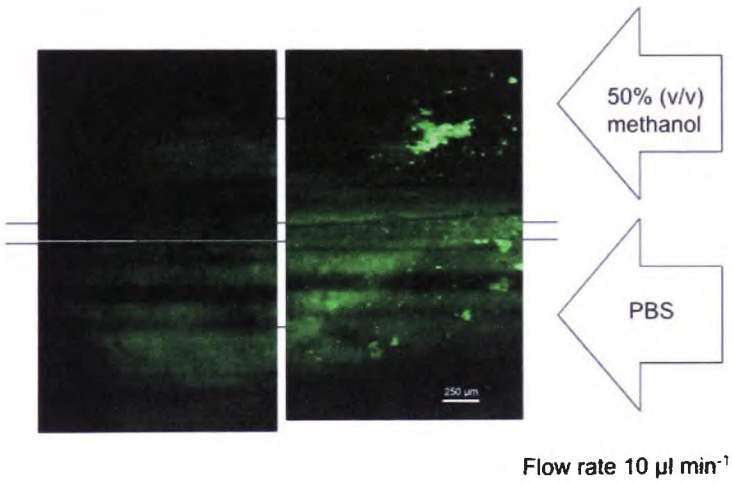

Figure 43. Composite of 4 confocal images of the rat tissue in the microfluidic device showing cell viability in the upper half of the tissue chamber and the interface between the two different solution streams using calcein AM. The tissue was interrogated with 50% (v/v) methanol in the upper stream and PBS in the lower stream (n=20). The flow rate for both flows was 10µl min^{-1}. Calcein AM was applied and these confocal images taken at the same tissue depth (120 µm). The fluorescence in the lower quadrants depicts areas of metabolically active cells, which have not been subjected to methanol.

Calcein fluorescence is however, retained in the lower half of the chamber where it was treated with PBS and little or no fluorescence is noted in the upper half except for an area in the upper right hand quadrant. One theory for this area of fluorescence could be due to the calcein probe diffusing further into the

tissue than the MeOH. The other theory for this occurrence could be that at the depth of the fluorescence, the MeOH had not yet been metabolized into its toxic metabolites and therefore had not yet affected the cells. The calcein fluorescence was also not as high as the fluorescence found in previous experiments. This could be due to the effect of chelatable iron on intracellular calcein. Fluorescent calcein binds with both Fe^{2+} and Fe^{3+} to form a metal-ligand complex which is non-fluorescent and has been used to estimate cellular iron levels.(323) Iron is ubiquitous metal in cells and is essential for the viability of the cell. The pool of cellular chelatable iron is usually found within the cytosol, the region of the cell where calcein AM is cleaved to form calcein. Petrat *et al* showed that rat hepatocytes and liver endothelial cells showed a substantial concentration (5.8 ± 2.6 μM in hepatocytes, 7.3 ± 2.6 μM in endothelial cells) of chelatable iron in the cytosol of these cells, compared to 0.3 -1.6 μM in other somatic cells.(324) Therefore, there was a high probability that some of the calcein probe bonded with the free iron within the cell, quenching the signal. In this thesis, tissue biopsies were used instead of precision cut tissue slices. The morphology of the tissue biopsy has undulations in the surface, which made it difficult to maintain the interface on the tissue. Another problem could be backpressure and has been discussed in Section 3.8.1.

Using multiple laminar flows to interrogate tissue slices has previously been successful and published by another group as discussed in Section 4.3.(171) Distilled solution containing concentrated unknown fluorescent dye was used in conjunction with a standard solution to verify flow over the 650 μm brain slice in a microfluidic chamber. The two solutions maintained equal flows

ranging from 0.5 to 1 ml min^{-1}, thereby exposing the two halves of the brain slice to different environments.

Ultimately, these sets of experiments were unsuccessful, as the result from one experiment could not be repeated even with adjustments to the flow profiles.

4.4 Interrogation of liver samples with different ethanol concentrations

The association of alcohol abuse with liver tissue damage has been the focus of considerable research, which has shown ethanol to be the direct cause of various abnormalities in liver architecture and functionality such as fatty liver, apoptosis, necrosis, cancer, fibrosis and cirrhosis.(325-327) However, the understanding of the mechanisms of alcoholic liver disease (ALD) progression has been difficult due to the lack of appropriate *in vitro* models that simulate the microenvironment of the liver organ. Whilst extensive knowledge has been gained through the application of primary hepatocytes in culture and hepatoma cells lines, both in tandem and isolation, these studies cannot provide a complete understanding of the complex intracellular interactions and regulatory factors that are exhibited in native tissue.

Ethanol is metabolized through various metabolic pathways in the liver as shown in Figure 44. The foremost oxidative pathway for the metabolism of ethanol includes alcohol dehydrogenase (ADH) that is present in the cytosol of hepatocytes and converts ethanol to acetaldehyde. Acetaldehyde is a highly reactive and toxic by-product, which damages tissue more significantly than ethanol alone and is also thought to contribute to the addictive development of

alcohol abuse.(328) At increased concentrations of ethanol (>100 mM) several enzymatic systems with high activity levels such as class II ADH, β3-ADH and cytochrome P450 2E1 (CYP2E1) are in attendance within the cell. The conversion of ethanol to acetaldehyde involves an intermediate carrier of electrons, NAD^+ that is reduced by two electrons to form NADH.

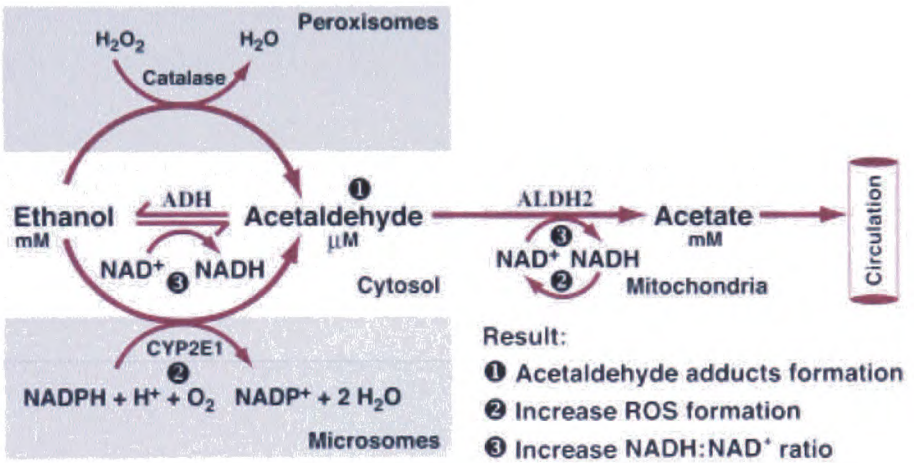

Figure 44. Oxidative pathways of ethanol metabolism. Image from S. Zakhari review(328) shows the enzymes alcohol dehydrogenase (ADH), cytochrome P450 2E1 (CYP2E1) and catalase all contribute to oxidative metabolism of ethanol.

As a consequence of these reactions the cytoplasm of the cell shrinks, and is exceptionally susceptible to injury from free radicals and further acetaldehyde concentrations. CYP2E1 is present in microsomes and has an essential role in metabolizing ethanol to acetaldehyde at increased ethanol concentrations. Acetaldehyde is metabolized mainly by aldehyde dehydrogenase 2 (ALDH2) in the mitochondria to form acetate and NADH. Catalase is located within peroxisomes and is a minor pathway in ethanol metabolism and requires H_2O_2 to oxidize ethanol. Chronic ethanol intake shows an increase in catalase activity and overall H_2O_2 production in rat models before

the pathway becomes overwhelmed through high concentrations of ethanol over time.(329)

After setting up as described in Section 3.13, the media was replaced with media supplemented with 20 mM, 50 mM, 100 mM, 150 mM and 200 mM ethanol in five parallel devices; a sixth device in which only unsupplemented media was run acted as a negative control. The eluent from the outlets of each of the microfluidic device was collected every hour in 0.5 ml microcentrifuge tubes for cell viability and functionality analysis.

4.4.1 Functionality analysis

To assess the functionality of the tissue within the microfluidic device production of albumin and urea was investigated. Serum albumin is an important carrier protein found in blood plasma, which is synthesized by the hepatocytes in the liver, where it helps maintain osmotic pressure and is a carrier of low water soluble molecules such as bile salts and free fatty acids. Increase in ethanol concentration is known to affect general protein synthesis.(330) Albumin levels in the eluent were determined by ELISA (Bethyl Laboratories Inc., USA) according to the manufacturer's guidelines. A 96-well flat bottom ELISA plate (SLS, UK) was coated overnight with 100 μl primary sheep anti-rat albumin antibody diluted in 0.05 M carbonate-bicarbonate buffer, pH 9.6 at 4°C. A 200 μl wash solution containing 50 mM Tris, 0.14 M NaCl, and 0.05% (v/v) Tween 20, pH 8.0 was used after each step and repeated three times. Plates were subsequently blocked with 200 μl 50 mM Tris, 0.14 M NaCl, containing 1% (w/v) BSA pH 8.0 for 30 minutes at ambient temperature. The rat serum reference standards (10,000, 500, 250, 125, 62.5, 31.25,15.625 and 7.8

ng ml^{-1} were diluted in 50 mM Tris, 0.14 M NaCl and 0.05% (v/v) Tween 20, pH 8.0 and 100 µl of each dilution was incubated on the plate with eluted samples for 1 hour. Next, the plates were incubated with 100 µl Horse Radish Peroxidase-conjugated detection antibody 1:5,000 in 50 mM Tris, 0.14 M NaCl and 0.05% (v/v) Tween 20, pH 8.0 for 1 hour. Finally, a colorimetric reaction was carried out by the addition of 50 µl undiluted tetramethyl benzidine (TMB) solution. The reaction was stopped with 25 µl of 2 M sulphuric acid and the absorbances were measured at λ = 450 nm.

Urea production has been commonly used as a specific marker of liver function.(331) Production of urea is a part of a cycle biochemical reactions that, in mammals, occurs only in hepatocytes. Ammonia is an extremely toxic waste product which has to be converted into a less toxic substance, urea. The conversion of ammonia to urea takes five steps; two in the mitochondria and three in the cytoplasm of hepatocytes as shown in Figure 45.

Urea concentrations in the media were determined using a colorimetric assay (QuantiChrom™ Urea Assay Kit, BioAssay Systems, USA) carried out using the manufacturer's protocol. Aliquot of 50 µl from the samples, blank (WME media) and the urea control (100 mg dL^{-1}) was transferred in duplicate wells in a clear 96-well flat bottom plate. 200 µl of the working reagent was added to each well and tapped lightly to mix. The plates were incubated for 10 minutes and read at an optical density at 520 nm, with 690 nm reference.

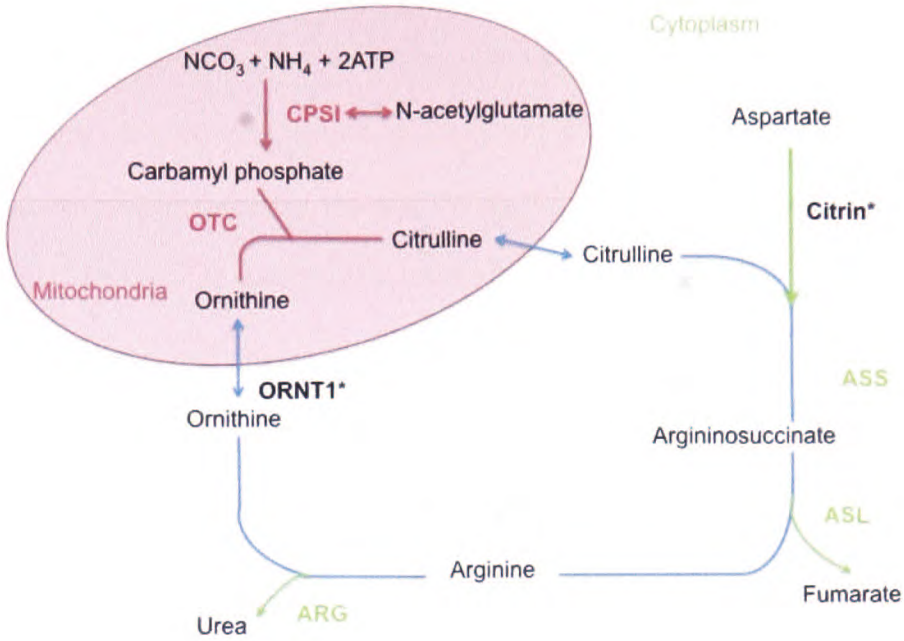

Figure 45. The urea cycle is composed of five catalytic enzymes, Carbamyl phosphate synthase I (**CPSI**), Ornithine transcarbamylase **(OTC),** Argininosuccinic acid synthetase **(ASS),** Argininosuccinic acid lyase **(ASL)** and Arginase **(ARG),** and at least two transport proteins (indicated with *) Citrin and ORNT1.

4.4.2 Fatty liver

The first pathologic alteration that occurs to the liver as a consequence of ethanol consumption is the development of fat in the liver, a condition called steatosis. It has been proposed that ethanol sensitizes the liver through the accumulation of fat to additional oxidative injury that leads to alcoholic liver disease.(332) The accretion of fat in the liver has been recognized as a factor that can be involved in more serious liver injury.(333) To discover whether there was a build up of fat in cells of the rat liver tissue after interrogation with increasing ethanol concentrations, an Oil Red O lipid stain was used. Oil Red O is a lysochrome (fat-soluble dye) diazo dye used for staining of neutral triglycerides and lipids.

Frozen sections (12 μm thick) were cut from the liver samples after maintenance in the microfluidic system using a Microm HM505E cryostat. Sections were selected from the centre of the sample and these were allowed to dry for 60 minutes and subsequently fixed with 10% (v/v) formalin for 10 minutes in a fume cupboard, then allowed to dry again for another 60 minutes. The slides were placed in absolute propylene glycol for 2 minutes before being immersed in Oil Red O for 10 minutes before rinsing with distilled water. The tissue was then placed in 85% (v/v) propylene glycol for five minutes to remove any excess stain, rinsed under running water and finally mounted in Depex using a coverslip. The tissue was then imaged using light microscopy using 40 x magnification.

4.4.3 The effects of increased ethanol concentration on liver sample viability and functionality

The concentrations of ethanol were selected as 20 mM, roughly equates to the legal drink drive limit in a blood sample in the United Kingdom (18.5 mM). Levels over 100 mM ethanol equate to the blood concentration of ethanol associated with a heavy consumer of alcohol.(334) Hourly aliquots were analyzed for WST-1 and LDH concentrations and all the individual absorbance results were subsequently averaged to give an overall result for the eight-hour monitoring period. The untreated tissue sample results (negative control) were used to establish the 'normal' baseline for WST-1 and LDH measurements as described in Section 3.13.1.

The WST-1 results gained from the different concentrations of ethanol were represented as percentage of the negative control and compared against each other as shown in Table 7.

All samples show an initial decrease in WST-1 metabolism occurred in the first day however by the fourth day, the liver tissue treated with 20 mM ethanol concentration shows approximately 80% parity with untreated liver samples.

Table 7. Percentage of viable rat liver tissue using WST-1 metabolism as an indicator after interrogation with 20, 50, 100, 150 and 200 mM compared with negative control of untreated liver samples (from aliquots collected over 8 h period). Data are expressed as the mean % of three separate experiments.

Day	20 mM	50 mM	100 mM	150 mM	200 mM
1	40.7 (± 19)	33.5 (± 14.1)	23.0 (± 13.6)	17.3 (± 5.8)	14.0 (± 5.21)
2	52.7 (± 23.3)	59.4 (± 23.6)	58.1 (± 23.9)	53.7 (± 12.6)	32.5 (± 9.5)
3	54.4 (± 7.6)	42.2 (± 12.8)	31.8 (± 11.3)	36.7 (± 16)	21.9 (± 8.7)
4	79.3 (± 17)	51.3 (± 8.6)	46.7 (± 12.3)	46.2 (± 9.5)	33.9 (± 12.8)

By comparison the 50, 100, 150 mM ethanol concentrations show a ~50% depression in enzyme activity compared with the untreated tissue in the same time period, with the 200 mM ethanol concentration showing only 34% activity after 4 days.

Ethanol is known to be a significant source of energy through its NAD metabolism as shown in Figure 44. NADH rapidly reduces WST-1 to formazan however; this reduction is strongly inhibited by superoxide dismutase (SOD), which is upregulated in ethanol metabolism.(335) In order to combat oxidative

stress, SOD is among the first line of defence in the detoxification of superoxide radicals to H_2O_2. As SOD is upregulated, inhibition of WST-1 occurs resulting in lower formazan production. This may impact the results of the test samples giving a lower indication of viability of the tissue than may actually be present.

Measurement of LDH activity in the eluent showed that cell death in the control liver sample remained at low levels for the 96 hours as show in Figure 46.

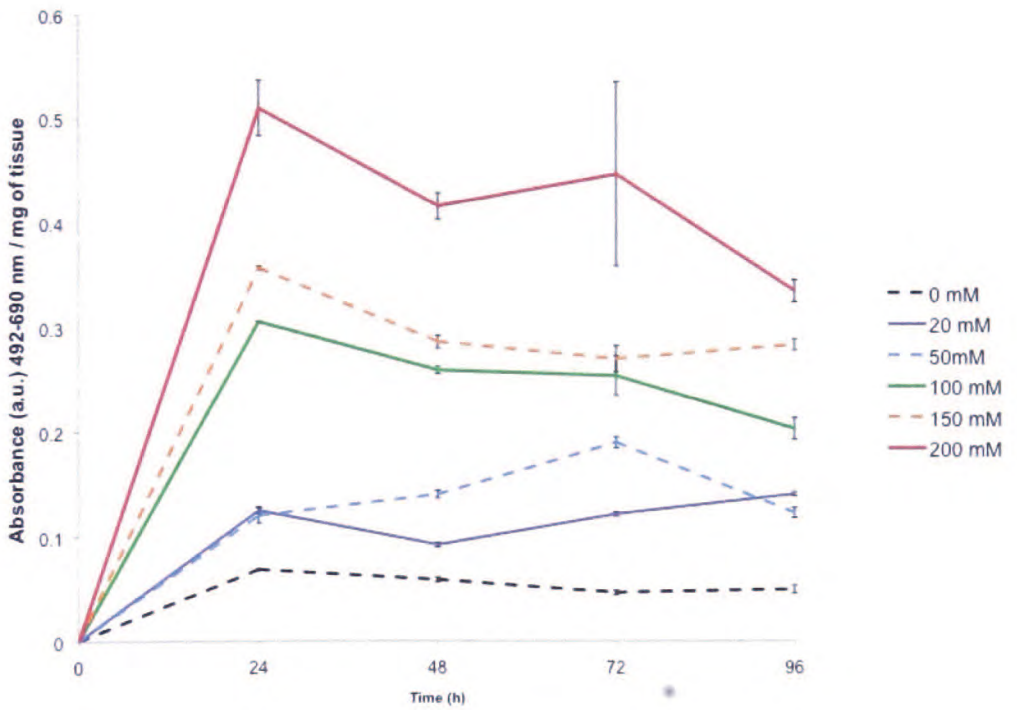

Figure 46. LDH activities in rat liver tissue samples after maintenance within a microfluidic device during interrogation with increasing ethanol concentrations. Liver samples were maintained at t_0, 24, 48, 72, 96 h in the absence of ethanol, control (dashed line, black), and in the presence of 20 mM (solid line, purple), 50 mM (dashed line, blue), 100 mM (solid line, green), 150 mM (dashed line, orange) and 200 mM (solid line, red) ethanol. Data are expressed as the mean % of three separate experiments, repeated in duplicates. ±S.E.M. of three separate experiments.

Exposure to ethanol levels above 100 mM resulted in an increase in LDH activity indicative of increased levels of cell death at these concentrations

compared to the control levels over the same time periods assayed. LDH activity at 20 and 50 mM show no marked difference compared with the control. This maybe attributed to the findings of an earlier study that indicated exposure to low ethanol concentrations reduces cell necrosis through the reduction of intracellular oxidative stress.(336) Both the LDH and WST-1 data signifies that ethanol concentrations in excess of 50 mM, after a period of two days resulted in a marked decrease in cell viability.

The ability of the liver tissue sample to continue to produce both serum albumin and urea under interrogation from increasing ethanol concentrations are shown in Figures 47 and 48.

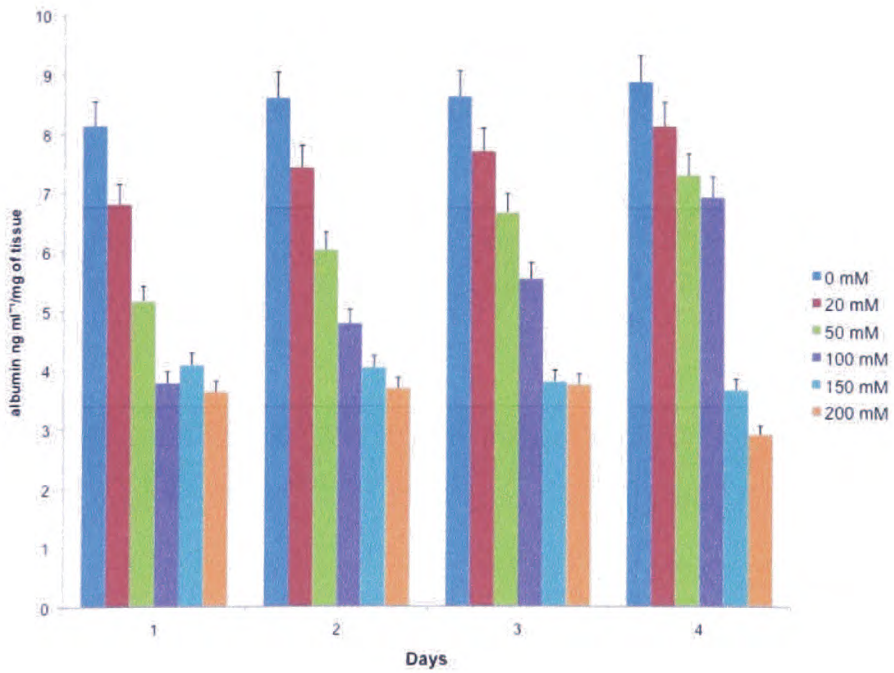

Figure 47. Albumin secretion by of rat liver tissue samples after maintenance within a microfluidic device and incubated with increasing ethanol concentrations. Aliquots were collected for eight hours every day and the levels of albumin determined. Data are expressed as the mean albumin levels ng ml^{-1} in the liver sample eluent ±S.E.M. of three separate experiments.

Increases in ethanol concentration are known to affect protein synthesis.(330) As shown in Figure 47, albumin was secreted by all the liver samples despite the interrogation with ethanol. As the ethanol concentration increases the amount of albumin decreases over the range of samples. Liver samples however, interrogated with 100 mM ethanol concentrations and below show a steady increase over the four-day exposure period although this level remains below the control (0mM). Ethanol concentrations of 150 mM and 200 mM show depressed secretion, evident at Day 1 with further decreases over time. The maximum concentration (200 mM) shows a decline of albumin secretion of two-thirds compared with the control.

As shown in Figure 48, urea was secreted by all liver samples regardless of their treatment. The control shows a 30% decrease of urea production from the start to the finish of the experiment. The sample treated with 20 mM ethanol exhibited an initial 80% increase, which dropped to a 37% increase over the four-day exposure period but still remained higher than the control. Ethanol treatment with 50 mM and 100 mM demonstrates an increase of urea production over the first three days however by day four, urea levels have dropped to between 75 – 50% compared with the control. Urea production in liver samples interrogated with 150 mM and 200 mM initially remain stable and comparable with the control. However by Day three, urea levels are depressed by 25-30% and at the end of day four; the levels were only 45% and 33% respectively. These results suggest that the metabolism of ethanol is involved in the decrease of albumin secretion and the increase of urea production at relatively low ethanol concentrations however; constant exposure over the period with concentrations above 50 mM causes urea levels to drop.

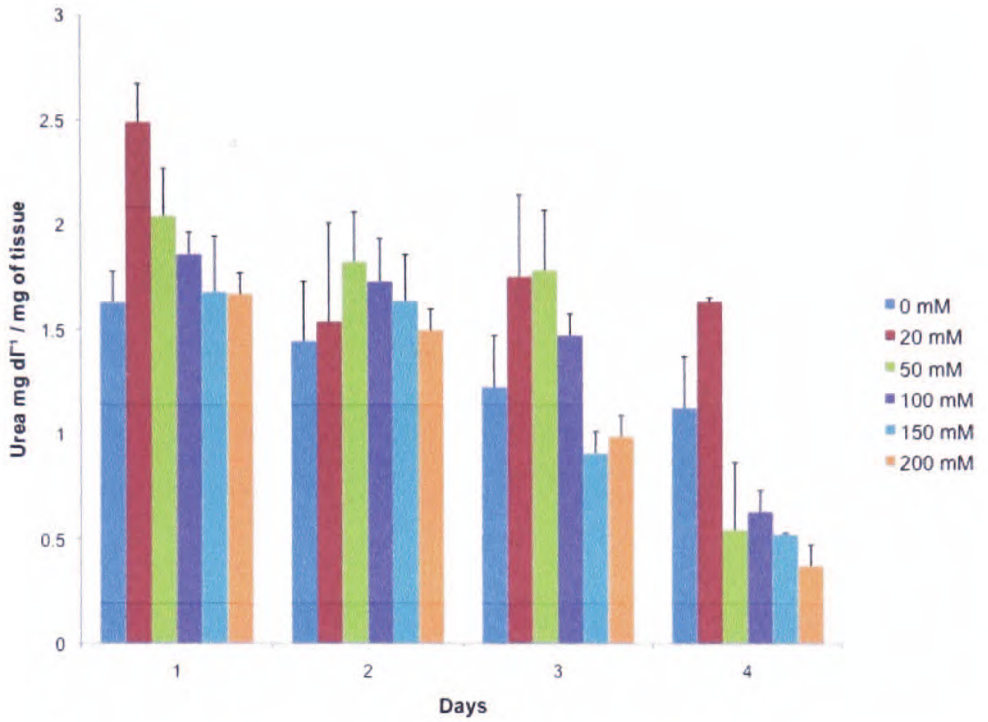

Figure 48. Urea production by of rat liver tissue samples after maintenance within a microfluidic device and incubated with increasing ethanol concentrations. Aliquots were collected for eight hours every day and the levels of urea determined. Data are expressed as the mean albumin levels ng ml^{-1} in the liver sample eluent ±S.E.M. of three separate experiments.

These results correlate with the viability of the cells as cell death is increasing over time. This is supported through finding from a previous study using isolated perfused liver.(337) This experiment was completed because the liver produces both albumin and urea and shows the effect of alcohol on the synthesis of proteins and removal of waste products.

H&E staining of the rat liver tissue after maintenance and interrogation with different concentrations of ethanol was used to analyze the integrity of the tissue and cell morphology. Figure 49 shows the control liver sample after four days maintenance in the microfluidic device. These samples were taken from the centre of the sample between 120 µm and 180 µm from the periphery. As

shown the cell nuclei of the hepatocytes have maintained their rounded appearance, with little or no shrinkage after 96 hours of culture in the microfluidic device. The cell membranes can be seen in several places, with the hepatocytes preserving their original hexagonal shape. In addition there is no discernible loss of the extracellular matrix between the cells. However, there are small gaps seen appearing in the structure of the tissue and the cells are beginning to look misshaped and there is evidence of some loss of cytoplasm as concentration increases (Figure 49b) as reported in a previous study.(338) As the concentration of ethanol increases (Figures 49c, d, e, f) the loss of ECM can be seen to increase with larger gaps appearing and the cells losing their shape, structure and cohesion this is exacerbated by the lost of viable hepatocytes. Ethanol has been shown to arrest the cell cycle and impair the replication of normal hepatocytes, even though the liver usually has a tremendous capacity to replace cells that are lost or damaged from other cytotoxic injuries.(326)

Fatty liver is a reversible condition associated with alcohol consumption where the liver stores triglycerides.(339) Oil Red O staining of the rat liver tissue biopsies treated with increasing ethanol concentrations are shown in Figure 50. No staining of fatty infiltration was observed in samples interrogated with 20, 50 and 100 mM over the exposure period (not shown). In contrast with the control (Figure 46A), the liver sample exposed to 150 mM ethanol demonstrates a small increase in staining by Oil Red O (Figure 46B) and the liver sample exposed to 200 mM ethanol showed a marked increase in staining (Figure 46C).

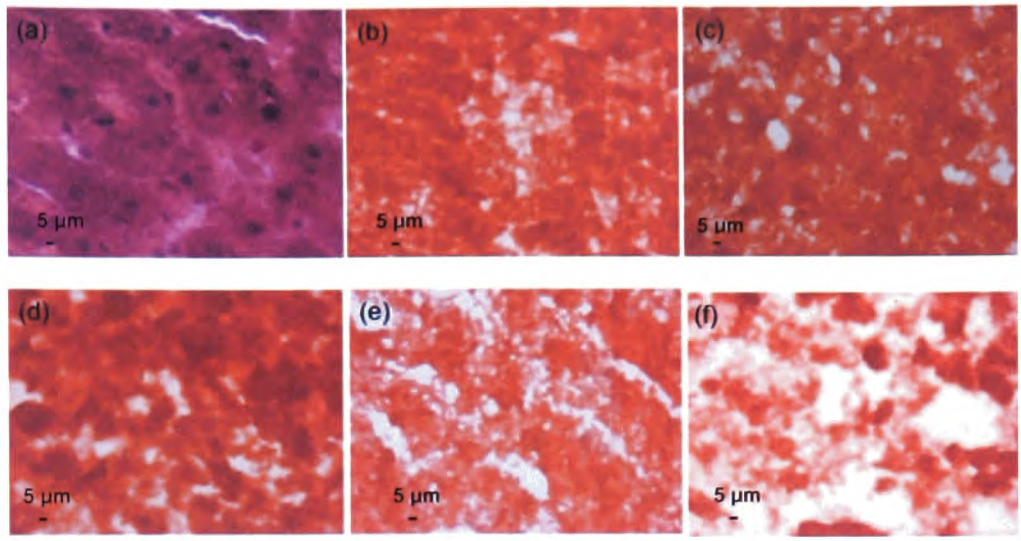

Figure 49. Haematoxylin and Eosin (H&E) staining of rat liver tissue samples after maintenance within a microfluidic device and incubated with increasing concentrations after maintenance in a microfluidic device. Liver samples were maintained in (a) 0 mM ethanol, (b) 20 mM ethanol, (c) 50 mM ethanol, (d) 100 mM ethanol, (e) 150 mM ethanol and (f) 200 mM ethanol. Samples were chosen between 200 µm and 300 µm from edge of tissue. Light microscopy images were taken at random on under x40 magnification and are representative of three separate experiments.

A recent study using PCLS and traditional explant culture methods, demonstrated that there was an increase in Oil Red O staining after the slices were incubated for over 48 hours with 25 mM ethanol compared to the control.(317) However, they also noted that there was an increase of Oil Red O staining in the control PCLS after culture compared with the PCLS examined before culture. High (>100 mM) concentrations of ethanol decrease the viability and functionality of the cells in the liver biopsy. Histological analysis of the liver sections showed the loss of ECM in the tissue and the increase of fatty deposits in the cells. Further analysis of the effects of ethanol on liver tissue in the microfluidic system could in the future give more information on the mechanisms involved in ethanol metabolism and how these can be used to treat ALD.

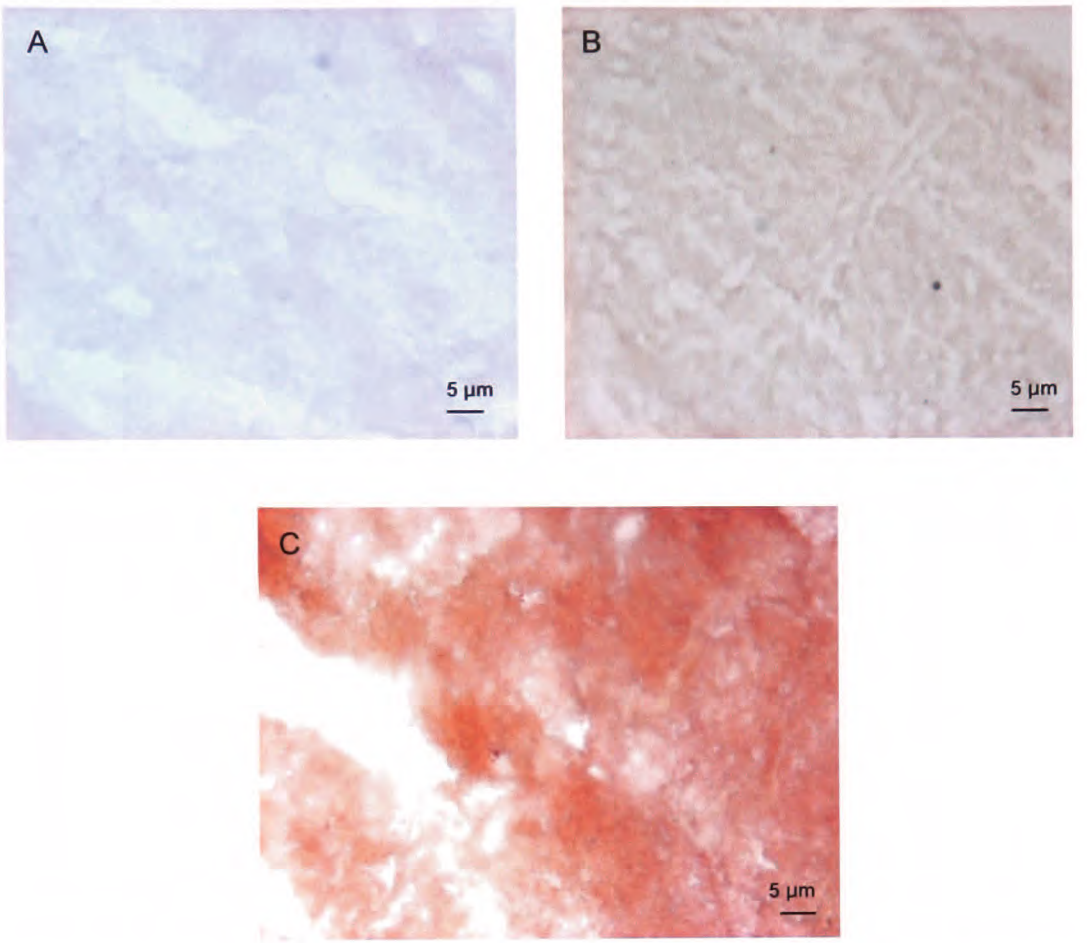

Figure 50. Oil Red O staining of rat liver tissue samples after maintenance within a microfluidic device and incubated with increasing ethanol concentrations. Liver samples were maintained in (A) 0 mM ethanol, (B) 150 mM ethanol and (C) 200 mM ethanol. Samples were chosen between 200 µm and 300 µm from edge of tissue. Light microscopy images were taken at random under x40 magnification and are representative of three separate experiments.

4.5 Anti-oxidant protection of vitamin C and E during interrogation with ethanol

As described in the last section, ethanol is an oxidant, which causes significant damage to cells. Within the hepatocyte, in addition to the enzymes used in metabolizing ethanol as discussed previously, there are anti-oxidant systems involving enzymatic and non-enzymatic pathways. Enzymes

concerned in the removal of ROS are: SODs, glutathione peroxidase, glutathione reductase along with the co-factors glutathione (GSH) and reduced nicotinamide adenosine dinucleotide phosphate (NADPH). Other important non-enzymatic anti-oxidants are vitamin E (α-tocopherol) and vitamin C (ascorbate) and have been the primary choice for investigating anti-oxidants as ALD patients have the greatest access to them. Vitamin E is found within the lipid phase of cell membranes and is a powerful anti-oxidant, it has also been shown that patients with ALD frequently exhibit reduced vitamin E levels.(340) The majority of studies into the effect of nutritional anti-oxidants to treat alcohol related injury are performed in cell culture, while the majority of alcohol studies are performed in animal models.(341-343) This is due to the relatively new concept of anti-oxidant use to treat ALD and the complexity of the disease progression.

After setting up the microfluidic systems with tissue as described in Section 3.13, the WME was replaced with WME supplemented with 250 mg l^{-1} Vitamin E and 100 mM ethanol in two parallel devices, two more devices contained 250 mg l^{-1} Vitamin E, 100 mM ethanol and WST-1 regent. Due to Vitamin E being lipid soluble, the media was shaken vigorously for 5 minutes to mix. The media was then filtered using 0.22 mm syringe filter to remove as many bubbles as possible before being put on the system. The eluent from the outlets of each of the microfluidic device was collected every hour in 0.5 ml microcentrifuge tubes for cell viability and functionality analysis. These experiments were repeated thrice. The Vitamin E was replaced in a subsequent set of experiments with 250 mg l^{-1} Vitamin C for comparison of effectiveness of

the different vitamins. The vitamin concentrations used were chosen as they had been previously been employed in earlier studies.(343-345)

4.5.1 Analysis of anti-oxidants effect on alcohol interrogation

As said previously, levels over 100 mM ethanol equate to the blood concentration of ethanol associated with a heavy consumer of alcohol and were shown in the previous experiments to be the lowest concentration of ethanol to cause cell damage and loss of function.(334) Using this ethanol concentration, the effect of the anti-oxidants, Vitamin E and Vitamin C on the viability and functionality of the liver samples were determined. Hourly aliquots were analyzed for LDH and WST-1 concentrations and the individual values were subsequently averaged to give an overall result for the eight-hour monitoring period. The untreated tissue sample results (negative control) were used to establish the 'normal' baseline for LDH and WST-1 measurements. All values were expressed per mg wet weight and all test conditions expressed as an increase or decrease of this baseline value.

Cell viability within the tissue sample, using WST-1 and LDH as markers, show that there is an improvement in viability of the liver sample by the addition of Vitamin E and Vitamin C to the media when treating the tissue with 100 mM ethanol. Both vitamins caused increases in WST-1 absorbance over ethanol alone, although the effects of Vitamin E were less marked by Day 3 and 4. As shown in Figure 51A, there was an increase of 60% in the viability of the Vitamin C treated biopsies than the ethanol sample however this increase is only 40% of the viability exhibited by the control sample on the first day. Vitamin

E treatment showed an 89% increase on the first day but this was not sustained over the course of the experiment.

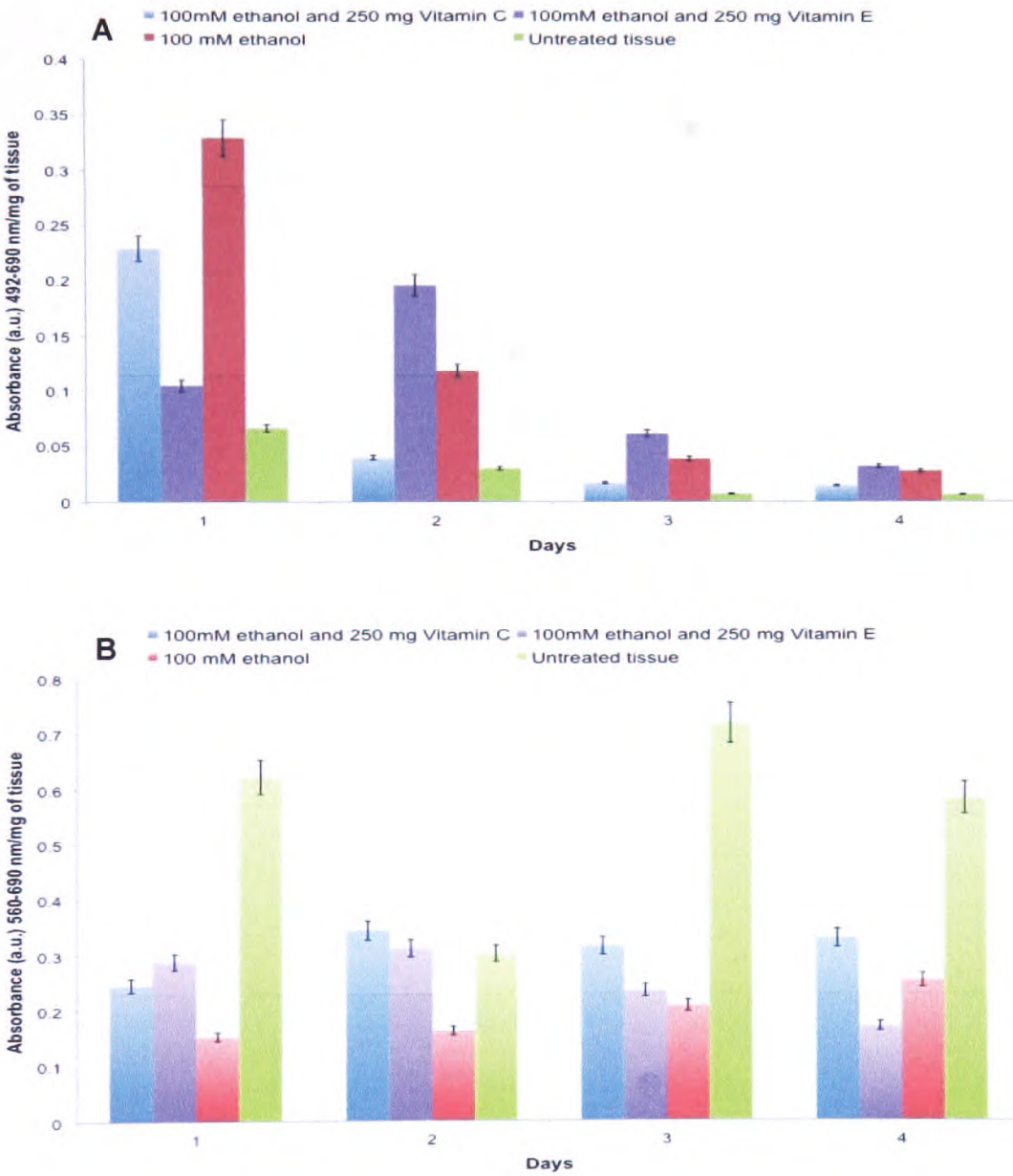

Figure 51. (A) WST-1 metabolism by of rat liver tissue samples after maintenance within a microfluidic device and incubated with 100 mM ethanol, 250 mg l^{-1} Vitamin C, 250 mg l^{-1} Vitamin E compared with untreated sample. (B) LDH release by of rat liver tissue samples after maintenance within a microfluidic device Aliquots were collected for eight hours every day. Data are expressed as the mean absorbance (a.u.) in the liver sample eluent ±S.E.M. of three separate experiments.

By Day 3 and 4, the biopsies treated with Vitamin C exhibited a higher viability index than those treated with Vitamin E, although both vitamins had limited effect when compared with the untreated samples.

Using the LDH marker, there is a 250% increase in cell death within the ethanol/vitamin C combination sample compared with the untreated sample on the first day as shown in Figure 51B. The vitamin E treated liver biopsy showed again a decrease in LDH release however, as shown by the WST-1 assay this was not sustained. The viability however, increased 60% in the vitamin C sample compared to the ethanol sample, which also reflects the WST-1 metabolism results. By the final day, cell death was 132% higher in the vitamin C sample than that in the untreated sample. The effect of the vitamin C compared to the ethanol sample increased the viability of the liver sample by 53%, just over half. This also reflects the effects from the WST-1 assay. Vitamin E however decreased the viability of the liver sample compared with the ethanol sample.

Previous studies in cell models have shown the same effects that the addition of vitamin C can mitigate the effects of ethanol.(346, 347) These same studies have also shown than Vitamin E has even better effect than Vitamin C, which was not observed in this thesis. The main problem that can be identified from the methodology was the process of actually getting the Vitamin E into the media for testing, as the vitamin is lipid based and therefore getting into the liquid phase was extremely difficult. It cannot be sure how many cells in the

tissue had access to the vitamin, and at what concentration during the testing but some effects were observed as shown above.

Albumin synthesis in the liver samples treated with vitamin C to combat ethanol damage as shown in Figure 52 showed slightly higher levels in the first 2 days of the experiment than the samples with ethanol alone (30% higher on Day 1 and 9% higher compared to 100 mM ethanol samples). However, this is not maintained in the last 2 days and the level of albumin in the media decreased to only 46% on Day 3 and 56% on Day 4 compared with the sample treated solely with ethanol. Urea production decreased in the combination test in all the days of the experiment compared with both ethanol and untreated samples Figure 53. The effect of vitamin E on the production of albumin and urea was abandoned due to time constraints.

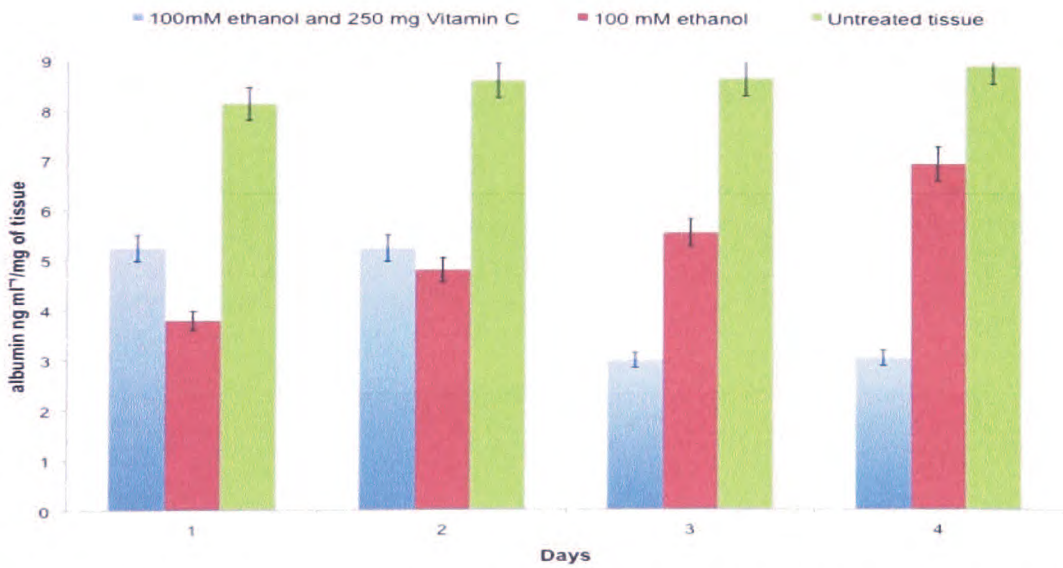

Figure 52. Albumin secretion by of rat liver tissue samples after maintenance within a microfluidic device and incubated with 100 mM ethanol with and without 250 mg ml^{-1} Vitamin C compared with untreated sample. Aliquots were collected for eight hours every day and the levels of albumin determined. Data are expressed as the mean albumin levels ng ml^{-1} in the liver sample eluent ±S.E.M. of three separate experiments.

The results presented are different from previous animal studies that have shown that vitamin C attenuate alcohol effects on albumin production, rather than decreasing it.(348, 349) However another study indicates that ethanol increases the production of uric acid in rat animal models and the addition of vitamin C reversed these effects, which correlates with these results presented in this section.(345) The exact mechanisms involved are yet unknown as there has been little research into the effect of alcohol intoxication on the production of urea in cell and animal models.

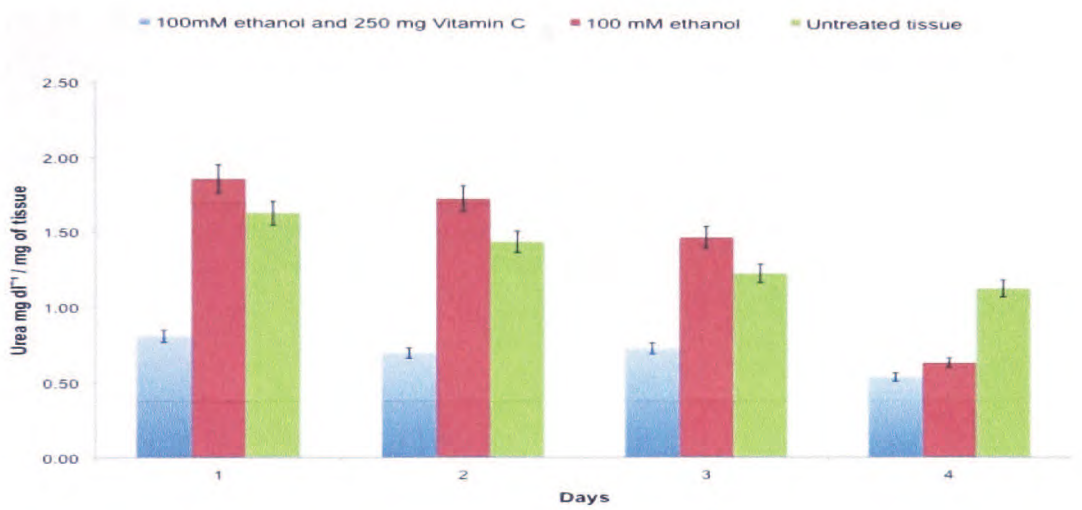

Figure 53. Urea production by of rat liver tissue samples after maintenance within a microfluidic device and incubated with 100 mM ethanol with and without 250 mg ml^{1} Vitamin C compared with untreated sample. Aliquots were collected for eight hours every day and the levels of urea determined. Data are expressed as the mean urea levels mg ml^{-1} in the liver sample eluent ±S.E.M. of three separate experiments.

In this chapter, it has been shown that rat liver samples were kept viable and functional over ninety-six hour time period. WST-1 was metabolised and reduced to formazan, which was subsequently detected off-chip along with the detection of LDH release from cells maintained and/or interrogated on-chip. Addition of different ethanol concentrations decreased the amount of formazan detected over the time period indicating the ethanol was affecting cell viability

over the time period compared to a control. The addition of ethanol to the liver samples exhibited many of the same characteristics noted in other studies which have used isolated hepatocytes and *in vivo* rat models of chronic ethanol intoxication including the decrease in viability, fatty liver progression, reduction of albumin production, change in cell morphology and decrease in urea levels.(317, 350) In this thesis, liver samples millimetres in thickness were used to ensure that even the cell types that were sparsely represented within the tissue such as cholangiocytes were included and the native complex ECM was maintained which is not present in cell-based models. Using microfluidic technology we have also mimicked the *in vivo* flow dynamics, which is not present in conventional cell and tissue representations.(116) Therefore, it is proposed that rat liver samples retain their biological functions and appeared to a novel and valuable model for the study of not only pathological but also physiological mechanisms. Using the concept of tissue based microfluidic systems to personalize medicine regimes; this became the focus of the final stage of the study.

5. Microfluidics for head and neck cancer diagnostics

'One changes one's ideas the way an animal sheds its coat, in patches: it's never a wholesale change from one day to the next.'

Umberto Eco 1932-

5.1 Introduction

Every year millions of patients worldwide will undergo tests to diagnose cancer. Male patients over the age of 50 years old, for example, will have their prostate-specific antigen (PSA) levels measured in an attempt to discover any possible prostate malignancy. Women will undergo mammograms to detect any potential breast tumours. However these tests are primitive, routinely producing false positives or false negatives and rely heavily on human observations rather then definitive results. For example, among 1,087 individuals participating in a cancer screening trial who received a battery of tests for prostate, ovarian, colorectal and lung cancer, 43 percent had at least one false positive test result.(351)

Discovering a better diagnostic technique than those used at present has been high priority for clinicians for several decades. The rise of molecular biology and the human genome project in 1980s and 1990s gave hope that numerous questions about prognosis and diagnosis of several pathological and physiological conditions would be answered as the code to the human genome was unlocked.(352) Unfortunately, as yet these questions remain largely unanswered because of the complexity of disease progression, in addition to

social and economic differences between individuals.(353, 354) For the past several years, pharmaceutical companies and research groups have become increasingly interested in biomarkers. A biomarker is a chemical that can be found in blood serum or nucleotide sequence in the DNA of the patient, such as the BRCA1 and BRCA2 gene sequence.(355, 356) The main objective of these studies is the possible exploitation of biomarkers. Ideally these markers can be detected early to save the expense of multi-year studies, for diagnostic tests to determine malignancy and the effectiveness of targeted therapies.(357, 358)

Previous research and marketing strategies in the pharmaceutical industry have been to develop drugs that can be administered as widely as possible to as many patients as feasible, with the aim that sufficient numbers benefit without detriment to those that do not.(359) These 'carpet' drugs give high monetary returns, which consequently drives the development and marketing of new therapeutics.(360) However in oncology, this model can break down due to the high cost of treatment coupled with the disinclination of NHS health trusts to pay for treatments that do not work in the minority (or possibly the majority) of cases.(361) This has given rise to 'niche' drugs or personalized medicine, whereby patients will only be prescribed drugs and funded, if the drugs demonstrate a significant probability that the patients will benefit. Therefore, several research groups are exploring biomarkers and techniques to identify positive responders in a patient cohort that is efficient, reliable and cost effective.

5.2 Microfluidic innovation in cancer research

Current studies of cancer dynamics within microfluidic systems have focused on evaluating the steps involved in cancer cell metastasis, detecting circulating tumour cells (CTC) and detection of biomarkers for diagnostic purposes. Exposure of tumour cells to different environmental conditions, such as shear stress and chemokine gradients, which represent changes found in capillaries *in vivo*, have been studied to measure the tractile force exerted by a cell.(362, 363) While these studies do not expand on chemokine research, they do present microfluidic systems that could be used to do so in the future.

Researchers have examined the site of attachment and adhesion of fibroblasts and tumour cells through isotrophic silicon microstructures and matrigel lined with human microvasular endothelial cells, highlighting the biomechanical properties.(364, 365) These studies present 3-D model systems for investigating the microenvironments of tumour tissue by trapping and culturing different cell lines in defined structures. The methods for detecting disparities in cell lines used in these studies seems cumbersome when compared to traditional analysis methods such as FACS. Others have examined cell deformability, to distinguish between normal, benign and metastatic cancer cells using microchannels, to develop a test for metastatic disease.(366, 367) These studies have demonstrated the effectiveness of cancer cells to deform to different sized gaps in the channels however, other previous studies have also examined deformability using traditional filters and culture systems and further analyzed the effect of anti-invasive drugs.(368, 369)

These microfluidic studies have not yet, given any new insight into the mechanisms of metastasis.

Microfluidic-based technology is ideally suited to diagnostic applications due to the inherent benefits described earlier, with many studies describing the design and testing of antibody-based microwell arrays and electrochemical detection within microfluidic channels for various secreted and surface-expressed tumour markers having been published.(370, 371) These studies include the capture of breast cancer cell lines using epithelial membrane antigen or EMA (CA 15-3) and epidermal growth factor receptor (EGFR) for further analysis. Chemotherapy resistance in cancerous cell lines has been assessed within a microchannel array that provided a more realistic representation of how cells would react *in vivo* than simply adding the drug to the cells in a static culture flask.(372) Another study has examined a multicellular tumour spheroid culture in a microchannel and described the assessment of oxygen and glucose concentration in static culture compared with perfusion, and shown that cell demand on nutrients quickly overtaking supply within static cultures. The study also assessed shear stress effects on spheroid growth, which had not been previously examined, and demonstrated the ability to grow several spheroids in a single culture.(373) These few studies while demonstrating the power of microfluidics to culture and identify different cancer cell properties are still in their infancy and have yet to answer any critical questions that have been proposed by traditional cell biology methods.

In a recent Gap analysis document(374) of cancer research, a document which analysed the gaps in current cancer research, several recommendations were highlighted: 'the need for improved preclinical models, research agents and technologies; development of three-dimensional cell culture models containing multiple cell types, which reflect the tissue architecture of the normal and diseased tissue; and an increase in research efforts into the role of the microenvironment in the development and treatment of cancer'. The work presented in this chapter will show how tissue-based microfluidic systems can address these points.

5.3 Tissue harvesting and preparation

Histopathological-confirmed samples from 9 patients undergoing surgery for HNC were studied. Ethics and NHS Trust approval was obtained from Hull and East Yorkshire Research Ethics Committee (07 / H1304) and Hull and East Yorkshire Hospitals NHS Trust (RO568) respectively. Samples were provided with no patient details apart from the origin of tumour. Tissue biopsies were removed during neck dissections and placed in containers filled with DMEM media at 4°C for transportation to the laboratory. Within 1 hour, the tissue was cut into approximately 3 mm^3 pieces, with the weight of each individual sample recorded.

5.4 Measurement of viability using LDH release, WST-1 metabolism and epi-fluorescent microscopy

To validate the application of microfluidics to model *in vivo* cancer microenvironment, HNSCC tissue samples were maintained in simulated *in vivo* conditions in a microfluidic system while the viability was examined using biochemical biomarkers, LDH release and WST-1 metabolism as described in section 3.13.1. A modification of this protocol was used to include HNC biopsies instead of rat liver tissue, with the application of 10% lysis buffer to the tissue after seventy hours of incubation in the microfluidic system to further demonstrate viability. Further experiments to analyze the viability of the tissue using epi-fluorescence microscopy and LavaCell™, as described in section 3.10, were taken after seventy hours incubation.

5.4.1 Analysis of the viability of HNSCC biopsies during maintenance in a microfluidic system

After an initial peak at the beginning of the experiment, thought to be due to damage caused to the surface of the tissue in harvesting, the LDH release decreased and then remained at low levels for the next 48 hours as shown in Figure 54. On the application of the lysis buffer after 70 hours, there was a significant increase in LDH release as the cytolytic agent penetrated the tissue causing disruption of the cell membranes. LDH levels remained high for the following 4 hours as more cells were exposed to the lysis buffer.

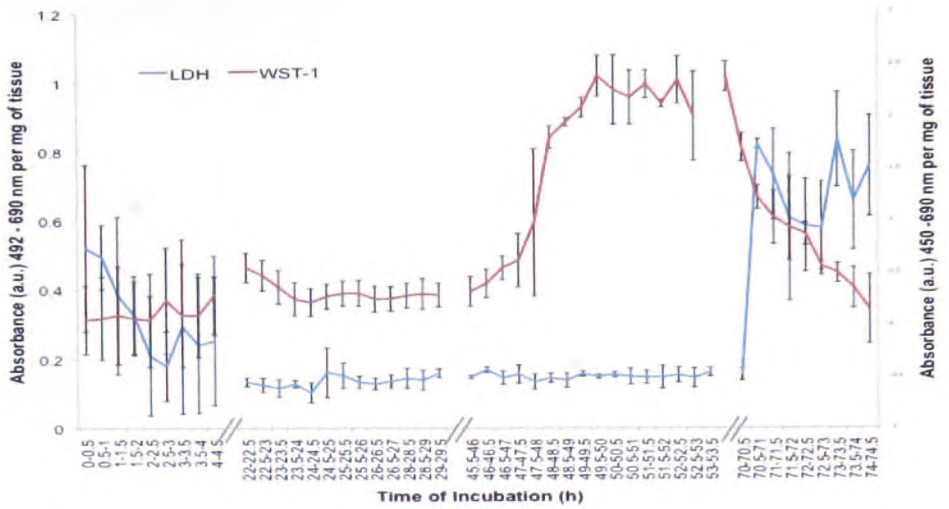

Figure 54. LDH release and WST-1 metabolism of primary HNSCC tissue with the addition of 10% lysis buffer after 70 hours. Aliquots were collected for eight hours every day. Data are expressed as the mean absorbance (a.u.) in the liver sample eluent ±S.E.M. of three separate experiments.

In contrast to LDH release, WST-1 metabolism showed a significant increase after 45 hours, with more formazan product being detected. The delay in detection of product is most probably due to the fact that only the outer cell layers would initially be exposed to the WST-1 reagent, therefore only relatively small amounts would be actively metabolized. As the reagent diffused further into the tissue, through the extracellular spaces, more cells would become exposed hence increasing the amount of metabolized reagent. The formazan salt would also take time to diffuse out of the tissue sample into the flowing media, analysis of more than fifty experiments of liver and different types of cancerous tissue have always shown a 35 – 50 hour delay in WST-1 detection in the eluent. After the application of lysis buffer at 70 hours of tissue maintenance, the amount of formazan detected decreases rapidly as the number of viable cells is reduced. These complementary analyses show that NHC tissue remains viable within the microfluidic system over the length of the experiment. The application of lysis buffer at the end of

the experiment showed that as cells were lysed the opposing viability biomarker levels reversed indicating cell death occurring which was not present before the application of the lysis buffer.

The experiment was repeated again thrice without the application of lysis buffer after seventy hours and instead LavaCell fluorescent probe was added to the system to assess viability. As shown in Figure 55, the tissue fluoresced highly in all areas examined showing that it was viable. Images collected using epi-fluorescence microscopy provide *in situ* assessment of tissue viability, along with ease and rapidity, which corroborates the biochemical results described above.

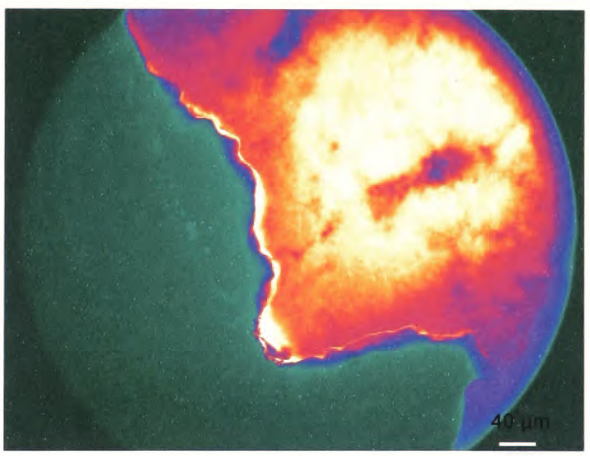

Figure 55. Image of HNC tissue following maintenance in the microfluidic device for 75 hours showing Lavacell™ fluorescence, highlighting the edge of the tissue distinguished from background. A 10 x objective was used. Image is representative of three separate experiments.

5.5 Viability of primary tumour tissue and secondary tumour (nodal) tissue

To understand whether the characteristics of the tumour tissue had an effect on the results, primary tumour tissue was compared with secondary

tumour tissue found in dissected lymph nodes using LDH release and WST-1 metabolism using the method described in Section 3.13.1.

5.5.1 Comparison of primary and secondary cancer using LDH and WST-1

The samples used in these experiments were of similar size and weight as discussed in Section 3.9. When comparing LDH release there was no significant difference as shown in Figure 56A, suggesting that the effects observed with WST-1 are more likely to be an inherent feature of the tissue biology rather than a facet of the architecture. The primary tumour biopsies showed markedly higher levels of formazan product, indicating increased mitochondrial activity, as compared with tissue from the secondary tumours as observed in Figure 56B.

The observed difference could be due to there being lower numbers of highly-proliferative tumour cells in the node or be a reflection of the distinct tissue architecture, i.e. that the nodal tissue was less diffuse and thus uptake of the WST-1 was slower. It could also be inferred that the incubation period in the current microfluidic experiment was too short for the secondary tumour tissue to enter the synthesis period and this could be another reason for the difference in WST-1 profiles in the primary and secondary tumour tissue; this hypothesis would need prolonged incubation times to test.

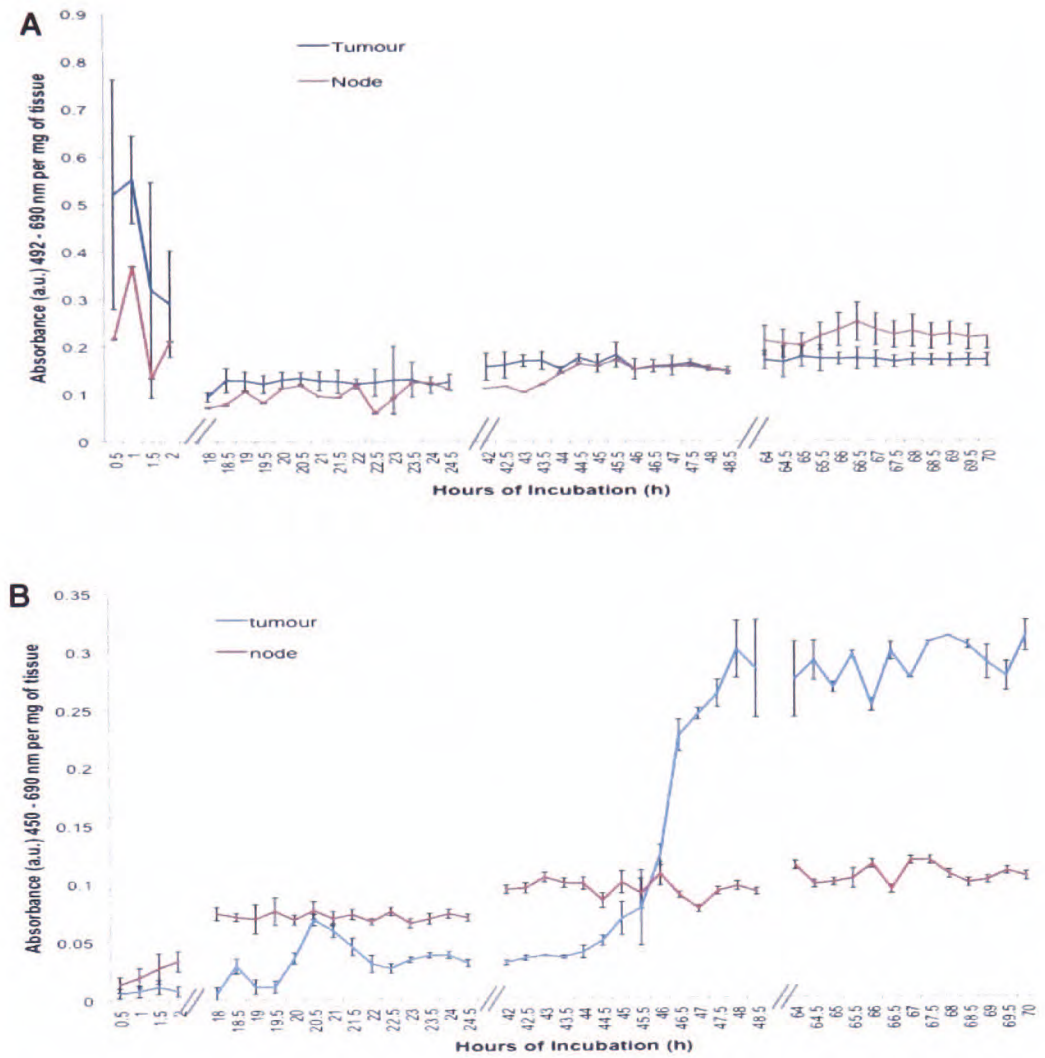

Figure 56. Comparison of (A) LDH release and (B) WST-1 metabolism in primary tumour tissue and secondary (node) tissue in microfluidic device Aliquots were collected for eight hours every day. ±S.E.M. of three separate experiments.

Comparisons between *in vitro* primary and secondary *in vitro* cancer tissue viability have been studied. A study using a murine model has shown that primary tumours inhibit secondary growth and when the primary tumour is removed accelerated metastatic tumour growth.(375) This study also assessed the time between the removal of the primary tumour and the administration of the chemotherapy drug, cyclophosphamide, and the effect on secondary tumours. They demonstrated that if the time period between surgery and chemotherapy was shorter than three days, the more effective the

chemotherapy. They also showed that if the time period was over seven days then the secondary cancer tissue grew, although very small, in size. The study concluded that the secondary tumour, because of the suppression of growth from the primary tumour, needed time to enter the synthesis period of the cell cycle and early intervention with chemotherapy drugs killed the cells as they entered this phase. Further investigations by another group using C57/BL6 mice [10/group] inoculated with Lewis lung carcinoma (3LL cells) [5×10^5 per animal] showed that tumour removal was followed by accelerated growth of locally recurrent tumours and metastases.(376) Using one group of mice as a control, another group was subdivided into two, with one (2A) killed after two weeks with the tumours and lungs excised and the second sub-group (2B), the tumours were removed and recurrent tumour growth evaluated for a further two weeks. Four weeks from the onset of the study, all remaining primary tumors and lungs were excised from both groups. After four weeks undisturbed growth, primary tumours in the control group reached a mean size of 2.85 ± 0.33 cm. After two weeks growth, primary tumours in groups 2A and 2B were comparable at 1.36 ± 0.44 m and 1.53 ± 0.29 cm, respectively. Two weeks after primary tumour excision, recurrent tumours in group 2B had reached a mean size of 2.65 ± 0.74 cm. Moreover, for several animals, recurrent tumours rapidly reached similar volumes to that of primary tumors in the control group. Primary tumours were typically encapsulated and nonadherent. In contrast, recurrent tumours were locally invasive and adherent to chest wall and wound. Histological examination revealed increased mitosis in recurrent tumors when compared with primary tumours. Recurrent tumours were also more locally invasive than primary tumours.

The microfluidic experiments have shown the ability to maintain and analyze the difference in primary and secondary tumours with further work needed to understand the mechanisms relating to the growth dynamics of both tumour categories and to establish whether the further results correlate with those found in the murine models.

5.6 Comparison of chemotherapy regimes on head and neck cancer in microfluidic microenvironment using extracellular biomarkers

Fast, obvious and easily accessible markers of cell death are needed for appraising early therapeutic efficiency for chemotherapy so that patients and their oncologists can choose whether to remain with a specified therapeutic strategy. Currently image based analysis of the response of a patient's tumour can take weeks, if not months after the start of treatment.(377) In recent laboratory studies, it has been shown that tumour cells undergoing apoptosis release cellular components into the culture media for example cytochrome *c*, DNA and nucleosomes.(378-380) In this last study, these biomarkers have been used to identify the effectiveness of 5-FU, CDDP and a combination of both drugs to kill HNC cancer tissue in a microfluidic system.

5.6 Chemotherapy Regimens

The eight microfluidic systems were set up as described in section 4.5. For the first 12 hours of the experiment, only DMEM media flowed through all the systems. After 12 hours, the media was changed in six of the microfluidic systems with two systems remaining with media only flowing through the tissue. For the six systems to receive drugs; two systems had 0.2 $\mu g\ ml^{-1}$ CDDP in DMEM, two systems had 1.0 $\mu g\ ml^{-1}$ 5-FU in DEM and the remaining two had

both 0.2 μg ml^{-1} CDDP and 1.0 μg ml^{-1} 5-FU in DMEM. These concentrations were taken from a previous study that was examining a 3D cell culture system, constructed from silicon and PDMS with multi-microchannels, for evaluating the effect of chemotherapy drugs on cancer cells and closely resemble the concentrations found in a patient's plasma undergoing chemotherapy treatment.(381) The treatment period was seven days with the total experiment lasting eight days. Eluent was collected constantly in 4 hourly aliquots throughout the day and night for the seven days of treatment. This change was necessary to capture any changes in the eluent as soon as they occurred. These samples, six for every twenty-four hours, were analyzed in duplicate and then the results averaged for the whole twenty-four hours to give daily totals.

5.6.1 Analysis of LDH release and WST-1 metabolism in HNSCC biopsies treated with chemotherapeutic drugs

The aim of these experiments was to determine the viability of cancer tumour tissue whilst treated with chemotherapeutic agents within a microfluidic system. As shown in Figure 57, all chemotherapy regimens invoked a greater release of LDH than untreated tumour tissue over the 7 day treatment period. LDH was released in the greatest concentration in the combination therapy of 5-FU and CDDP. In the first 5 days of treatment, the amount of LDH released was approximately double the amount released by the untreated sample. By the final 2 days, the amount of LDH released triple the amount released by the control. CDDP induced a greater death response than 5-FU alone. The combination therapy however, showed the greatest variation between samples as shown in the error bars on the graph.

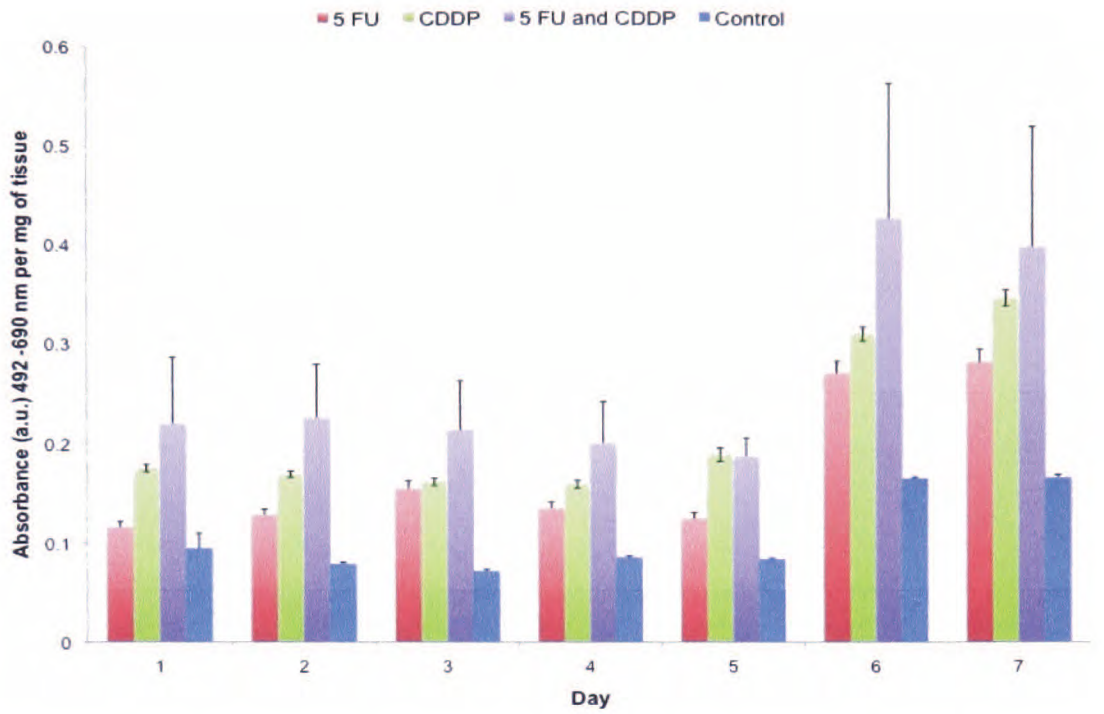

Figure 57. LDH released from HNC tissue during treatment with different chemotherapy regimes compared with untreated cancer tissue biopsies. Data are expressed as the mean absorbance levels of LDH in each the cancer sample collected every 24 hours. ±S.E.M. of three separate experiments.

In Figure 58, the effects of the chemotherapeutic agents on WST-1 metabolism are highly noticeable from Day 5. In the untreated control samples, WST-1 metabolism at Day 5 is over four and half times more than the samples treated with the chemotherapy drugs and this is maintained over the next two days of treatment. There is no marked difference in the amount of WST-1 metabolized between the three different regimes however, in these tests 5-FU treated samples seem to have a slightly greater effect over the two other treatments. This could be a reflection of the 5-FU and CDDP acting *via* different mechanisms and differences in the tumour viability before the incorporation into the microfluidic system.

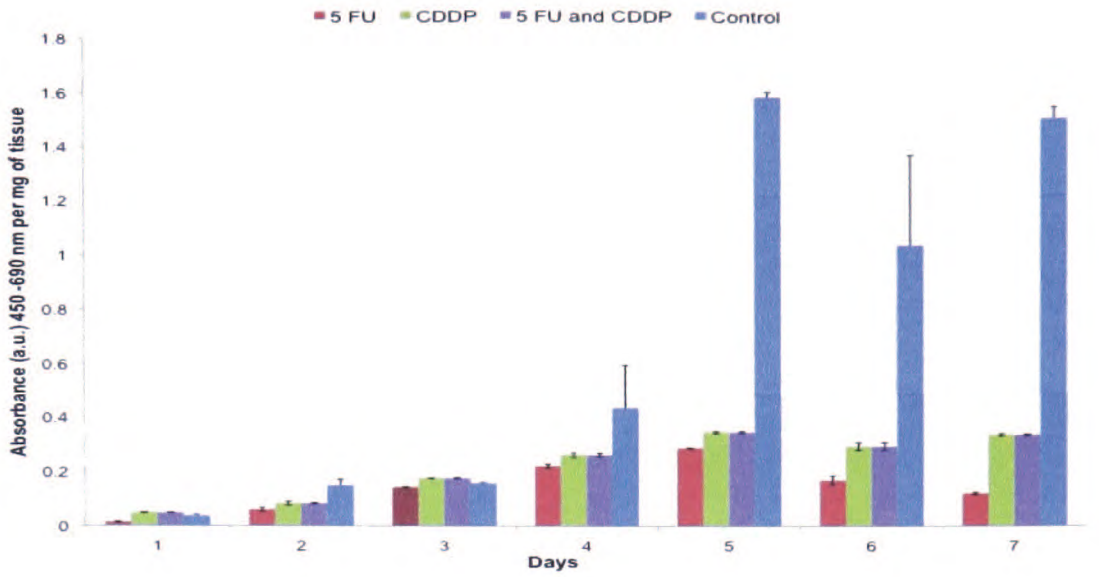

Figure 58. WST-1 metabolism in HNC tissue during treatment with different chemotherapy regimes compared to untreated cancer tissue biopsies. Aliquots were collected every 4 hours over the 7 day period. Data are expressed as the mean absorbance levels in the cancer sample eluent ±S.E.M. of three separate experiments.

This current study effectively mimics previous *in vivo* data using concurrent chemotherapy, with 5-FU and CDDP, and radiotherapy (CCRT) that were shown to be effective in the treatment of locoregionally advance nasopharyngeal carcinoma (NPC). A study of prognostic factors after CCRT in 34 patients demonstrated that increased serum LDH levels after treatment were strongly associated with distant metastasis-free survival.(382) A later study with 111 NPC patients showed that elevated serum LDH before treatment correlated with adverse prognostic factors of survival.(383) The most recent study into serum LDH levels as a prognostic factor in 61 patients with NPC treated with chemotherapy has revealed that pre-treatment LDH level as the only statistically significant prognostic factor for disease-free survival (DFS) and overall survival (OS). Four year DFS and OS rates for patients with normal serum LDH levels were 55.9% and 68.7% respectively. However, patients with high serum levels the DFS and OS rates were 21.3% and 28.5% respectively.

Previous work using WST-1 has been restricted to cell lines where the effect of tamoxifen alone and tamoxifen plus 5-FU on the proliferation of two types of gastric adenocarcinoma cell lines (KATOIII and MKN28 cells) was studied.(384) The effect of the combination of drugs resulted in anti-proliferative activity in KATOIII cells but MKN28 drugs continued to proliferate in a dose-dependant manner suggesting that some tumours have resistance mechanisms. Metabolism of WST-1 by the cell lines treated with 5-FU showed similar results to those treated with tamoxifen. Research published investigating the effect of CDDP using WST-1 demonstrated that Saos2/p53 cells were twice as sensitive to CDDP alone than Saos2 cells.(385)

These microfluidic experiments have shown the ability to model cell death by chemotherapeutic agents in HNC explants and these results are similar to those published using cell models and most importantly those found in cancer patients. Future work could include the use of other chemotherapeutic agents such as docetaxel, and the maintenance and subsequent interrogation of different cancer explants such as lung or liver tumour biopsies.

5.6.3 Viability analysis of metastatic cells

Metastasis is the spread of cancer cells from a primary tumour and subsquent colonization of distant secondary sites.(386) Metastases to regional lymph nodes are discovered at diagnosis and surgery in approximately one-third of breast, colorectal, uterine cervix and oral cavity and pharynx cancer patients.(387) High mortality rates associated with cancer are largely caused by the metastatic spread.(218) Metastasis is a multi-process involving cancer cell motility, intravasation, transit in the blood or lymph, extravasation and growth at

a new location.(388) Microfluidics has the ability to maintain tissue in its native interconnected state as shown and replicate the conditions for all the parameters of metastasis especially motility and transit in microchannels, which mimic circulatory vessels.

Cancer cells were collected in the eluent from the microfluidic system after the seven day incubation period. Eluent was collected for 3 hours in 1.5 ml micro centrifuge tubes and centrifuged at 100*g* for 5 minutes. The supernatant containing cell debris was removed by aspiration. The cells were resuspended in DMEM. To quantify cell viability equal volumes of 2% (w/v) TB and cell solution were mixed and the cell count enumerated using a haemocytometer. Counts were measured in duplicate and the percentage viability determined.

5.6.4 Analysis of metastatic cell viability after chemotherapeutic intervention

The aim of the experiment was to determine whether chemotherapeutic agents destroyed 'metastatic' cells released from the tumour tissue in the microfluidic system. The cells collected at the end of experiment resulted in approximately 3,000 cells being released from an untreated 3 mm^3 biopsy; based on haemocytometer measurements and are shown in Figure 59. The percentage of cancer cells, which survived the chemotherapy interrogation, is shown in Table 8.

The results indicate that 72% (n=3) of cells were alive from the untreated tumour biopsy, which is comparable with values determined previously in Section 3.12.1. The viability of the cancer cells treated with the chemotherapy

decreased to only 63 - 42% of the untreated tumour biopsy. The combination therapy showed the greatest reduction in cell viability in the treatment regimens in correlation with the LDH data in Section 5.7.1.

Table 8. Percentage of viable metastatic cancer cells recovered after primary tumour tissue was maintained and interrogated in microfluidic system for seven days (n=3)

Drug Regimen	*Percentage of viable cells collected in eluent from microfluidic system*
Untreated samples	72% ± 15.6
5-FU only	45% ± 22.3
CDDP only	44% ± 20.2
5-FU and CDDP combination	30% ± 23.7

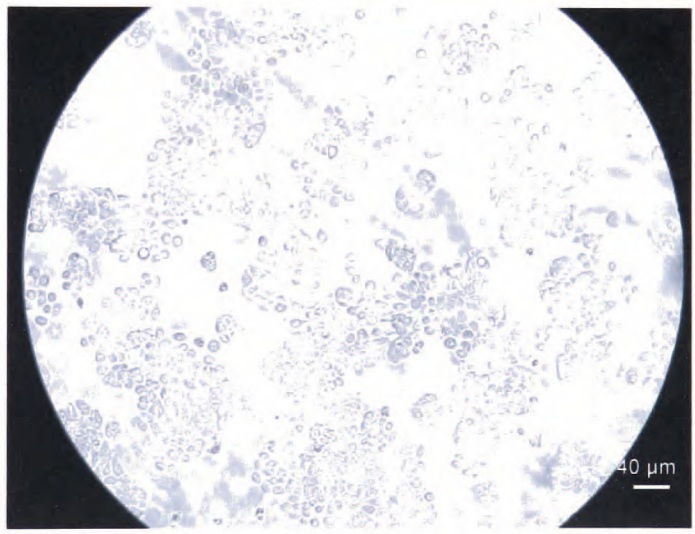

Figure 59. Cancer cells collected from untreated tumour tissue maintained in a microfluidic system. (n=3) Magnification 10 x

Furthermore this would be expected as present clinical practice of HNC management advocates the combination therapy as the desired method of treatment.(250)

5.6.5 Cytochrome c analysis

Cytochrome c is a 14.5 kDa protein, as shown in Figure 55, that is located in the inner mitochondria membrane in healthy cells and is a key component of the electron transport chain in the respiration, functioning as an electron shuttle.(389) It an efficient biological electron-transporter and it plays a vital role in cellular oxidations in both animals and plants. It is regarded as a common catalyst of respiration, forming a necessary electron-bridge between the respirable substrates and oxygen.

Figure 60. Cytochrome c with heme, currently the focus of many studies in biomarker research.(390)

During apoptosis, cytochrome *c* is liberated from the mitochondria into the cytoplasm, where it is then released into the culture media.(391) Within 1 hour after treatment, cytochrome *c* was found in the media whereas LDH was released much later.(392) In necrosis, a study has shown that cytochrome *c* remains within the cell and not found within the media. There is much speculation of the biological significance of the release of cytochrome *c*, with studies showing various anti-inflammatory effects, guiding phagocytes to sites

of injury, and increasing the effect of apoptosis and cell shrinkage by inducing K^+ efflux from cells.(392-394)

To quantify the release of cytochrome *c* within the tissue sample, a quantitative sandwich enzyme immunoassay technique (Quantikine®, Human Cytochrome *c*, R&D Systems, USA) was carried out following the manufacturer's protocol. A 96-well flat bottom ELISA plate was provided coated with monoclonal antibody against human cytochrome c. The cytochrome c reference standards (20, 10, 5, 2.5, 1.25, 0.625 ng ml^{-1}) and 100 µl of each standard and sample was incubated on the plate with 100 µl of the Calibrator Diluent RD5P for two hours. After the plate was washed a total of four times with wash buffer, the plates were incubated with 200 µl of Cytochrome *c* Conjugate for two hours. After another four washes, a colorimetric reaction was carried out by the addition of 200 µl TMB solution. The reaction was stopped with 50 µl of 2 M sulphuric acid and the absorbances were measured at λ = 450 nm. The individual four hours samples, six aliquots in twenty-four hours, were analyzed in duplicate with the results averaged over the twenty-four hours and are expressed as daily results. The experiment was repeated three times. The blank used was the unused media. Cytochrome *c* has a half-life of eight days(395) and therefore samples were kept at 4°C until the experiment was completed after seven days and all samples were analyzed on the same plate.

5.6.6 Determination of Cytochrome c release from HNSCC biopsies

The aim of this experiment was to determine whether cytochrome *c* was released from tumour biopsies maintained within a microfluidic system. Eluent collected from the microfluidic system was analyzed using the commercial

start of therapy. Cancer patients that responded to treatment and survived three years later however had lower serum levels of cytochrome *c* (25 ng ml^{-1}) within the first three days. In another *in vivo* based study it was also shown that elevated cytochrome *c* levels were observed in serum from patients with haematological malignancies and that during treatment these levels increased, that correlated with increased cell death determined through LDH release.(392) A study aimed at investigating the prognostic significance of several biomarkers, including cytochrome *c,* in surgically treated parotid cancer patients treated with adjuvant radiotherapy showed, through immunohistochemical examination of paraffin-embedded tissue specimens, from 27 patients that cytochrome *c* expression does not predict survival in parotid cancer patients.(396)

5.6.7 Nucleosomes and DNA analysis

Nucleosomes supply a mechanism for chromatin condensation and consist of four pairs of histones, encircled by dsDNA as shown in Figure 62. dsDNA is methodically cleaved by endonucleases between the histones/nucleosomes during apoptosis and fragments are released into the extracellular space.(397)

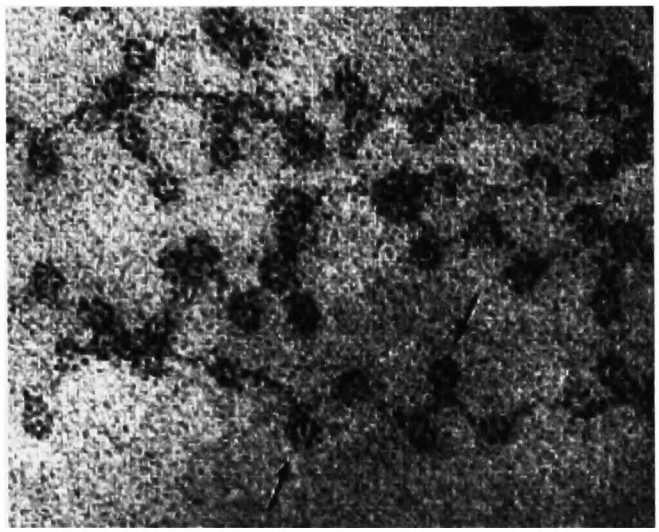

Figure 62. Electron micrograph shows chromatin from the nucleus of a chicken red blood cell. The arrangement of DNA on nucleosomes has been described as 'beads on a string'.(98)

To quantify the release of dsDNA within HNC biopsy a Quant-iT™ PicoGreen® dsDNA Assay Kit was used as described in Section 3.12. The release of dsDNA was plotted against the release of LDH, as described in Section 3.12.1, to determine whether there were any corresponding trends. The results are expressed as an average determined from triplicate samples. The blank used was the unused media.

To quantify the release of nucleosomes within the tissue sample, a quantitative sandwich enzyme immunoassay.technique (Cell Death Detection ELISA^{PLUS}, Roche, UK) was carried out following the manufacturer's protocol. A 96-well flat bottom ELISA plate was provided coated with streptavidin. A 20 μl aliquot of each sample and a positive control containing lyophilized and stabilized DNA-Histone-Complex was incubated on the plate with 80 μl of the immunoreagent. The immunoreagent contains a mixture of anti-histone biotin monoclonal murine antibodies (clone H11-4) and Anti-DNA-horseradish

peroxidase monoclonal murine antibodies (clone MCA-33). The microplate was subsequently placed on a shaking platform at 300 rpm for two hours. During the incubation period, the anti-histone antibody binds to the histone-component of the nucleosomes and simultaneously captures the immunocomplex to the streptavidin-coated microplate *via* biotinylation.

Additionally, the Anti-DNA-horseradish peroxidase antibody reacts with the DNA-component of the nucleosomes. After the plate was washed for a total of three times with wash buffer, a colorimetric reaction was carried out by the addition of 100 µl 2,2'-azino-bis(3-ethylbenzthiazoline-6-sulphonic acid) (ABTS) and placed back on the shaking platform at 250 rpm. The reaction was stopped after twenty minutes with 100 µl of ABTS stop solution supplied by the manufacturer and the absorbances were measured at λ = 405 nm. The individual four hour samples, six aliquots in twenty-four hours, were analyzed in duplicate with the results averaged over the twenty-four hours and are expressed as daily results. The experiment was repeated three times. The blank used was the unused media. The samples were kept at 4°C until the experiment was completed and all samples were analyzed on the same plate.

5.6.8 dsDNA and nucleosome release from HNC biopsies

Measuring changes in dsDNA and nucleosomes release from NHC tumour tissue within a microfluidic system was the purpose of these experiments. Eluent collected from the microfluidic system was analyzed firstly using a fluorescent dye for dsDNA and secondly, an immunoassay containing a monoclonal antibody specific for histones and dsDNA. The graph in Figure 63 shows the release of dsDNA from an untreated cancer sample. This experiment

was conducted only once as the release of DNA appeared erratic and bears no resemblance to the underlying LDH trend after 29 hours of maintenance in the microfluidic system. It can therefore be assumed that dsDNA has been released from viable cells within the biopsy as the LDH results denote negligible numbers of apoptotic or necrotic cells. The rises and falls could be due to proliferating cells, as it has been shown previously in Sections 5.4.1 and 5.5.1 that the WST-1 absorbance also increased after two days of incubation, and the flow dynamics of the system such as diffusion into the tissue of WST-1 and the release into the media of formazan from inside the tissue biopsy.

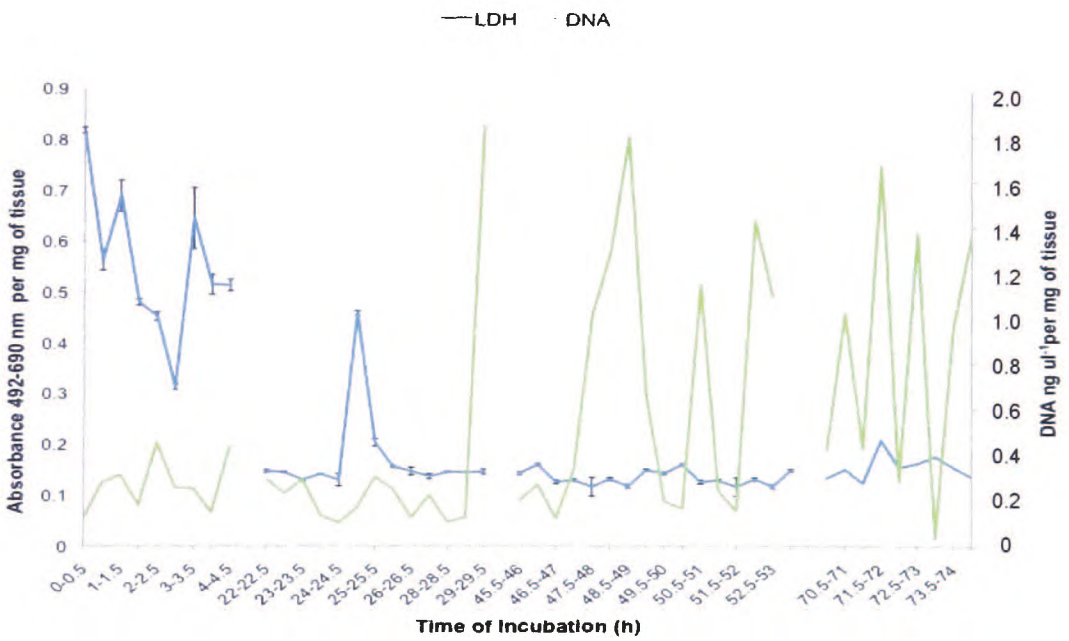

Figure 63. DNA release compared with LDH release from an untreated HNC tumour biopsy in microfluidic device. Gaps in the graph equate to times unmonitored overnight.

There is no other possible explanation for the enormously fluctuating DNA concentrations such as with loss of DNA to other surfaces within the device (chip surfaces, tumour surface) and is more likely due to the erratic nature of the cell cycle of the cancer cells, as described in the introduction chapter.

Circulation cell free DNA (cfDNA) has gained considerable interest for oncology researchers seeking to isolate specific cancer markers over last decade. Previous studies have reported DNA fragments in the serum of cancer patients, apparently because apoptosis and necrosis are happening in and around the tumour.(399) Macrophages would usually remove this debris, however due to limited circulatory access movement of macrophages around the tumour can be restricted. Soluble DNA fragments have been identified in the supernatant of Jurkat T cells induced to undergo apoptosis with 1.2 M staurosporine, or necrosis with 2.5 M oligomycin and 1.2 M staurosporine *in vitro*.(400)

The prevalent belief within the oncology field presumes that cfDNA arises from apoptotic or necrotic cancer cells in relation to cancer metastasis.(401) However, reanalysis of the current literature has proposed that cfDNA is principally secreted by living cancer cells rather than from apoptotic or necrotic cells. For example in response to radiotherapy, in high percentage of patients with lymphoma, lung, ovary, uterus and cervical cancers, cfDNA was significantly decreased to 66–90% of pre-treatment rather than being increased. These results suggest that the significant portion of cfDNA may derive from living cancer cells.(399)

Secondly, oncogene-containing cfDNA may behave like oncoviruses and represent an alternative pathway for cancer metastasis as circulation DNA contain oncogenes, hypermethylated tumour suppressor genes and aberrant

microsatellites, that are identical to those found in the patient's tumour tissue.(402) *In vitro* experiments have also demonstrated that free DNA can enter and transform normal cells and these can grow into neoplasms when injected into mice.(403)

Lastly, cancer has the propensity to colonize in specific tissues (such as lymph nodes) since there are DNA binding proteins or receptors on the cell surface.(404-407) Further analysis regarding the origin and function of cfDNA could have major implications for cancer biologists and medicine if these conclusions are accurate.

To complement the DNA analysis, nucleosomes were examined using an immunoassay. In Figure 64, all of the eluent collected from the treated samples showed an elevated level of nucleosomes compared with the control sample.

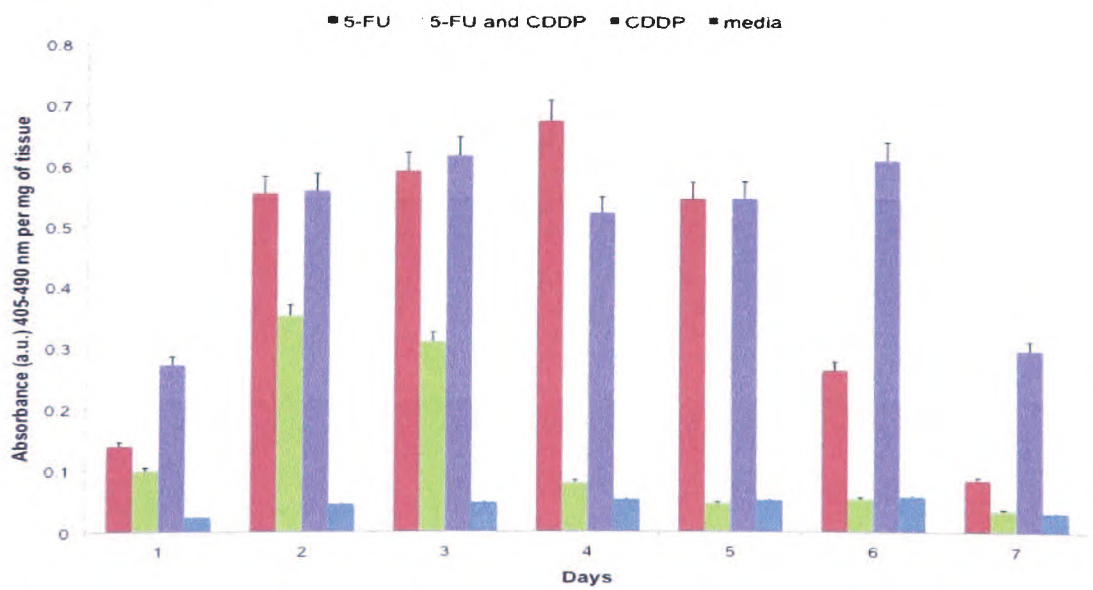

Figure 64. Nucleosomes and DNA released from HNC tissue during treatment with different chemotherapy regimes compared to untreated cancer tissue biopsies. Data are expressed as the mean absorbance levels over 24 hours in the cancer sample eluent ±S.E.M. of three separate experiments.

The nucleosomes released in the control sample remained relatively stable over the experimental period with the average absorbance levels per mg of tissue remaining at 0.44 AU ±0.01. The samples with the highest level of nucleosome expression over the entire experiment were the HNC biopsies treated with only CDDP with the average absorbance per mg of tissue recorded at 0.481 AU ±0.149. This was almost 11 times higher than the levels recorded from the control sample. The 5-FU administered biopsies showed the same profile with the highest absorbance from all treatments on Day 4 at 0.676 AU ±0.0338, this was 13 times higher than the control sample on the same day. However from Day 5 the concentration of nucleosomes released from the 5-FU biopsies steadily decreases to only 12% of this high by Day 7.

The cancer biopsies treated with both chemotherapeutic agents showed a similar profile however, they exhibited lower concentrations than the single drug samples (three times lower than CDDP and 5-FU) and by Day 5 the concentration was almost parallel to those in the control samples. This was surprising, as it would be assumed that the effect of the combination of drugs would cause a higher degree of cell death than the single drug regimen. The study of released nucleosomes as a biomarker of cancer effectiveness is still developing. A previous study demonstrated the release of nucleosomes from tumour cells *in vitro* and *in vivo* after treatment with CDDP.(379) Using HeLa cells *in vitro*, nucleosome expression increased after 24 hours however, in subsequent murine models bearing HeLa tumours a decrease in nucleosome expression after 24 hours was shown. A study of non-small cell lung cancer

patients undertaking chemotherapy (8 mg/m^2 mitomycin c, 25 mg/m^2 vinorelbin, and 80 mg/m^2 CDDP) showed, using the same assay as was used in this thesis, that there was an increase in nucleosomes within serum samples followed by a decrease during intervals in between treatment.(408) Patients who responded to treatment or were in remission encountered less of an early increase (pre-therapeutic value, 344 AU; maximum value, 436 AU) in nucleosomes level followed by a significant decrease (140 AU) after 8 days. Patients that did not respond exhibited a higher initial increase (pre-therapeutic value, 442 AU; maximum value, 632 AU) and these levels did not decrease as rapidly (290 AU) as those patients that did respond to treatment. The reason put forward for these phenomena is the variable rates in cell death and proliferation in the aggressive tumours along with greater access to blood vasculature in patients with metastasis. At time of writing, there has been no research into nucleosome expression in HNC patients during treatment.

Head and neck cancer has a low survival rate and while there have been advances in clinical treatment regimes, translation of these improvements into decreases in the mortality rate have not been achieved. Developments in *in vitro* pre-clinical models to assess the effectiveness of established and novel chemotherapy drugs in patients before treatment commences, would allow a more informed decision by both the clinical team and the patient. Both the scientific and medical fields have acknowledged that the measurement of biomarkers would be an effective tool in clarifying whether the cancer treatment has been successful. To this end, many studies in cancer biomarkers have been completed, utilizing cell lines and patients themselves. These studies have been productive in providing invaluable information nonetheless; they all

have their limitations. Models that use cell lines lack the complexity of the *in vivo* microenvironment. Patient studies have been the most informative, but there have been questions about the exact nature of the results and what is actually being demonstrated. Tissue-based microfluidic systems are able to replicate the *in vivo* microenvironment of the tumour, while also containing multiple cell types and maintaining the native tissue architecture. It has been shown that the viability of the tumour biopsy remained intact and by implementing current chemotherapy regimens, a response has been observed in several clinically relevant biomarkers. This work provides an important first step into the development of a pre-clinical model, which can be used to provide further intelligence into the progression and treatment of cancer.

6. Conclusion

'It's more fun to arrive a conclusion than to justify it.'

Malcolm Forbes 1919-1990

The last decade has been an exciting time for biological microfluidic studies however; there has been little investigation into tissue-based systems. The reason for the lack of interest in tissue-based microfluidics is twofold; firstly, cell culture has been used in biological studies for over ninety years with a high degree of success in modelling physiological and pathological dynamics. The parameters of maintaining and growing different cell types have been extensively examined and defined. The success of this research is that there has been little change in the cell culture methodology since the 1980s. The second reason is that even though tissue and organ culture has been shown to be more reflective of the mechanisms found *in vivo,* maintaining tissue viability and more importantly functionality *in vitro* through traditional methods is exceedingly difficult. However, the research presented in this thesis demonstrated the potential that microfluidics has in mimicking *in vivo* dynamics through the maintenance of tissue.

The first experimental section of this thesis focused the design and fabrication the microfluidic device and system. The preliminary investigations of maintaining tissue viability and morphology where examined using microscopy, histology and biochemical assays. This work showed that the microfluidic

chamber system provided sufficient oxygen and nutrients for the tissue to remain healthy without any major loss of ECM or increase of non-viable cells within the sample and that these patterns were repeatable for individual biopsies over time. The ability to interrogate the tissue to envoke a response was also tested and proven, alongside the ability to study the cells both within tissue environment and individually through disaggregation. After constructing the microfluidic device and verifying the flow profiles and with the success of the viability studies using LDH measurements and fluorescence assays showing that the tissue was remaining viable within the microfluidic system with the addition lysis buffer verifying the viability.

The second section examined the possibility of using the system as a future model of hepatotoxicity by insulting the tissue with several different chemicals, the main being ethanol. The functionality of the liver was assessed both prior to interrogation and afterwards, and demonstrated not only the ability to maintain function of liver tissue over five days but also the ability to effect the function of liver sample over the same time period. Models of *in vivo* liver dynamics are being actively sought and whilst this system was not used to examine fully liver tissue differentiation and function, it is a vital step forward. It has been shown that rat liver samples were kept viable and functional over ninety-six hour time period. WST-1 was metabolised and reduced to formazan, which was subsequently detected off-chip along with the detection of LDH release from cells maintained and/or interrogated on-chip. Addition of different ethanol concentrations decreased the amount of formazan detected over the time period indicating the ethanol was affecting cell viability over the time period compared to a control. The addition of ethanol to the liver samples exhibited

many of the same characteristics noted in other studies which have used isolated hepatocytes and *in vivo* rat models of chronic ethanol intoxication including the decrease in viability, fatty liver progression, reduction of albumin production, change in cell morphology and decrease in urea levels.(317, 350) In this thesis, liver samples millimetres in thickness were used to ensure that even the cell types that were sparsely represented within the tissue such as cholangiocytes were included and the native complex ECM was maintained which is not present in cell-based models. Using microfluidic technology we have also mimicked the *in vivo* flow dynamics, which is not present in conventional cell and tissue representations.(116) Therefore, it is proposed that rat liver samples retain their biological functions and appeared to a novel and valuable model for the study of not only pathological but also physiological mechanisms.

The final chapter examined the feasibility of the microfluidic system to model the cancer microenvironment for future pre-clinical and personalized patient models. Viability of the head and neck cancer tissue was assured over eight days of culture with the tissue subsequently treated with commonly used chemotherapy drugs with the analysis of biomarkers, which have been identified in clinical studies. Head and neck cancer has a low survival rate and while there have been advances in clinical treatment regimes, translation of these improvements into decreases in the mortality rate have not been achieved. Developments in *in vitro* pre-clinical models to assess the effectiveness of established and novel chemotherapy drugs in patients before treatment commences, would allow a more informed decision by both the clinical team and the patient. Both the scientific and medical fields have acknowledged that

the measurement of biomarkers would be an effective tool in clarifying whether the cancer treatment has been successful. To this end, many studies in cancer biomarkers have been completed, utilizing cell lines and patients themselves. These studies have been productive in providing invaluable information nonetheless; they all have their limitations. Models that use cell lines lack the complexity of the *in vivo* microenvironment. Patient studies have been the most informative, but there have been questions about the exact nature of the results and what is actually being demonstrated. Tissue-based microfluidic systems are able to replicate the *in vivo* microenvironment of the tumour, while also containing multiple cell types and maintaining the native tissue architecture. It has been shown that the viability of the tumour biopsy remained intact and by implementing current chemotherapy regimens, a response has been observed in several clinically relevant biomarkers. This work provides an important first step into the development of a pre-clinical model, which can be used to provide further intelligence into the progression and treatment of cancer.

The challenge of the microfluidic community, in respect to tissue and organ biology, is to move beyond the need to replicate conventional cell-based methodologies within microfluidic systems and appreciate the gaps in biological knowledge that microfluidic technology can fill. This thesis has examined the ability to investigate and alter the microenvironment of an *ex vivo* tissue sample has the potential to open new avenues in cell signaling, molecular biology, systematics, and developmental biology that with current methods and techniques is impossible.

7. Future Work

'Imagination is more important than knowledge. Knowledge is limited. Imagination encircles the world.'

Albert Einstein 1879-1955

It is usual at the end of a thesis for the author to suggest future opportunities that their research has afforded. In the case of this thesis, a more apt statement would be, 'what can't be done'. The vast majority of studies into cell biology have used cell-based models that many biologists agree only give a fraction of the whole picture and that snapshot is sometimes so distorted that it bears no relation to the original image. The tissue-based microfluidic model demonstrated within this thesis is 'one small step' to a future 'giant leap' in bringing into focus the complexity of *in vivo* dynamics. In the first chapter, many of the current avenues of research in cell biology using microfluidic technology were acknowledged. Many of these studies could be transferred to tissue-based methodologies with little or no difficulty, allowing a greater understanding of cell kinetics within the context of a tissue environment.

Continuation of the current studies described in this thesis would be the addition of downstream modules to the microfluidic system to allow the culture and analysis of tissue all on the same platform. Interrogation and then subsequent disaggregation of the tissue to the single cell, could allow the ability to replicate the 3D *in vivo* microenvironment followed by the rapid analysis of single cells to substantiate individual effects on different cells, cell products and

ECM. This would be achieved by the coupling the tissue chamber to a separation chamber and holding areas as illustrated in Figure 65, which were designed by the author, and Jane Woods.

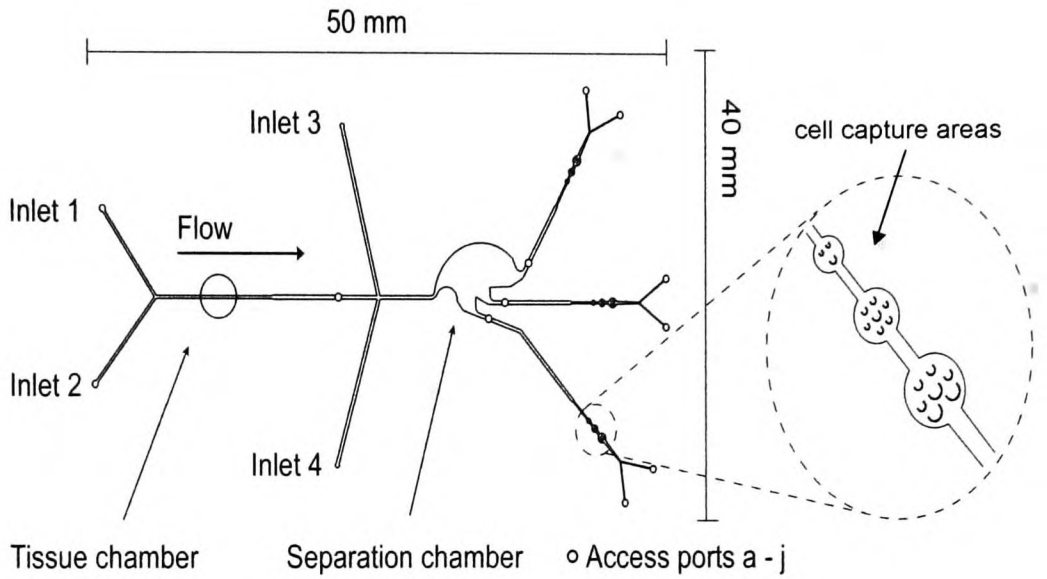

Figure 65. Schematic of microfluidic device for the maintenance of tissue, disaggregation and separation of cells, cell products and ECM.

Further refinements of the system would be to add different analysis modules at the end of each 'arm', as shown in Figure 66. These modules could include a polymerase chain reaction (PCR) component, for the analysis of DNA from lysed cells or extracellular fragments, a microarray, for the analysis of individual intracellular and extracellular proteins, and the final module could be a flow cell section for the analysis of enzyme function.

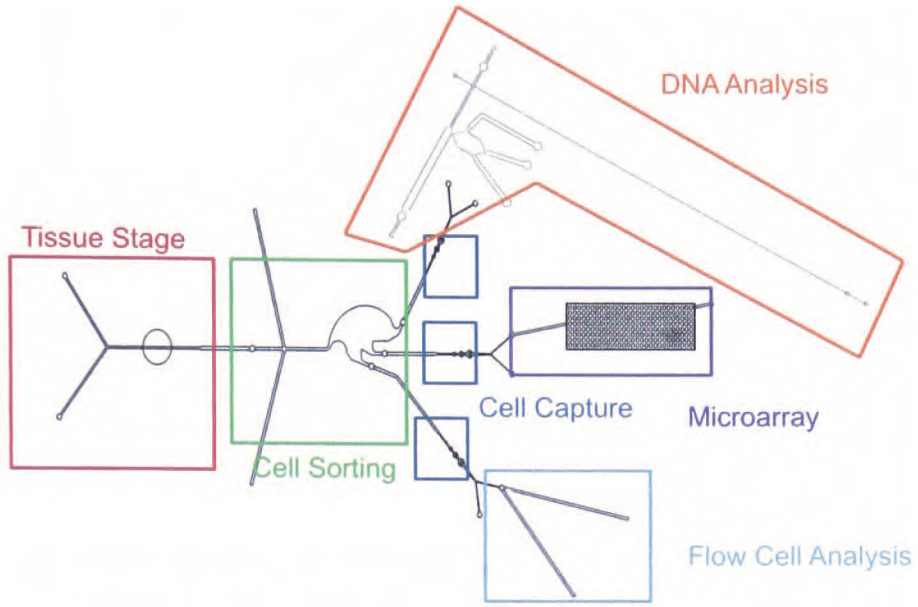

Figure 66. Schematic of envisioned 'lab on a chip' for the analysis of tissue culture.

These components coupled on the same system would allow the analysis of a single or indeed many different important cellular pathways from small samples, giving access to large amount of information which is not currently possible using conventional methodology. This would be definitely classed as a 'lab on a chip'.

8. Publications

Articles

Hattersley SM, Dyer CE, Greenman J, Haswell SJ. Development of a microfluidic device for the maintenance and interrogation of viable tissue biopsies. Lab on a Chip. 2008;8(11):1842-6.

Hattersley S.M, Slyvester D, Dyer C.E, Stafford N.D, Haswell S.J, Greenman J. An innovative explant tissue model using microfluidics for the study of tumour tissue responses. In preparation

Conference presentations

Poster: Tissue processing in a microfluidic environment, S.M. Hattersley, J. Greenman and S.J. Haswell, Analytical Research Forum 2007, 16 - 18 July 2007, University of Strathclyde, Glasgow, United Kingdom

Oral: *In situ* tissue interrogation and cell isolation using a microfluidic device, 22nd International Symposium on Microscale Bioseparations and Methods for Systems Biology (MSB 2008), Freie Universität, Berlin, Germany, March 9-13, 2008.

Poster: Development of a microfluidic device for them and interrogation of viable tissue biopsies, S.M. Hattersley, C.E. Dyer, J. Greenman and S.J.

Haswell, Analytical Research Forum 2008, University of Hull, Kingston upon Hull, United Kingdom, 21 - 23 July 2008.

Poster: On-chip disaggregation of primary human cancer cells from tumour biopsies for analysis in a microfluidic device, J. Woods, S.M. Hattersley, L.A. Madden, P.T. Docker, K.C. Jiang, C.E. Dyer, J. Greenman and S.J. Haswell, The 12th International Conference on Miniaturized Systems for Chemistry and Life Sciences, μTAS 2008 Conference, San Diego, USA, October 12-16, 2008.

Poster: A tissue-based microfluidic system for preclinical toxicology and chemotherapy studies: another 'small' step towards personalized medicine Samantha M. Hattersley, Jane Woods, Charlotte E. Dyer, John Greenman and Stephen J. Haswell, The 5th International Conference on Microtechnologies in Medicine and Biology, MMB 2009 Conference, Quebec City, Canada, April 1-9, 2009.

Poster: Development of microfluidic based devices for studying tumour biology and evaluating treatment response in head and neck cancer biopsies, D. Sylvester, S.M. Hattersley, S.J. Haswell, N.D Stafford, J. Greenman, Hull University Biomedical Sciences Research Day, University of Hull, Kingston upon Hull, United Kingdom, 21st July 2010

Poster: Development of microfluidic based devices for studying tumour biology and evaluating treatment response in head and neck cancer biopsies,

D. Sylvester, S.M. Hattersley, S.J. Haswell, N.D Stafford, J. Greenman, ENT UK Annual Conference in association with the Otorhinolaryngological Research Society, University Hospital, Coventry, United Kingdom, 10th September 2010,

Poster: Microfluidic devices for evaluating head and neck tumour biology, D. Sylvester, S.M. Hattersley, C.E. Dyer, S.J. Haswell, N.D Stafford, J. Greenman, American Academy of Otolaryngology Head and Neck Surgery Foundation 2010 Annual Meeting, Boston, USA, 26th-30th September 2010

Poster: Development of microfluidic based devices for studying tumour biology and evaluating treatment response in head and neck cancer biopsies, D. Sylvester, S.M. Hattersley, C.E. Dyer, S.J. Haswell, N.D Stafford, J. Greenman, The 14th International Conference on Miniaturized Systems for Chemistry and Life Sciences, μTAS 2010 Conference, Groningen, The Netherlands, 3-7 October 2010

9. References

1. El-Ali J, Sorger PK, Jensen KF. Cells on chips. Nature. 2006;442(7101):403-11.

2. Squires TM, Quake SR. Microfluidics: Fluid physics at the nanoliter scale. Reviews of Modern Physics. 2005;77(3):977-1026.

3. Doroszewski J, Skierski J, Przadka L. Interaction of neoplastic cells with glass surface under flow conditions. Experimental Cell Research. 1977;104(2):335-43.

4. Greenwood PA, Greenway GM. Sample manipulation in micro total analytical systems. TrAC - Trends in Analytical Chemistry. 2002;21(11):726-40.

5. Gad-el-Hak M. The Fluid Mechanics of Microdevices -The Freeman Scholar Lecture. Journal of Fluids Engineering. 1999;121:5-33.

6. Fluid Mechanics: Overview. eFunda Inc; 2010 [28 November 2010].

7. Berk BC. Atheroprotective signaling mechanisms activated by steady laminar flow in endothelial cells. Circulation. 2008;117(8):1082-9.

8. Tardy Y, Resnick N, Nagel T, Gimbrone Jr MA, Dewey Jr CF. Shear stress gradients remodel endothelial monolayers in vitro via a cell proliferation-migration-loss cycle. Arteriosclerosis, Thrombosis, and Vascular Biology. 1997;17(11):3102-6.

9. Fagerberg B, Ryndel M, Kjelldahl J, Akyurek LM, Rosengren L, Karlstrom L, et al. Differences in lesion severity and cellular composition between in vivo assessed upstream and downstream sides of human symptomatic carotid atherosclerotic plaques. Journal of Vascular Research. 2010;47(3):221-30.

10. Takayama S, McDonald JC, Ostuni E, Liang MN, Kenis PJA, Ismagilov RF, et al. Patterning cells and their environments using multiple laminar fluid flows in capillary networks. Proceedings of the National Academy of Sciences of the United States of America. 1999;96(10):5545-8.

11. Takayama S, Ostuni E, LeDuc P, Naruse K, Ingber DE, Whitesides GM. Selective Chemical Treatment of Cellular Microdomains Using Multiple Laminar Streams. Chemistry & Biology. 2003;10(2):123-30.

12. Zhang MY, Lee PJ, Hung PJ, Johnson T, Lee LP, Mofrad MRK. Microfluidic environment for high density hepatocyte culture. BIOMEDICAL MICRODEVICES. 2008;10(1):117-21. doi: 10.1007/s10544-007-9116-9.

13. Wu MH, Huang SB, Cui ZF, Cui Z, Lee GB. A high throughput perfusion-based microbioreactor platform integrated with pneumatic micropumps for three-dimensional cell culture. Biomedical Microdevices. 2008;10(2):309-19. doi: 10.1007/s10544-007-9138-3|ISSN 1387-2176.

14. Simms HA, Bowman CA, Anseth KS. Using living radical polymerization to enable facile incorporation of materials in microfluidic cell culture devices. Biomaterials. 2008;29(14):2228-36. doi: 10.1016/j.biomaterials.2008.02.001|ISSN 0142-9612.

15. Park J, Li Y, Berthiaume F, Toner M, Yarmush ML, Tilles AW. Radial flow hepatocyte bioreactor using stacked microfabricated grooved substrates. Biotechnology and Bioengineering. 2008;99(2):455-67.

16. Hung PJ, Lee PJ, Sabounchi P, Lin R, Lee LP. Continuous perfusion microfluidic cell culture array for high-throughput cell-based assays. Biotechnology and Bioengineering. 2005;89(1):1-8.

17. Leclerc E, Corlu A, Griscom L, Baudoin R, Legallais C. Guidance of liver and kidney organotypic cultures inside rectangular silicone microchannels. Biomaterials. 2006;27(22):4109-19.

18. Ong S-E, Zhang S, Du H, Fu Y. Fundamental principles and applications of microfluidic systems. Front Biosci. 2008;13:2757-73.

19. Zhao B, Moore JS, Beebe DJ. Surface-directed liquid flow inside microchannels. Science. 2001;291(5506):1023-6.

20. Gravesen P, Branebjerg J, Jensen OS. Microfluidics - A review. Journal of Micromechanics and Microengineering. 1993;3(4):168-82.

21. Bayraktar T, Pidugu SB. Characterization of liquid flows in microfluidic systems. International Journal of Heat and Mass Transfer. 2006;49(5-6):815-24. doi: 10.1016/j.ijheatmasstransfer.2005.11.007.

22. Hetsroni G, Mosyak A, Pogrebnyak E, Yarin LP. Fluid flow in micro-channels. International Journal of Heat and Mass Transfer. 2005;48(10):1982-98. doi: 10.1016/j.ijheatmasstransfer.2004.12.019.

23. Zhu G, Alexeev A, Balazs AC. Designing constricted microchannels to selectively entrap soft particles. Macromolecules. 2007;40(14):5176-81.

24. Krishnan A. Taylor made microdevices. 2006 [cited 2006 Nov 2006]; Available from: https://http://www.aesociety.org/areas/electrokinetics.php.

25. Izquierdo S, Fueyo N. Optimal preconditioning of lattice Boltzmann methods. Journal of Computational Physics. 2009;228(17):6479-95.

26. Hong ZC, Zhen CE, Yang CY. Fluid dynamics and heat transfer analysis of three dimensional microchannel flows with microstructures. Numerical Heat Transfer; Part A: Applications. 2008;54(3):293-314.

27. Bao FB, Lin JZ, Shi X, editors. Simulation of gas flow and heat transfer in micro Poiseuille flow. 3rd IEEE International Conference on Nano/Micro Engineered and Molecular Systems, NEMS; 2008.

28. Chen S, Tian Z. Simulation of microchannel flow using the lattice Boltzmann method. Physica A: Statistical Mechanics and its Applications.

29. Cai C, Boyd ID, Fan J, Candler GV. Direct simulation methods for low-speed microchannel flows. Journal of thermophysics and heat transfer. 2000;14(3):368-78.

30. Raisee M, Shad MM, Hosseinalipoor SM, Farokhirad S, editors. Two-dimensional unstructured direct simulation Monte Carlo method for micro/nanochannel gas flows2009; Pohang.

31. Arce P. What is Electrokinetics? : The American Electrophoresis Society; 2010 [cited 2010 2 December 2010]; Available from: http://www.aesociety.org/areas/electrokinetics.php.

32. Haeberle S, Zengerle R. Microfluidic platforms for lab-on-a-chip applications. Lab on a Chip. 2007;7(9):1094-110.

33. Barz DPJ, Ehrhard P. Simulation of flow and mass transport in a meander microchannel subject to electroosmotic pumping. Microscale Thermophys Eng. 2005;9(3):305-16. doi: 10.1080/10893950500196493.

34. Wang W, Zhou F, Zhao L, Zhang JR, Zhu JJ. Measurement of electroosmotic flow in capillary and microchip electrophoresis. Journal of Chromatography A. 2007;1170(1-2):1-8.

35. Kang Y, Li D. Electrokinetic motion of particles and cells in microchannels. Microfluidics and Nanofluidics. 2009;6(4):431-60.

36. Liu BF, Xu B, Zhang G, Du W, Luo Q. Micro-separation toward systems biology. J Chromatogr A. 2006;1106(1-2):19-28.

37. Vykoukal J, Yang J, Becker FF, Gascoyne PRC, Krulevitch P, Ackler H, et al. A combined dielectrophoretic and field-flow fractionation microsystem for biomedical separation and analysis. Micro Total Analysis Systems 2000, Proceedings. 2000:127-30.

38. Hughes MP. Dielectrophoretic behavior of latex nanospheres: Low-frequency dispersion. Journal of Colloid and Interface Science. 2002;250(2):291-4.

39. Keh HJ, Liu YC. Electrokinetic Flow in a Circular Capillary with a Surface Charge Layer. Journal of Colloid and Interface Science. 1995;172(1):222-9.

40. Kamholz AE, Weigl BH, Finlayson BA, Yager P. Quantitative analysis of molecular interaction in a microfluidic channel: The T-sensor. ANALYTICAL CHEMISTRY. 1999;71(23):5340-7.

41. Walker GM, Zeringue HC, Beebe DJ. Microenvironment design considerations for cellular scale studies. Lab on a Chip. 2004;4(2):91-7.

42. Smith GD, Takayama S. Gamete and embryo isolation and culture with microfluidics. Theriogenology. 2007;68(SUPPL. 1).

43. Walum E, Hedander J, Garberg P. Research perspectives for pre-screening alternatives to animal experimentation: On the relevance of cytotoxicity measurements, barrier passage determinations and high throughput screening in vitro to select potentially hazardous compounds in large sets of chemicals. Toxicology and Applied Pharmacology. 2005;207(2, Supplement 1):393-7.

44. Harrison R. Observations on the living developing nerve fiber. The Anatomical record 1907;1:116-28.

45. Wigley CB. The cell culture laboratory. In: Davis JM, editor. Basic Cell Culture. 2nd ed. Oxford: Oxford University Press; 2002. p. 1-27.

46. Pizzoferrato A, Ciapetti G, Stea S, Cenni E, Arciola CR, Granchi D, et al. Cell culture methods for testing biocompatibility. Clinical Materials. 1994;15(3):173-90.

47. Carrel A. Journal of Experimental Medicine. 1912;15:516.

48. Hayflick L, Moorhead PS. The serial cultivation of human diploid cell strains. Experimental Cell Research. 1961;25(3):585-621.

49. Abmayr SM, Balagopalan L, Galletta BJ, Hong SJ. Cell and molecular biology of myoblast fusion. International Review of Cytology2003. p. 33-89.

50. Katz JP, Kaestner KH. Cellular and molecular mechanisms of carcinogenesis. Gastroenterology Clinics of North America. 2002;31(2):379-94.

51. Kiechle FL. DNA technology, the clinical laboratory, and the future. Archives of Pathology and Laboratory Medicine. 2001;125(1):72-6.

52. Domon T, Yamazaki Y, Fukui A, Ohnishi Y, Takahashi S, Yamamoto T, et al. Ultrastructural study of cell-cell interaction between osteoclasts and osteoblasts/stroma cells in vitro. Annals of Anatomy - Anatomischer Anzeiger. 2002;184(3):221-7.

53. Porter BD, Lin ASP, Peister A, Hutmacher D, Guldberg RE. Noninvasive image analysis of 3D construct mineralization in a perfusion bioreactor. Biomaterials. 2007;28(15):2525-33.

54. Kemp RB. The application of heat conduction microcalorimetry to study the metabolism and pharmaceutical modulation of cultured mammalian cells. Thermochimica Acta. 2001;380(2):229-44.

55. MacDonald C. Primary culture and the establishment of cell lines. In: Davis JM, editor. Basic Cell Culture. 2nd ed. Oxford: Oxford University Press; 2002. p. 191-225.

56. Goldstein S. Aging in vitro. Growth of cultured cells from the Galapagos tortoise. Experimental Cell Research. 1974;83(2):297-302.

57. Rohme D. Evidence for a relationship between longevity of mammalian species and life spans of normal fibroblasts in vitro and erythrocytes in vivo. Proceedings of the National Academy of Sciences of the United States of America. 1981;78(8 I):5009-13.

58. Sherwood SW, Rush D, Ellsworth JL, Schimke RT. Defining cellular senescence in IMR-90 cells: A flow cytometric analysis. Proceedings of the National Academy of Sciences of the United States of America. 1988;85(23):9086-90.

59. Yamanaka S. Strategies and New Developments in the Generation of Patient-Specific Pluripotent Stem Cells. Cell Stem Cell. 2007;1(1):39-49.

60. Oback B, Wells DN. Cloning cattle: The methods in the madness. Advances in Experimental Medicine and Biology2007. p. 30-57.

61. Brendler-Schwaab SY, Schmezer P, Liegibel U, Weber S, Michalek K, Tompa A, et al. Cells of different tissues for in vitro and in vivo studies in toxicology: Compilation of isolation methods. Toxicology in Vitro. 1994;8(6):1285-302.

62. Novelli M, Savoia P, Cambieri I, Ponti R, Comessatti A, Lisa F, et al. Collagenase digestion and mechanical disaggregation as a method to extract and immunophenotype tumour lymphocytes in cutaneous T-cell lymphomas. Clinical and Experimental Dermatology. 2000;25(5):423-31.

63. Cunningham RE. Tissue disaggregation. Methods in molecular biology (Clifton, NJ). 2010;588:327-30.

64. Cooke JE, Godin I, Ffrench-Constant C, Heasman J, Wylie CC. Culture and manipulation of primordial germ cells. Methods in Enzymology. 1993;225:37-58.

65. Alexeev V, Igoucheva O, Domashenko A, Cotsarelis G, Yoon K. Localized in vivo genotypic and phenotypic correction of the albino mutation in skin by RNA-DNA oligonucleotide. Nature Biotechnology. 2000;18(1):43-7.

66. Falchetti ML, Falcone G, D'Ambrosio E, Verna R, Alema S, Levi A. Induction of telomerase activity in v-myc-transformed avian cells. Oncogene. 1999;18(7):1515-9.

67. Mitchell MS, Bodine ET, Hill S, Princler G, Lloyd P, Mitsuya H, et al. Phenotypic and genotypic comparisons of human T-cell leukemia virus type 1 reverse transcriptases from infected T-cell lines and patient samples. J Virol. 2007;81(9):4422-8.

68. Santerre RF, Cook RA, Crisel RMD, Sharp JD, Schmidt RJ, Williams DC, et al. Insulin synthesis in a clonal cell-line of simian virus-40- transformed hamster pancreatic beta cells. Proceedings of the National Academy of Sciences of the United States of America-Biological Sciences. 1981;78(7):4339-43.

69. Dimri G, Band H, Band V. Mammary epithelial cell transformation: Insights from cell culture and mouse models. Breast Cancer Research. 2005;7(4):171-9.

70. Filaci G, Gerloni M, Rizzi M, Castiglioni P, Chang HD, Wheeler MC, et al. Spontaneous transgenesis of human B lymphocytes. Gene Therapy. 2004;11(1):42-51.

71. Reich NC, Levine AJ. Growth regulation of a cellular tumour antigen, p53, in nontransformed cells. Nature. 1984;308(5955):199-201.

72. Rosenberger RF, Gounaris E, Kolettas E. Mechanisms responsible for the limited lifespan and immortal phenotypes in cultured mammalian cells. Journal of Theoretical Biology. 1991;148(3):383-92.

73. Jones RT, Hudson EA, Resau JH. A review of in vitro and in vivo culture techniques for the study of pancreatic carcinogenesis. Cancer. 1981;47(6 Suppl):1490-6.

74. Anderson G, Jenkinson EJ. Use of explant technology in the study of in vitro immune responses. Journal of Immunological Methods. 1998;216(1-2):155-63.

75. Sen J, Venkataraman L, Shinkai Y, Pierce JW, Alt FW, Burakoff SJ, et al. Expression and induction of nuclear factor-Œ∫B-related proteins in thymocytes. J Immunol. 1995;154(7):3213-21.

76. Anderson G, Moore NC, Owen JJT, Jenkinson EJ. 1996. p. 73-99.

77. Nakayama T, June CH, Munitz TI, Sheard M, McCarthy SA, Sharrow SO, et al. Inhibition of T cell receptor expression and function in immature CD4+CD8+ cells by CD4. Science. 1990;249(4976):1558-61.

78. Moore NC, Jenkinson EJ, Owen JJT. Effects of the thymic microenvironment on the response of thymocytes to stimulation. European Journal of Immunology. 1992;22(10):2533-7.

79. Resau JH, Sakamoto K, Cottrell JR, Hudson EA, Meltzer SJ. Explant organ culture: A review. Cytotechnology. 1991;7(3):137-49.

80. Mukesh M, Bionaz M, Graugnard DE, Drackley JK, Loor JJ. Adipose tissue depots of Holstein cows are immune responsive: Inflammatory gene expression in vitro. Domestic Animal Endocrinology. 2010;38(3):168-78.

81. Gurzov EN, Izquierdo M. Cyclin E1 knockdown induces apoptosis in cancer cells. Neurological Research. 2006;28(5):493-9.

82. Shard AG, Tomlins PE. Biocompatibility and the efficacy of medical implants. Regenerative Medicine. 2006;1(6):789-800.

83. Scuteri A, Donzelli E, Ravasi M, Tredici G. Adult mesenchymal stem cells support cisplatin-treated dorsal root ganglion survival. Neurosci Lett. 2008;445(1):68-72.

84. Pappa A, Brown D, Koutalos Y, DeGregori J, White C, Vasiliou V. Human aldehyde dehydrogenase 3A1 inhibits proliferation and promotes survival of human corneal epithelial cells. Journal of Biological Chemistry. 2005;280(30):27998-8006.

85. Hartwig S, Ho J, Pandey P, Macisaac K, Taglienti M, Xiang M, et al. Genomic characterization of Wilms' tumor suppressor 1 targets in nephron progenitor cells during kidney development. Development (Cambridge, England). 2010;137(7):1189-203.

86. Chansard M, Iwahana E, Liang J, Fukuhara C. Regulation of cAMP-induced arylalkylamine N-acetyltransferase, Period1, and MKP-1 gene expression by mitogen-activated protein kinases in the rat pineal gland. Molecular Brain Research. 2005;139(2):333-40.

87. Choi M, Stottmann RW, Yang YP, Meyers EN, Klingensmith J. The bone morphogenetic protein antagonist noggin regulates mammalian cardiac morphogenesis. Circulation Research. 2007;100(2):220-8.

88. Jackson MT, Smith MM, Smith SM, Jackson CJ, Xue M, Little CB. Activation of cartilage matrix metalloproteinases by activated protein C. Arthritis and Rheumatism. 2009;60(3):780-91.

89. Feuermann Y, Mabjeesh SJ, Niv-Spector L, Levin D, Shamay A. Prolactin affects leptin action in the bovine mammary gland via the mammary fat pad. J Endocrinol. 2006;191(2):407-13.

90. Giacobini P, Messina A, Wray S, Giampietro C, Crepaldi T, Carmeliet P, et al. Hepatocyte growth factor acts as a motogen and guidance signal for gonadotropin hormone-releasing hormone-1 neuronal migration. Journal of Neuroscience. 2007;27(2):431-45.

91. Gitton Y, Tibaldi L, Dupont E, Levi G, Joliot A. Efficient CPP-mediated Cre protein delivery to developing and adult CNS tissues. Bmc Biotechnol. 2009;9.

92. Ichikawa M, Yoshida J, Saito K, Sagawa H, Tokita Y, Watanabe M. Differential effects of two ROCK inhibitors, Fasudil and Y-27632, on optic nerve regeneration in adult cats. Brain Res. 2008;1201(C):23-33.

93. Itoh A, Horiuchi M, Bannerman P, Pleasure D, Itoh T. Impaired regenerative response of primary sensory neurons in ZPK/DLK gene-trap mice. Biochemical and Biophysical Research Communications. 2009;383(2):258-62.

94. Jones VC, McKeown L, Verkhratsky A, Jones OT. LV-pIN-KDEL: A novel lentiviral vector demonstrates the morphology, dynamics and continuity of the endoplasmic reticulum in live neurones. BMC Neuroscience. 2008;9.

95. Kirjavainen A, Sulg M, Heyd F, Alitalo K, Yla-Herttuala S, Moroy T, et al. Prox1 interacts with Atoh1 and Gfi1, and regulates cellular differentiation in the inner ear sensory epithelia. Developmental Biology. 2008;322(1):33-45.

96. Hazen VM, Phan K, Yamauchi K, Butler SJ. Assaying the ability of diffusible signaling molecules to reorient embryonic spinal commissural axons. Journal of visualized experiments : JoVE. 2010;(37).

97. McLaughlin PJ, Sassani JW, Klocek MS, Zagon IS. Diabetic keratopathy and treatment by modulation of the opioid growth factor (OGF)-OGF receptor (OGFr) axis with naltrexone: A review. Brain Research Bulletin. 2010;81(2-3):236-47.

98. Parra LM, Zou Y. Sonic hedgehog induces response of commissural axons to Semaphorin repulsion during midline crossing. Nature Neuroscience. 2010;13(1):29-35.

99. Hu L, Lawson DM. In vitro prolactin release from pituitaries of ovariectomized, estradiol -treated holtzman rats: A direct comparison of dispersed cells and tissue explants. Life Sci. 1996;58(3):229-37.

100. Menzies KK, Lefevre C, Macmillan KL, Nicholas KR. Insulin regulates milk protein synthesis at multiple levels in the bovine mammary gland. Functional and Integrative Genomics. 2009;9(2):197-217.

101. Casas A, Batlle A. Photodynamic therapy in Argentina. Photodiagnosis and Photodynamic Therapy. 2006;3(4):205-13.

102. Bhola P, Banerjee S, Mukherjee J, Balasubramanium A, Arun V, Karim Z, et al. Preclinical in vivo evaluation of rapamycin in human malignant peripheral nerve sheath explant xenograft. Int J Cancer. 2010;126(2):563-71.

103. Palmer AW, Wilson CG, Baum EJ, Levenston ME. Composition-function relationships during IL-1-induced cartilage degradation and recovery. Osteoarthritis and Cartilage. 2009;17(8):1029-39.

104. Tsai WC, Hsu CC, Chen HC, Hsu YH, Lin MS, Wu CW, et al. Ciprofloxacin-mediated inhibition of tenocyte migration and down-regulation of focal adhesion kinase phosphorylation. Eur J Pharmacol. 2009;607(1-3):23-6.

105. Ager EI, Pask AJ, Shaw G, Renfree MB. Expression and protein localisation of IGF2 in the marsupial placenta. Bmc Dev Biol. 2008;8.

106. Blackmore M, Letourneau PC. L1, Œ≤1 integrin, and cadherins mediate axonal regeneration in the embryonic spinal cord. Journal of Neurobiology. 2006;66(14):1564-83.

107. Garnham PCC. The placenta in malaria with special reference to reticulo-endothelial immunity. Transactions of the Royal Society of Tropical Medicine and Hygiene. 1938;32(1).

108. Koizumi A, Zeck G, Ben Y, Masland RH, Jakobs TC. Organotypic culture of physiologically functional adult mammalian retinas. PLoS ONE. 2007;2(2).

109. Hedlund M, Stenqvist AC, Nagaeva O, Kjellberg L, Wulff M, Baranov V, et al. Human placenta expresses and secretes NKG2D ligands via exosomes

that down-modulate the cognate receptor expression: evidence for immunosuppressive function. Journal of immunology (Baltimore, Md : 1950). 2009;183(1):340-51.

110. Cohen J, Johnson AR. Differential effects of laminin and merosin on neurite outgrowth by developing retinal ganglion cells. Journal of Cell Science. 1991;100(SUPPL. 15):1-7.

111. Sparrow JR, Hicks D, Barnstable CJ. Cell commitment and differentiation in explants of embryonic rat neural retina. Comparison with the developmental potential of dissociated retina. Developmental Brain Research. 1990;51(1):69-84.

112. Gotlieb AI, Boden P. Porcine aortic organ culture: A model to study the cellular response to vascular injury. In Vitro. 1984;20(7):535-42.

113. Keenan KP, Combs JW, McDowell EM. Regeneration of hamster tracheal epithelium after mechanical injury. III. Large and small lesions: Comparative stathmokinetic and single pulse and continuous thymidine labeling autoradiographic studies. Virchows Archiv Abteilung B Cell Pathology. 1982;41(3):231-52.

114. Luke DA. Epithelial proliferation in explants of mouse palatal mucosa cultured in contact and apart. Virchows Archiv Abteilung B Cell Pathology. 1980;33(3):275-80.

115. Smoot DT, Rosenthal LE, Mobley HLT, Iseri O, Zhu S, Resau JH. Development of a human stomach explant organ culture system to study the pathogenesis of Helicobacter pylori. Digestion. 1990;46(1):46-54.

116. Strehl R, Tallheden T, Sj√∂gren-Jansson E, Minuth WW, Lindahl A. Long-term maintenance of human articular cartilage in culture for biomaterial testing. Biomaterials. 2005;26(22):4540-9.

117. Shurtz-Swirski R, Cohen Y, Barnea ER. Patterns of secretion of human chorionic gonadotrophin by superfused placental explants and the embryo-placental relationship following maternal use of medications. Human Reproduction. 1992;7(3):300-4.

118. Rao CV, Wolf DM, Arkin AP. Control, exploitation and tolerance of intracellular noise. Nature. 2002;420(6912):231-7.

119. Nevill JT, Cooper R, Dueck M, Breslauer DN, Lee LP. Integrated microfluidic cell culture and lysis on a chip. Lab on a Chip. 2007;7(12):1689-95.

120. Kim L, Vahey MD, Lee HY, Voldman J. Microfluidic arrays for logarithmically perfused embryonic stem cell culture. Lab on a Chip. 2006;6(3):394-406.

121. Lee P, Lin R, Moon J, Lee LP. Microfluidic alignment of collagen fibers for in vitro cell culture. Biomedical Microdevices. 2006;8(1):35-41.

122. Chennazhy KP, Krishnan LK. Effect of passage number and matrix characteristics on differentiation of endothelial cells cultured for tissue engineering. Biomaterials. 2005;26(28):5658-67.

123. Santos M, Nguyen BT, Thompson JS. Factors affecting in vitro growth of harvested enterocytes. Cell Transplant. 1992;1(4):299-306.

124. Mourzina Y, Kaliaguine D, Schulte P, Offenhausser A. Patterning chemical stimulation of reconstructed neuronal networks. Analytica Chimica Acta. 2006;575(2):281-9.

125. Mehenti NZ, Fishman HA, Bent SF. A model neural interface based on functional chemical stimulation. Biomedical Microdevices. 2007;9(4):579-86. doi: 10.1007/s10544-007-9069-z|ISSN 1387-2176.

126. Nakashima Y, Yasuda T. Cell differentiation guidance using chemical stimulation controlled by a microfluidic device. Sensors and Actuators a-Physical. 2007;139:252-8. doi: 10.1016/j.sna.2007.05.035|ISSN 0924-4247.

127. Li XJ, Li PCH. Contraction study of a single cardiac muscle cell in a microfluidic chip. Methods in Molecular Biology. 2006:199-225.

128. Allshire A, Piper HM, Cuthbertson KSR, Cobbold PH. Cytosolic free Ca2+ in single rat heart cells during anoxia and reoxygenation. Biochem J. 1987;244(2):381-5.

129. Greene LA, Aletta JM, Rukenstein A, Green SH. PC12 pheochromocytoma cells: Culture, nerve growth factor treatment, and experimental exploitation. Methods in Enzymology. 1987;147:207-16.

130. Rothstein JD, Martin L, Levey AI, Dykes-Hoberg M, Jin L, Wu D, et al. Localization of neuronal and glial glutamate transporters. Neuron. 1994;13(3):713-25.

131. Shevkoplyas SS, Yoshida T, Gifford SC, Bitensky MW. Direct measurement of the impact of impaired erythrocyte deformability on microvascular network perfusion in a microfluidic device. Lab on a Chip. 2006;6(7):914-20.

132. Hsiai TK, Cho SK, Wong PK, Ing MH, Salazar A, Hama S, et al. Micro sensors: Linking real-time oscillatory shear stress with vascular inflammatory responses. Annals of Biomedical Engineering. 2004;32(2):189-201.

133. Tanaka Y, Kikukawa Y, Sato K, Sugh Y, Kitamori T. Culture and leukocyte adhesion assay of human arterial endothelial cells in a glass microchip. Analytical Sciences. 2007;23(3):261-6.

134. Jaggi RD, Sandoz R, Effenhauser CS. Microfluidic depletion of red blood cells from whole blood in high-aspect-ratio microchannels. Microfluidics and Nanofluidics. 2007;3(1):47-53.

135. Munaka T, Abe H, Kanai M, Sakamoto T, Nakanishi H, Yamaoka T, et al. Real-time monitoring of antibody secretion from hybridomas on a microchip by time-resolved luminescence anisotropy analysis. Analytical Biochemistry. 2006;353(1):1-6.

136. Ostrovidov S, Jiang JL, Sakai Y, Fujii T. Membrane-based PDMS microbioreactor for perfused 3D primary rat hepatocyte cultures. Biomedical Microdevices. 2004;6(4):279-87.

137. Dishinger JF, Kennedy RT. Serial immunoassays in parallel on a microfluidic chip for monitoring hormone secretion from living cells. Analytical Chemistry. 2007;79(3):947-54.

138. Amatore C, Arbault S, Chen Y, Crozatier C, Tapsoba I. Electrochemical detection in a microfluidic device of oxidative stress generated by macrophage cells. Lab on a Chip. 2007;7(2):233-8.

139. Park J, Bansal T, Pinelis M, Maharbiz MM. A microsystem for sensing and patterning oxidative microgradients during cell culture. Lab on a Chip. 2006;6(5):611-22. doi: 10.1039/b516483d.

140. Lin F, Butcher EC. T cell chemotaxis in a simple microfluidic device. Lab on a Chip. 2006;6(11):1462-9.

141. Torisawa Y-s, Shiku H, Yasukawa T, Nishizawa M, Matsue T. Multi-channel 3-D cell culture device integrated on a silicon chip for anticancer drug sensitivity test. Biomaterials. 2005;26(14):2165-72.

142. Kane BJ, Zinner MJ, Yarmush ML, Toner M. Liver-specific functional studies in a microfluidic array of primary mammalian hepatocytes. Analytical Chemistry. 2006;78(13):4291-8.

143. Hogan J. Lab on a chip: a little goes a long way. Nature. 2006;442(7101):351-2.

144. Toh YC, Lim TC, Tai D, Xiao G, Van Noort D, Yu H. A microfluidic 3D hepatocyte chip for drug toxicity testing. Lab on a Chip - Miniaturisation for Chemistry and Biology. 2009;9(14):2026-35.

145. Pappas D, Wang K. Cellular separations: A review of new challenges in analytical chemistry. Analytica Chimica Acta 2007;601(1):26-35.

146. Yang S, Undar A, Zahn JD. A microfluidic device for continuous, real time blood plasma separation. Lab on a Chip. 2006;6(7):871-80.

147. Han KH, Frazier AB. Paramagnetic capture mode magnetophoretic microseparator for high efficiency blood cell separations. Lab on a Chip. 2006;6(2):265-73.

148. Choi S, Song S, Choi C, Park JK. Continuous blood cell separation by hydrophoretic filtration. Lab on a Chip. 2007;7(11):1532-8.

149. Zhang MY, Lee PJ, Hung PJ, Johnson T, Lee LP, Mofrad MRK. Microfluidic environment for high density hepatocyte culture. Biomedical Microdevices. 2008;10:117-21.

150. Yang M, Zhang X. Electrical assisted patterning of cardiac myocytes with controlled macroscopic anisotropy using a microfluidic dielectrophoresis chip. Sensors and Actuators a-Physical. 2007;135(1):73-9.

151. Nalayanda DD, Puleo CM, Fulton WB, Wang TH, Abdullah F. Characterization of pulmonary cell growth parameters in a continuous perfusion microfluidic environment. Exp Lung Res. 2007;33(6):321-35.

152. Bruzewicz BA, McGuigan, P.A., Whitesides, G.M. Fabrication of a modular tissue construct in a microfluidic chip. Lab Chip. 2008;8:663-71.

153. Ling Y, Rubin J, Deng Y, Huang C, Demirci U, Karp JM, et al. A cell-laden microfluidic hydrogel. Lab on a Chip. 2007;7(6):756-62.

154. Iyer VR, Eisen MB, Ross DT, Schuler G, Moore T, Lee JCF, et al. The transcriptional program in the response of human fibroblasts to serum. Science. 1999;283(5398):83-7.

155. Ho CT, Lin RZ, Chang WY, Chang HY, Liu CH. Rapid heterogeneous liver-cell on-chip patterning via the enhanced field-induced dielectrophoresis trap. Lab on a Chip. 2006;6(6):724-34.

156. Khademhosseini A, Eng G, Yeh J, Kucharczyk PA, Langer R, Vunjak-Novakovic G, et al. Microfluidic patterning for fabrication of contractile cardiac organoids. Biomedical Microdevices. 2007;9(2):149-57.

157. Balis FM. Evolution of anticancer drug discovery and role of cell-based screening. Journal of The National Cancer Institute. 2002;94:78-9.

158. Bowers SLK, Banerjee I, Baudino TA. The extracellular matrix: At the center of it all. Journal of Molecular and Cellular Cardiology. 2010;48(3):474-82.

159. Koch M, Laub F, Zhou P, Hahn RA, Tanaka S, Burgeson RE, et al. Collagen XXIV, a Vertebrate Fibrillar Collagen with Structural Features of Invertebrate Collagens: Selective expression in developing cornea and bone. Journal of Biological Chemistry. 2003;278(44):43236-44.

160. Cattaruzza S, Perris R. Proteoglycan control of cell movement during wound healing and cancer spreading. Matrix Biology. 2005;24(6):400-17.

161. Kievit FM, Florczyk SJ, Leung MC, Veiseh O, Park JO, Disis ML, et al. Chitosan-alginate 3D scaffolds as a mimic of the glioma tumor microenvironment. Biomaterials. 2010;31(22):5903-10.

162. Chatterjee K, Lin-Gibson S, Wallace WE, Parekh SH, Lee YJ, Cicerone MT, et al. The effect of 3D hydrogel scaffold modulus on osteoblast differentiation and mineralization revealed by combinatorial screening. Biomaterials. 2010;31(19):5051-62.

163. Da Silva CL, Gon√ßalves R, Dos Santos F, Andrade PZ, Almeida-Porada G, Cabral JMS. Dynamic cell-cell interactions between cord blood haematopoietic progenitors and the cellular niche are essential for the expansion of CD34+, CD34+CD38- and early lymphoid CD7+ cells. Journal of Tissue Engineering and Regenerative Medicine. 2010;4(2):149-58.

164. Thompson A, Brennan, K., Cox, A., Gee, J., Harcourt, D., Harris, A., Harvie, M., Holen, I., Howell, A., Nicholson, R., Steel, M., and Streuli, C. . Evaluation of the current knowledge limitations in breast cancer research: a gap analysis. Breast Cancer Research 2008;10(R26).

165. Raty S, Walters EM, Davis J, Zeringue H, Beebe DJ, Rodriguez-Zas SL, et al. Embryonic development in the mouse is enhanced via microchannel culture. Lab on a Chip 2004;4(3):186-90.

166. Loeschcke V, Krebs RA, Dahlgaard J, Michalak P. High-temperature stress and the evolution of thermal resistance in Drosophila. EXS. 1997;83:175-90.

167. Lucchetta EM, Lee JH, Fu LA, Patel NH, Ismagilov RF. Dynamics of Drosophila embryonic patterning network perturbed in space and time using microfluidics. Nature. 2005;434(7037):1134-8.

168. Smith KR. Gene therapy: Theoretical and bioethical concepts. Arch Med Res. 2003;34(4):247-68.

169. Winkel GK, Pedersen RA. Fate of the inner cell mass in mouse embryos as studied by microinjection of lineage tracers. Developmental Biology. 1988;127(1):143-56.

170. Choi Y, McClain MA, LaPlaca MC, Frazier AB, Allen MG. Three dimensional MEMS microfluidic perfusion system for thick brain slice cultures. Biomedical Microdevices. 2007;9(1):7-13.

171. Blake AJ, Pearce TM, Rao NS, Johnson SM, Williams JC. Multilayer PDMS microfluidic chamber for controlling brain slice microenvironment. Lab on a Chip. 2007;7(7):842-9.

172. Van Midwoud PM, Groothuis GMM, Merema MT, Verpoorte E. Microfluidic biochip for the perifusion of precision-cut rat liver slices for metabolism and toxicology studies. Biotechnology and Bioengineering. 2010;105(1):184-94.

173. Cohen S. View of the Liver and Gallbladder. Merek; 2006.

174. Grattagliano I, Bonfrate L, Diogo CV, Wang HH, Wang DQH, Portincasa P. Biochemical mechanisms in drug-induced liver injury: Certainties and doubts. World J Gastroentero. 2009;15(39):4865-76.

175. Olpin SE. Metabolic disorders presenting as liver disease. Paediatrics and Child Health. 2010;20(1):1-6.

176. Khan Z, Crawford, J.M., Stolz, D.B. Ultrastructure of the hepatocyte. In: Rodes J, editor. Textbook of Hepatology. 3rd Edition ed. Oxford: Blackwell Publishing; 2007. p. 20-8.

177. Zajicek G. Time dimension in histopathology. Pathology Research and Practice. 1992;188(4-5):410-2.

178. Feldmann G. The cytoskeleton of the hepatocyte. Structure and functions. Journal of Hepatology. 1989;8(3):380-6.

179. Ichihara A, Nakamura T, Tanaka K. Use of hepatocytes in primary culture for biochemical studies on liver functions. Molecular and Cellular Biochemistry. 1982;43(3):145-60.

180. Jeejeebhoy KN, Philips MJ. Isolated mammalian hepatocytes in culture. Gastroenterology. 1976;71(6):1086-96.

181. Kevresan S, Kuhajda K, Kandrac J, Fawcett JP, Mikov M. Biosynthesis of bile acids in mammalian liver. European Journal of Drug Metabolism and Pharmacokinetics. 2006;31(3):145-56.

182. Pelkonen O, Kapitulnik J, Gundert-Remy U, Boobis AR, Stockis A. Local kinetics and dynamics of xenobiotics. Critical Reviews in Toxicology. 2008;38(8):697-720.

183. Donato MT, Lahoz A, Castell JV, GÃ³mez-LechÃ³n MJ. Cell lines: A tool for in vitro drug metabolism studies. Current Drug Metabolism. 2008;9(1):1-11.

184. Braet F, Wisse E. Structural and functional aspects of liver sinusoidal endothelial cell fenestrae: A review. Comparative Hepatology. 2002;1.

185. Liver Lobe. [12 November 2008]; Available from: http://www.technion.ac.il/~mdcourse/274203/slides/Liver/1-Liver%20Lobule%20-A.jpg.

186. Horn T, Christofferson P, Henriksen JH. Alcoholic liver injury: Defenestration in noncirrhotic livers - A scanning electron microscopic study. Hepatology. 1987;7(1):77-82.

187. Fraser R, Clark SA, Day WA, Murray FEM. Nicotine decreases the porosity of the rat liver sieve: A possible mechanism for hypercholesterolaemia. British Journal of Experimental Pathology. 1988;69(3):345-50.

188. Braet F, De Zanger R, Sasaoki T, Baekeland M, Janssens P, Smedsrod B, et al. Assessment of a method of isolation, purification, and cultivation of rat liver sinusoidal endothelial cells. Laboratory Investigation. 1994;70(6):944-52.

189. Semela D, Shah, V.H. Liver sinusoidal endothelial cells. In: Rodes J, editor. Textbook of Hepatology. Oxford: Blackwell Publishing; 2007

190. Henderson NC, Forbes SJ. Hepatic fibrogenesis: From within and outwith. Toxicology. 2008;254(3):130-5.

191. Pinzani M. The hepatic stellate cell. In: Rodes J, editor. Textbook of Hepatology. Oxford: Blackwell Publishing; 2007.

192. Sato M, Suzuki S, Senoo H. Hepatic stellate cells: Unique characteristics in cell biology and phenotype. Cell Structure and Function. 2003;28(2):105-12.

193. Blomhoff R, Wake K. Perisinusoidal stellate cells of the liver: Important roles in retinol metabolism and fibrosis. FASEB Journal. 1991;5(3):271-7.

194. Ueno T, Bioulac-Sage P, Balabaud C, Rosenbaum J. Innervation of the sinusoidal wall: Regulation of the sinusoidal diameter. Anatomical Record - Part A Discoveries in Molecular, Cellular, and Evolutionary Biology. 2004;280(1):868-73.

195. Amenta PS, Harrison D. Expression and potential role of the extracellular matrix in hepatic ontogenesis: A review. Microscopy Research and Technique. 1997;39(4):372-86.

196. Martinez-Hernandez A, Amenta PS. The hepatic extracellular matrix. I. Components and distribution in normal liver. Virchows Archiv - A Pathological Anatomy and Histopathology. 1993;423(1):1-11.

197. Huang BQ, Masyuk TV, Muff MA, Tietz PS, Masyuk AI, LaRusso NF. Isolation and characterization of cholangiocyte primary cilia. American Journal of Physiology - Gastrointestinal and Liver Physiology. 2006;291(3).

198. Trauner M, Boyer JL. Bile salt transporters: Molecular characterization, function, and regulation. Physiological Reviews. 2003;83(2):633-71.

199. Jaeschke H. Kupffer Cells. In: Rodes J, editor. Textbook of Hepatology. Oxford: Blackwell Publishing; 2007.

200. McCuskey RS, McCuskey PA. Fine structure and function of Kupffer cells. Journal of Electron Microscopy Technique. 1990;14(3):237-46.

201. Knook DL, Barkway C, Sleyster EC. Lysosomal enzyme content of Kupffer and endothelial liver cells isolated from germfree and clean conventional rats. Infection and Immunity. 1981;33(2):620-2.

202. Jaeschke H, Farhood A, Bautista AP, Spolarics Z, Spitzer JJ. Complement activates Kupffer cells and neutrophils during reperfusion after hepatic ischemia. American Journal of Physiology - Gastrointestinal and Liver Physiology. 1993;264(4 27-4).

203. Jaeschke H, Gores GJ, Cederbaum AI, Hinson JA, Pessayre D, Lemasters JJ. Mechanisms of hepatotoxicity. Toxicological Sciences. 2002;65(2):166-76.

204. Takei Y, Arteel GE, Bergheim I, Lambert JC, McMullen MR, Nagy LE, et al. Roles of Kupffer cells in alcoholic liver disease. Alcoholism: Clinical and Experimental Research. 2005;29(6):1116-20.

205. Luo DZ, Vermijlen D, Ahishali B, Triantis V, Plakoutsi G, Braet F, et al. On the cell biology of pit cells, the liver-specific NK cells. World Journal of Gastroenterology. 2000;6(1):1-11.

206. Wisse E, Van't Noordende JM, Van Der Meulen J, Daems Th W. The pit cell: description of a new type of cell occurring in rat liver sinusoids and peripheral blood. Cell and Tissue Research. 1976;173(4):423-35.

207. Nakatani K, Kaneda K, Seki S, Nakajima Y. Pit cells as liver-associated natural killer cells: Morphology and function. Medical Electron Microscopy. 2004;37(1):29-36.

208. Bouwens L, Jacobs R, Remels L, Wisse E. Natural cytotoxicity of rat hepatic natural killer cells and macrophages against a syngeneic colon adenocarcinoma. Cancer Immunology Immunotherapy. 1988;27(2):137-41.

209. Sell S. Is there a liver stem cell? Cancer Research. 1990;50(13):3811-5.

210. Golding M, Sarraf CE, Lalani EN, Anilkumar TV, Edwards RJ, Nagy P, et al. Oval cell differentiation into hepatocytes in the acetylaminofluorene- treated regenerating rat liver. Hepatology. 1995;22(4 I):1243-53.

211. Alison MR. Regulation of hepatic growth. Physiological Reviews. 1986;66(3):499-541.

212. Shiojiri N, Lemire JM, Fausto N. Cell lineages and oval cell progenitors in rat liver development. Cancer Research. 1991;51(10):2611-20.

213. Yasui O, Miura N, Terada K, Kawarada Y, Koyama K, Sugiyama T. Isolation of oval cells from long-evans cinnamon rats and their transformation into hepatocytes in vivo in the rat liver. Hepatology. 1997;25(2):329-34.

214. Chu Chieh H, Evarts RP, Nakatsukasa H, Marsden ER, Thorgeirsson SS. Occurrence of oval-type cells in hepatitis B virus-associated human hepatocarcinogenesis. Hepatology. 1992;16(6):1327-33.

215. Ruck P, Xiao JC, Pietsch T, Von Schweinitz D, Kaiserling E. Hepatic stem-like cells in hepatoblastoma: Expression of cytokeratin 7, albumin and oval cell associated antigens detected by OV-1 and OV-6. Histopathology. 1997;31(4):324-9.

216. Abenoza P, Manivel JC, Wick MR, Hagen K, Dehner LP. Hepatoblastoma: An immunohistochemical and ultrastructural study. Human Pathology. 1987;18(10):1025-35.

217. Marcus KJ, Tishler RB. Head and Neck Carcinomas Across the Age Spectrum: Epidemiology, Therapy, and Late Effects. Seminars in Radiation Oncology. 2010;20(1):52-7.

218. Hanahan D, Weinberg RA. The hallmarks of cancer. Cell. 2000;100(1):57-70.

219. Christofori G. Changing neighbours, changing behaviour: cell adhesion molecule-mediated signalling during tumour progression. Embo Journal. 2003;22(10):2318-23.

220. Derycke L, Van Marck V, Depypere H, Bracke M. Molecular targets of growth, differentiation, tissue integrity, and ectopic cell death in cancer cells. Cancer Biother Radiopharm. 2005;20(6):579-88.

221. Pajonk F, Vlashi E, McBride WH. Radiation resistance of cancer stem cells: The 4 R's of radiobiology revisited. Stem Cells. 2010;28(4):639-48.

222. Stefanko E, Wr√≥bel T. Mechanisms of resistance to cancer chemotherapy. Advances in Clinical and Experimental Medicine. 2010;19(1):5-12.

223. Morse EE. Diagnosis of lymphoma in the new millennium. Ann Clin Lab Sci. 1998;28(6):370-9.

224. Craft AW. Childhood cancer - Mainly curable so where next? Acta Paediatrica, International Journal of Paediatrics. 2000;89(4):386-92.

225. Timar J, Csuka O, Remenar E, Repassy G, Kasler M. Progression of head and neck squamous cell cancer. Cancer Metast Rev. 2005;24(1):107-27.

226. Drug-Expert.com. Head and Neck Cancer. 2010.

227. Statistics OfN. Cancer Statistics registrations: Registrations of cancer diagnosed in 2007, United Kingdom. 2010;Series MB1 (no.38.).

228. Jerjes W, Upile T, Petrie A, Riskalla A, Hamdoon Z, Vourvachis M, et al. Clinicopathological parameters, recurrence, locoregional and distant metastasis in 115 T1-T2 oral squamous cell carcinoma patients. Head and Neck Oncology. 2010;2(1).

229. Boussen H, Bouaouina N, Mokni-Baizig N, Gamoudi A, Chouchane L, Benna F, et al. Nasopharyngeal carcinoma. Recent data. Les carcinomes du nasopharynx: Donn√©es actuelles. 2005;53(1):45-51.

230. Lalami Y, De Castro Jr G, Bernard-Marty C, Awada A. Management of head and neck cancer in elderly patients. Drugs and Aging. 2009;26(7):571-83.

231. Curado MP, Hashibe M. Recent changes in the epidemiology of head and neck cancer. Current Opinion in Oncology. 2009;21(3):194-200.

232. Altieri A, Bosetti C, Talamini R, Gallus S, Franceschi S, Levi F, et al. Cessation of smoking and drinking and the risk of laryngeal cancer. British Journal of Cancer. 2002;87(11):1227-9.

233. Balaram P, Sridhar H, Rajkumar T, Vaccarella S, Herrero R, Nandakumar A, et al. Oral cancer in Southern India: The influence of smoking, drinking, paan-chewing and oral hygiene. International Journal of Cancer. 2002;98(3):440-5.

234. Lubin JH, Purdue M, Kelsey K, Zhang ZF, Winn D, Wei Q, et al. Total exposure and exposure rate effects for alcohol and smoking and risk of head and neck cancer: A pooled analysis of case-control studies. American Journal of Epidemiology. 2009;170(8):937-47.

235. Lanford D. Head and Neck Alliance. 2010 [25 Feb 2010]; Available from: http://www.headandneck.org/.

236. Chen YC, Christiani DC, Su HJJ, Hsueh YM, Smith TJ, Ryan LM, et al. Early-life or lifetime sun exposure, sun reaction, and the risk of squamous cell carcinoma in an Asian population. Cancer Causes and Control. 2010:1-6.

237. Glombitza F, Guntinas-Lichius O, Petersen I. HPV status in head and neck tumors. Pathology Research and Practice.

238. Baez A. Genetic and environmental factors in head and neck cancer genesis. Journal of Environmental Science and Health - Part C Environmental Carcinogenesis and Ecotoxicology Reviews. 2008;26(2):174-200.

239. Chang KP, Hsu CL, Chang YL, Tsang NM, Chen CK, Lee TJ, et al. Complementary serum test of antibodies to Epstein-Barr virus nuclear antigen-1 and early antigen: A possible alternative for primary screening of nasopharyngeal carcinoma. Oral Oncology. 2008;44(8):784-92.

240. Ndiaye IC, Diom ES, Diop F, Tall A, Ndiaye M, Essalki I, et al. Squamous carcinoma of the hypopharynx in children in S√©n√©gal: Between disarray and enigma. International Journal of Pediatric Otorhinolaryngology. 2009;73(3):357-61.

241. Slyvester D. Personal Communication. 2010.

242. El Hag IA, Kollur SM, Chiedozi LC. The role of FNA in the initial management of thyroid lesions: 7-year experience in a district general hospital. Cytopathology. 2003;14(3):126-30.

243. Spector JG, Sessions DG, Haughey BH, Chao KSC, Simpson J, El Mofty S, et al. Delayed regional metastases, distant metastases, and second primary malignancies in squamous cell carcinomas of the larynx and hypopharynx. Laryngoscope. 2001;111(6):1079-87.

244. Ozdek A, Sarac S, Akyol MU, Unal OF, Sungur A. Histopathological predictors of occult lymph node metastases in supraglottic squamous cell carcinomas. European Archives of Oto-Rhino-Laryngology. 2000;257(7):389-92.

245. MacGuill MJ, Barrett C, Ravi N, MacDonald G, Reynolds JV. Isolated tumour cells in pathological node-negative lymph nodes adversely affect prognosis in cancer of the oesophagus or oesophagogastric junction. Journal of Clinical Pathology. 2007;60(10):1108-11.

246. Jatrana S, Crampton P, Filoche S. The case for integrating oral health into primary health care. New Zealand Medical Journal. 2009;122(1301):43-52.

247. Diagnosis and management of head and neck cancer. In: Scotland NHS-, editor. Edinburgh: Scottish Intercollegiate Guidelines Network; 2006.

248. Specenier PM, Vermorken JB. Neoadjuvant chemotherapy in head and neck cancer: Should it be revisited? Cancer Letters. 2007;256(2):166-77.

249. Specenier PM, Van den Weyngaert D, Van Laer C, Weyler J, Van den Brande J, Huizing MT, et al. Phase II feasibility study of concurrent radiotherapy and gemcitabine in chemonaive patients with squamous cell carcinoma of the head and neck: long-term follow up data. Ann Oncol. 2007;18(11):1856-60.

250. Network SIG. Diagnosis and management of head and neck

cancer- A national clinical guideline In: Scotland N, editor.2006.

251. Marur S, Forastiere AA. Head and neck cancer: Changing epidemiology, diagnosis, and treatment. Mayo Clin Proc. 2008;83(4):489-501.

252. Gibson MK, Forastiere AA. Reassessment of the role of induction chemotherapy for head and neck cancer. Lancet Oncology. 2006;7(7):565-74.

253. Kubota A, Furukawa M, Fujita Y, Yagi H. Concurrent chemoradiotherapy for resectable locoregionally advanced squamous cell carcinoma of the head

and neck-analysis of factors associated with toxicity and efficacy. Journal of Otolaryngology of Japan. 2010;113(3):101-9.

254. Grem JL. 5-Fluorouracil: Forty-plus and still ticking. A review of its preclinical and clinical development. Investigational New Drugs. 2000;18(4):299-313.

255. Cohen SM, Lippard SJ. Cisplatin: From DNA damage to cancer chemotherapy. Progress in Nucleic Acid Research and Molecular Biology 2001.

256. Rosenberg B, VanCamp L, Trosko JE, Mansour VH. Platinum compounds: A new class of potent antitumour agents [24]. Nature. 1969;222(5191):385-6.

257. Jamieson ER, Lippard SJ. Structure, recognition, and processing of cisplatin-DNA adducts. Chemical Reviews. 1999;99(9):2467-98.

258. Johnson NP, Butour JL, Villani G, Wimmer FL, Defais M, Pierson V, et al. Metal antitumor compounds: The mechanism of action of platinum complexes. Prog Clin Biochem Med. 1989;10:1-24.

259. Rabik CA, Dolan ME. Molecular mechanisms of resistance and toxicity associated with platinating agents. Cancer Treatment Reviews. 2007;33(1):9-23.

260. Brabec V, Kasparkova J. Molecular aspects of resistance to antitumor platinum drugs. Drug Resistance Updates. 2002;5(3-4):147-61.

261. Siddik ZH. Cisplatin: Mode of cytotoxic action and molecular basis of resistance. Oncogene. 2003;22(47 REV. ISS. 6):7265-79.

262. Berrocal A, Blasco S, Del Pozo N. Targeted therapies in head and neck carcinoma. Nuevas dianas terap√©uticas en tumores de cabeza y cuello. 2010;24(2):62-71.

263. Chitapanarux I, Lorvidhaya V, Tharavichitkul E, Mayurasakorn S, Sittitrai P, Pattarasakulchai T, et al. A phase II study of docetaxel and carboplatin with concurrent radiation therapy for locally advanced head and neck cancer. Auris Nasus Larynx.

264. Breslauer DN, Lee PJ, Lee LP. Microfluidics-based systems biology. Mol Biosyst. 2006;2(2):97-112.

265. Harrison DJ, Fluri K, Seiler K, Fan Z, Effenhauser CS, Manz A. Micromachining a miniaturized capillary electrophoresis-based chemical analysis system on a chip. Science. 1993;261(5123):895-7.

266. Paguirigan AL, Beebe DJ. From the cellular perspective: Exploring differences in the cellular baseline in macroscale and microfluidic cultures. Integrative Biology. 2009;1(2):182-95.

267. Chisti Y. Hydrodynamic damage to animal cells. Critical Reviews in Biotechnology. 2001;21(2):67-110.

268. Attia UM, Marson S, Alcock JR. Micro-injection moulding of polymer microfluidic devices. Microfluidics and Nanofluidics. 2009;7(1):1-28.

269. Zhang H, Wang W, Quan C, Fan S. Engineering considerations for process development in mammalian cell cultivation. Current Pharmaceutical Biotechnology. 2010;11(1):103-12.

270. Cheng CM, Steward Jr RL, LeDuc PR. Probing cell structure by controlling the mechanical environment with cell-substrate interactions. Journal of Biomechanics. 2009;42(2):187-92.

271. Gao Z, Lister K, Desai JP. Constitutive Modeling of Liver Tissue: Experiment and Theory. Annals of Biomedical Engineering. 2009:1-12.

272. Tarn MD. Standard Operating Procedures for the Fabrication of Glass Microchips. 2008.

273. de Graaf IAM, Draaisma AL, Schoeman O, Fahy GM, Groothuis GMM, Koster HJ. Cryopreservation of rat precision-cut liver and kidney slices by rapid freezing and vitrification. Cryobiology. 2007;54(1):1-12.

274. Wowk B. Thermodynamic aspects of vitrification. Cryobiology. 2010;60(1):11-22.

275. Luciano AM, Chigioni S, Lodde V, Franciosi F, Luvoni GC, Modina SC. Effect of different cryopreservation protocols on cytoskeleton and gap junction mediated communication integrity in feline germinal vesicle stage oocytes. Cryobiology. 2009;59(1):90-5.

276. Jamal HZ, Weglarz TC, Sandgren EP. Cryopreserved mouse hepatocytes retain regenerative capacity in vivo. Gastroenterology. 2000;118(2):390-4.

277. Terry C, Mitry RR, Lehec SC, Muiesan P, Rela M, Heaton ND, et al. The effects of cryopreservation on human hepatocytes obtained from different sources of liver tissue. Cell Transplant. 2005;14(8):585-94.

278. Fisher RA, Bu D, Thompson M, Wolfe L, Ritter JK. Optimization of conditions for clinical human hepatocyte infusion. Cell Transplant. 2004;13(6):677-89.

279. Lemasters JJ, Trollinger DR, Qian T, Cascio WE, Ohata H. Confocal imaging of Ca2+, pH, electrical potential, and membrane permeability in single living cells. Green Fluorescent Protein1999. p. 341-58.

280. Niven GW, Mulholland F. Cell membrane integrity and lysis in Lactococcus lactis: the detection of a population of permeable cells in post-logarithmic phase cultures. Journal of Applied Microbiology. 1998;84(1):90-6.

281. Martindale JL, Holbrook NJ. Cellular response to oxidative stress: Signaling for suicide and survival. Journal of Cellular Physiology. 2002;192(1):1-15.

282. Munoz M, Villar I, Garcia-Erce JA. An update on iron physiology. World journal of gastroenterology : WJG. 2009;15(37):4617-26.

283. Baregamian N, Song J, Jeschke MG, Evers BM, Chung DH. IGF-1 Protects Intestinal Epithelial Cells From Oxidative Stress-Induced Apoptosis. Journal of Surgical Research. 2006;136(1):31-7.

284. Chen Y-C, Chow J-M, Lin C-W, Wu C-Y, Shen S-C. Baicalein inhibition of oxidative-stress-induced apoptosis via modulation of ERKs activation and induction of HO-1 gene expression in rat glioma cells C6. Toxicology and Applied Pharmacology. 2006;216(2):263-73.

285. Deisseroth AaD, A.L. Catalase: Physical and chemical properties, mechanism of catalase, and physiological role. Physiological Reviews. 1970;50:319-75.

286. Fleischaker Jr RJ, Sinskey AJ. Oxygen demand and supply in cell culture. European Journal of Applied Microbiology and Biotechnology. 1981;12(4):193-7.

287. Merkel TC, Bondar VI, Nagai K, Freeman BD, Pinnau I. Gas sorption, diffusion, and permeation in poly(dimethylsiloxane). Journal of Polymer Science, Part B: Polymer Physics. 2000;38(3):415-34.

288. Leclerc E, Sakai Y, Fujii T. Cell culture in 3-dimensional microfluidic structure of PDMS (polydimenthylsiloxane). BIOMEDICAL MICRODEVICES. 2003;5(2):109-14.

289. Lin Q, Yun Z. Impact of the hypoxic tumor microenvironment on the regulation of cancer stem cell characteristics. Cancer Biology and Therapy. 2010;9(12):949-56.

290. Brahimi-Horn MC, Chiche J, Pouyss√©gur J. Hypoxia and cancer. Journal of Molecular Medicine. 2007;85(12):1301-7.

291. Mehta G, Mehta K, Sud D, Song JW, Bersano-Begey T, Futai N, et al. Quantitative measurement and control of oxygen levels in microfluidic poly(dimethylsiloxane) bioreactors during cell culture. Biomedical Microdevices. 2007;9(2):123-34.

292. Sud D, Mehta G, Mehta K, Linderman J, Takayama S, Mycek MA. Optical imaging in microfluidic bioreactors enables oxygen monitoring for continuous cell culture. J Biomed Opt. 2006;11(5). doi: 10.1117/1.2355665|issn 1083-3668.

293. Sankaran NB, Mandal PK, Bhattacharya B, Samanta A. Fluorescence response of mono - And tetraazacrown derivatives of 4-aminophthalimide with and without some transition and post transition metal ions. Journal of Materials Chemistry. 2005;15(27-28):2854-9.

294. Rigby GP, Ahmed S, Horseman G, Vadgama P. In vivo glucose monitoring with open microflow - Influences of fluid composition and preliminary evaluation in man. Analytica Chimica Acta. 1999;385(1-3):23-32.

295. Martini FH. The digestive system. Fundamentals of Anatomy and Physiology. 6th Edition ed: Pearson Education International; 2004. p. 875-928.

296. Gerritsen HC, Sanders R, Draaijer A, Ince C, Levine YK. Fluorescence lifetime imaging of oxygen in living cells. Journal of Fluorescence. 1997;7(1):11-5.

297. Jauregui HO, McMillan PN, Driscoll J, Naik S. Attachment and long term survival of adult rat hepatocytes in primary monolayer cultures: Comparison of different substrata and tissue culture media formulations. In Vitro. 1986;22(1):13-22.

298. Richards J, Imagawa W, Balakrishnan A, Edery M, Nandi S. The lack of effect of phenol red or estradiol on the growth response of human, rat, and mouse mammary cells in primary culture. Endocrinology. 1988;123(3):1335-40.

299. Watson TF. Fact and artefact in confocal microscopy. Advances in dental research. 1997;11(4):433-41.

300. Webb CD, Graumann PL, Kahana JA, Teleman AA, Silver PA, Losick R. Use of time-lapse microscopy to visualize rapid movement of the replication origin region of the chromosome during the cell cycle in Bacillus subtilis. Molecular Microbiology. 1998;28(5):883-92.

301. Bruns S, Kniemeyer O, Hasenberg M, Aimanianda V, Nietzsche S, Thywissen A, et al. Production of extracellular traps against Aspergillus fumigatus in vitro and in infected lung tissue is dependent on invading neutrophils and influenced by hydrophobin RodA. Plos Pathogens. 2010;6(4).

302. Godinez WJ, Lampe M, Worz S, Muller B, Eils R, Rohr K. Deterministic and probabilistic approaches for tracking virus particles in time-lapse fluorescence microscopy image sequences. Medical Image Analysis. 2009;13(2):325-42.

303. Kulesa PM, Stark DA, Steen J, Lansford R, Kasemeier-Kulesa JC. Watching the assembly of an organ a single cell at a time using confocal multi-position photoactivation and multi-time acquisition. Organogenesis. 2009;5(4):156-65.

304. Choi HY, Veal DA, Karuso P. Epicocconone, a new cell-permeable long stokes' shift fluorescent stain for live cell imaging and multiplexing. Journal of Fluorescence. 2006;16(4):475-82.

305. Bayliss MK, Skett, P. In: Jones GE, editor. Human Cell Culture Protocols. Humana Press1996.

306. Wang D, Bodovitz S. Single cell analysis: The new frontier in 'omics'. Trends in Biotechnology. 2010;28(6):281-90.

307. Ishiyama M, Tominaga H, Shiga M, Sasamoto K, Ohkura Y, Ueno K, et al. Novel cell proliferation and cytotoxicity assays using a tetrazolium salt that produces a water-soluble formazan dye. In Vitro Toxicology: Journal of Molecular and Cellular Toxicology. 1995;8(2):187-90.

308. Diagnostics R. Cell Proliferation Reagent WST-1 2007.

309. Uhl V, Pilarczyk G, Greulich KO. Fluorescence microscopic observation of catalysis by single or few LDH-1 enzyme molecules. Biol Chem. 1998;379(8-9):1175-80.

310. Legrand C, Bour JM, Jacob C, Capiaumont J, Martial A, Marc A, et al. Lactate dehydrogenase (LDH) activity of the number of dead cells in the medium of cultured eukaryotic cells as marker. J Biotechnol. 1992;25(3):231-43.

311. Invitrogen. Quant-iTTM PicoGreen® dsDNA Reagent and Kits. In: Invitrogen, editor.2008.

312. Toussaint MJM, Nederbragt H. Lack of effect of extracellular matrix or 3T3 feeder layer on the maintenance of differentiation or survival time of cultured rat hepatocytes. Toxicology in Vitro. 1995;9(1):83-90.

313. Zeisberg M, Kramer K, Sindhi N, Sarkar P, Upton M, Kalluri R. De-differentiation of primary human hepatocytes depends on the composition of specialized liver basement membrane. Molecular and Cellular Biochemistry. 2006;283(1-2):181-9.

314. Sundstrom L, Morrison Iii B, Bradley M, Pringle A. Organotypic cultures as tools for functional screening in the CNS. Drug Discovery Today. 2005;10(14):993-1000.

315. Wang S, Rijk JCW, Riethoff-Poortman JH, Van Kuijk S, Peijnenburg AACM, Bovee TFH. Bovine liver slices combined with an androgen transcriptional activation assay: An in-vitro model to study the metabolism and bioactivity of steroids. Analytical and Bioanalytical Chemistry. 2010;397(2):631-41.

316. Harrigan JA, McGarrigle BP, Sutter TR, Olson JR. Tissue specific induction of cytochrome P450 (CYP) 1A1 and 1B1 in rat liver and lung following in vitro (tissue slice) and in vivo exposure to benzo(a)pyrene. Toxicology in Vitro. 2006;20(4):426-38.

317. Klassen LW, Thiele GM, Duryee MJ, Schaffert CS, DeVeney AL, Hunter CD, et al. An in vitro method of alcoholic liver injury using precision-cut liver slices from rats. Biochem Pharmacol. 2008;76(3):426-36.

318. Kaji H, Nishizawa M, Matsue T. Localized chemical stimulation to micropatterned cells using multiple laminar fluid flows. Lab on a Chip - Miniaturisation for Chemistry and Biology. 2003;3(3):208-11.

319. Zhou M, Diwu Z, Panchuk-Voloshina N, Haugland RP. A Stable Nonfluorescent Derivative of Resorufin for the Fluorometric Determination of Trace Hydrogen Peroxide: Applications in Detecting the Activity of Phagocyte NADPH Oxidase and Other Oxidases. Analytical Biochemistry. 1997;253(2):162-8.

320. Rajamani R, Muthuvel A, Senthilvelan M, Sheeladevi R. Oxidative stress induced by methotrexate alone and in the presence of methanol in discrete regions of the rodent brain, retina and optic nerve. Toxicology Letters. 2006;165(3):265-73.

321. Chan TC, Williams SR, Clark RF. Formic Acid Skin Burns Resulting in Systemic Toxicity. Annals of Emergency Medicine. 1995;26(3):383-6.

322. Liesivuori J, Savolainen, H. Methanol and formic acid toxicity: biochemical mechanisms. Pharmacology and Toxicology. 1991;69:157-63.

323. Hasinoff BB. The intracellular iron sensor calcein is catalytically oxidatively degraded by iron(II) in a hydrogen peroxide-dependent reaction. Journal of Inorganic Biochemistry. 2003;95(2-3):157-64.

324. Petrat F, De Groot, H., Rauen, U. Subcellular distribution of chelatable iron: a laser scanning microscopic study in isolated hepatocytes and liver endothelial cells. Biochemical Journal. 2001;356:61-9.

325. Albano E. Oxidative mechanisms in the pathogenesis of alcoholic liver disease. Molecular Aspects of Medicine. 2008;29(1-2):9-16.

326. Clemens DL. Effects of ethanol on hepatic cellular replication and cell cycle progression. World Journal of Gastroenterology. 2007;13(37):4955-9.

327. Seitz HK, Becker P. Alcohol metabolism and cancer risk. Alcohol Research and Health. 2007;30(1):38-47.

328. Zakhari S. Overview: How is alcohol metabolized by the body? Alcohol Research and Health. 2006;29(4):245-54.

329. Misra UK, Bradford BU, Handler JA, Thurman RG. Chronic ethanol treatment induces H2O2 production selectively in pericentral regions of the liver lobule. Alcoholism: Clinical and Experimental Research. 1992;16(5):839-42.

330. Ohtake H, Kato S, Murawaki Y. Acute and chronic effect of ethanol on hepatic albumin synthesis in rat liver in vitro. Research Communications in Chemical Pathology and Pharmacology. 1986;53(2):213-31.

331. Peters S, Haagsman HP, van Norren K. Arginase release by primary hepatocytes and liver slices results in rapid conversion of arginine to urea in cell culture media. Toxicology in Vitro. 2008;22(4):1094-8. doi: 10.1016/j.tiv.2008.01.016.

332. Tsukamoto H, Machida K, Dynnyk A, Mkrtchyan H. "Second hit" models of alcoholic liver disease. Semin Liver Dis. 2009;29(2):178-87.

333. Zeng T, Xie KQ. Ethanol and liver: Recent advances in the mechanisms of ethanol-induced hepatosteatosis. Arch Toxicol. 2009;83(12):1075-81.

334. Wu DM, Zhai QW, Shi XL. Alcohol-induced oxidative stress and cell responses. J Gastroen Hepatol. 2006;21:S26-S9.

335. Berridge MV, M.V., Tan, A.S., McCoy, K.D. and Wang, R., . The biochemical and cellular basis of cell proliferation assays that use tetrazolium salts. . Biochemica. 1996;4:15-20.

336. Castilla R, GonzÃ¡lez R, Fouad D, Fraga E, Muntana J. Dual effect of ethanol on death in primary culture of human and rat hepatocytes. Alcohol and Alcoholism. 2004;39(4):290-6.

337. Rothschild MA, Oratz M, Schreiber SS. Effects of nutrition and alcohol on albumin synthesis. Alcoholism: Clinical and Experimental Research. 1983;7(1):28-30.

338. Gavaler JS, Perez HA, Estes L, Van Thiel DH. Morphologic alterations of rat Leydig cells induced by ethanol. Pharmacology Biochemistry and Behavior. 1984;18(SUPPL. 1):341-7.

339. Iseri OA, Lieber CS, Gottlieb LS. The ultrastructure of fatty liver induced by prolonged ethanol ingestion. American Journal of Pathology. 1966;48(4):535-55.

340. Delamaza MP, Petermann M, Bunout D, Hirsch S. Effects of Long-Term Vitamin-E Supplementation in Alcoholic Cirrhotics. J Am Coll Nutr. 1995;14(2):192-6.

341. McDonough KH. Antioxidant nutrients and alcohol. Toxicology. 2003;189(1-2):89-97.

342. Odeleye OE, Eskelson CD, Watson RR, Mufti SI, Chvapil M. Vitamin-E Reduction of Lipid-Peroxidation Products in Rats Fed Cod Liver Oil and Ethanol. Alcohol. 1991;8(4):273-7.

343. Ozdil S, Bolkent E, Yanardag R, Arda-Pirincci P. Protective effects of ascorbic acid, DL-alpha-tocopherol acetate, and sodium selenate on ethanol-induced liver damage of rats. Biol Trace Elem Res. 2004;97(2):149-61.

344. Arulmozhi V, Krishnaveni M, Karthishwaran K, Dhamodharan G, Mirunalini S. Antioxidant and antihyperlipidemic effect of Solanum nigrum fruit extract on the experimental model against chronic ethanol toxicity. Pharmacognosy Magazine. 2010;6(21):42-50.

345. Yanardag R, Ozsoy-Sacan O, Ozdil S, Bolkent S. Combined effects of vitamin C, vitamin E, and sodium selenate supplementation on absolute

ethanol-induced injury in various organs of rats. Int J Toxicol. 2007;26(6):513-23.

346. Wu D, Cederbaum AI. Ethanol cytotoxicity to a transfected HepG2 cell line expressing human cytochrome P4502E1. Journal of Biological Chemistry. 1996;271(39):23914-9.

347. Glascott Jr PA, Gilfor E, Serroni A, Farber JL. Independent antioxidant action of vitamins E and C in cultured rat hepatocytes intoxicated with allyl alcohol. Biochem Pharmacol. 1996;52(8):1245-52.

348. Ram√≠rez-Far√≠as C, Madrigal-Santill√°n E, Guti√©rrez-Salinas J, Rodr√≠guez-S√°nchez N, Mart√≠nez-Cruz M, Valle-Jones I, et al. Protective effect of some vitamins against the toxic action of ethanol on liver regeneration induced by partial hepatectomy in rats. World J Gastroentero. 2008;14(6):899-907.

349. Koyuturk M, Bolkent S, Ozdil S, Arbak S, Yanardag R. The protective effect of vitamin C, vitamin E and selenium combination therapy on ethanol-induced duodenal mucosal injury. Human and Experimental Toxicology. 2004;23(8):391-8.

350. [Anon]. Alcohol-induced liver damage. J Natl Med Assoc. 1999;91(12):646-.

351. Research AAFC. False Positive Screening For Cancer Found To Be Frequent And Costly.: ScienceDaily; 2004 [updated 2004, December 30August 3, 2008]; Available from: http://www.sciencedaily.com /releases/2004/12/041220002224.htm.

352. Beretta L. Proteomics from the clinical perspective: Many hopes and much debate. Nature Methods. 2007;4(10):785-6.

353. Hartman M, Loy EY, Ku CS, Chia KS. Molecular epidemiology and its current clinical use in cancer management. The Lancet Oncology. 2010;11(4):383-90.

354. McKinney C, Merriman TR. The human genome and understanding of common disease: Present and future technologies. Cellular and Molecular Life Sciences. 2007;64(7-8):961-78.

355. Akervall J. Gene profiling in squamous cell carcinoma of the head and neck. Cancer Metast Rev. 2005;24(1):87-94.

356. Despierre E, Lambrechts D, Neven P, Amant F, Lambrechts S, Vergote I. The molecular genetic basis of ovarian cancer and its roadmap towards a better treatment. Gynecologic Oncology. 2010;117(2):358-65.

357. Cho WCS. Contribution of oncoproteomics to cancer biomarker discovery. Molecular Cancer. 2007;6.

358. Yeom YI, Kim SY, Lee HG, Song EY. Cancer biomarkers in 'omics age. Biochip Journal. 2009;2(3):160-74.

359. Walley T, Haycox A. Pharmacoeconomics: Basic concepts and terminology. Brit J Clin Pharmaco. 1997;43(4):343-8.

360. Weintraub WS. Pharmacoeconomic concepts in antiplatelet therapy: Understanding cost-effectiveness analyses using clopidogrel as an example. Journal of Cardiovascular Pharmacology and Therapeutics. 2008;13(2):107-19.

361. Donnelly L. NHS's refusal to fund cancer treatment costs mother £21,000. London 2008 [cited 13 September 2008]; Available from: http://www.telegraph.co.uk/health/2910780/NHSs-refusal-to-fund-cancer-treatment-costs-mother-21000.html.

362. Walker GM, Sai J, Richmond A, Stremler M, Chun CY, Wikswo JP. Effects of flow and diffusion on chemotaxis studies in a microfabricated gradient generator. Lab on a Chip - Miniaturisation for Chemistry and Biology. 2005;5(6):611-8.

363. Verdier C, Couzon C, Duperray A. Critical stresses for cancer cell detachment in microchannels. European Biophysics Journal. 2009;38(8):1035-47.

364. Nikkhah M, Strobl JS, Agah M. Attachment and response of human fibroblast and breast cancer cells to three dimensional silicon microstructures of different geometries. BIOMEDICAL MICRODEVICES. 2009;11(2):429-41.

365. Cheung LSL, Zheng X, Stopa A, Baygents JC, Guzman R, Schroeder JA, et al. Detachment of captured cancer cells under flow acceleration in a bio-functionalized microchannel. Lab on a Chip - Miniaturisation for Chemistry and Biology. 2009;9(12):1721-31.

366. Hou HW, Li QS, Lee GYH, Kumar AP, Ong CN, Lim CT. Deformability study of breast cancer cells using microfluidics. BIOMEDICAL MICRODEVICES. 2009;11(3):557-64.

367. Chaw KC, Manimaran M, Tay EH, Swaminathan S. Multi-step microfluidic device for studying cancer metastasis. Lab on a Chip - Miniaturisation for Chemistry and Biology. 2007;7(8):1041-7.

368. Gabor H, Weiss L. Perturbations in cancer cell deformability and resistance to shear forces. Invasion and Metastasis. 1986;6(3):166-79.

369. Welch DR, Lobl TJ, Seftor EA, Wack PJ, Aeed PA, Yohem KH, et al. Use of the Membrane Invasion Culture System (MICS) as a screen for anti-invasive agents. Int J Cancer. 1989;43(3):449-57.

370. Du Z, Cheng KH, Vaughn MW, Collie NL, Gollahon LS. Recognition and capture of breast cancer cells using an antibody-based platform in a microelectromechanical systems device. BIOMEDICAL MICRODEVICES. 2007;9(1):35-42.

371. Henry OY, Fragoso A, Beni V, Laboria N, S√°nchez JLA, Latta D, et al. Design and testing of a packaged microfluidic cell for the multiplexed electrochemical detection of cancer markers. ELECTROPHORESIS. 2009;30(19):3398-405.

372. Ying-Yan W, Tao W, Xin L, Hong-Wei G, Bing-Cheng L, Qi W. The analysis of chemotherapy resistance in human lung cancer cell line with microchip-based system. BIOMEDICAL MICRODEVICES. 2008;10(3):429-35.

373. Hu G, Li D. Three-dimensional modeling of transport of nutrients for multicellular tumor spheroid culture in a microchannel. Biomedical Microdevices. 2007;9(3):315-23.

374. Thompson A, Brennan K, Cox A, Gee J, Harcourt D, Harris A, et al. Evaluation of the current knowledge limitations in breast cancer research: a gap analysis. Breast cancer research : BCR. 2008;10(2).

375. Fisher B, Gunduz N, Saffer EA. Influence of the interval between primary tumor removal and chemotherapy on kinetics and growth of metastases. Cancer Res. 1983;43(4):1488-92.

376. Qadri SSA, Wang JH, Coffey JC, Alam M, O'Donnell A, Aherne T, et al. Can surgery for cancer accelerate the progression of secondary tumors within residual minimal disease at both local and systemic levels? Annals of Thoracic Surgery. 2005;80(3):1046-51.

377. Beachy SH, Repasky EA. Using extracellular biomarkers for monitoring efficacy of therapeutics in cancer patients: An update. Cancer Immunology, Immunotherapy. 2008;57(6):759-75.

378. Barczyk K, Kreuter M, Pryjma J, Booy EP, Maddika S, Ghavami S, et al. Serum cytochrome c indicates in vivo apoptosis and can serve as a prognostic marker during cancer therapy. Int J Cancer. 2005;116(2):167-73.

379. Trejo-Becerril C, Perez-Cardenas E, Trevino-Cuevas H, Taja-Chayeb L, Garcia-Lopez P, Segura-Pacheco B, et al. Circulating nucleosomes and response to chemotherapy: An in vitro, in vivo and clinical study on cervical cancer patients. Int J Cancer. 2003;104(6):663-8.

380. Sheard MA, Vojtesek B, Simickova M, Valik D. Release of cytokeratin-18 and -19 fragments (TPS and CYFRA 21-1) into the extracellular space during apoptosis. Journal of Cellular Biochemistry. 2002;85(4):670-7.

381. Torisawa YS, Takagi A, Nashimoto Y, Yasukawa T, Shiku H, Matsue T. A multicellular spheroid array to and viability realize spheroid formation, culture, assay on a chip. Biomaterials. 2007;28(3):559-66.

382. Cheng SH, Jian JJM, Tsai SYC, Chan KY, Yen LK, Chu NM, et al. Prognostic features and treatment outcome in locoregionally advanced nasopharyngeal carcinoma following concurrent chemotherapy and radiotherapy. Int J Radiat Oncol. 1998;41(4):755-62.

383. Hong RL, Ting LL, Ko JY, Hsu MM, Sheen TS, Lou PJ, et al. Induction chemotherapy with mitomycin, epirubicin, cisplatin, fluorouracil, and leucovorin followed by radiotherapy in the treatment of locoregionally advanced nasopharyngeal carcinoma. J Clin Oncol. 2001;19(23):4305-13.

384. Hosoya Y, Kitoh Y, Kobayashi E, Okabe R, Fujimura A, Kanazawa K. Combination effects of tamoxifen plus 5-fluorouracil on gastric cancer cell lines in vitro. Cancer Letters. 1999;140(1-2):139-43.

385. Tsuchiya H, Mori Y, Ueda Y, Okada G, Tomita K. Sensitization and caffeine potentiation of cisplatin cytotoxicity resulting from introduction of wild-type p53 gene in human osteosarcoma. Anticancer Res. 2000;20(1 A):235-42.

386. Sahai E. Illuminating the metastatic process. Nat Rev Cancer. 2007;7(10):737-49.

387. Registrations of cancer diagnosed in 2007, England. In: Statistics NOo, editor.2007.

388. Zhang LJ, Li H, Zhang LY, Gu Y, Song Y, Li F, et al. Metastasis: Inherent vs. acquired phenotype. Med Hypotheses. 2010;74(5):874-6.

389. Schultz DR, Harrington Jr WJ. Apoptosis: Programmed cell death at a molecular level. Seminars in Arthritis and Rheumatism. 2003;32(6):345-69.

390. Resource for Biocomputing V, and Informatics at the University of California, San Francisco. Structure of horse heart cytochrome c (PDB:1HRC). In: c c, editor. UCSF Chimera2008.

391. Zou H, Henzel WJ, Liu X, Lutschg A, Wang X. Apaf-1, a human protein homologous to C. elegans CED-4, participates in cytochrome c-dependent activation of caspase-3. Cell. 1997;90(3):405-13.

392. Renz A, Berdel WE, Kreuter M, Belka C, Schulze-Osthoff K, Los M. Rapid extracellular release of cytochrome c is specific for apoptosis and marks cell death in vivo. Blood. 2001;98(5):1542-8.

393. Ahlemeyer B, Klumpp S, Krieglstein J. Release of cytochrome c into the extracellular space contributes to neuronal apoptosis induced by staurosporine. Brain Res. 2002;934(2):107-16.

394. Platoshyn O, Zhang S, McDaniel SS, Yuan JXJ. Cytochrome c activates K+ channels before inducing apoptosis. American Journal of Physiology - Cell Physiology. 2002;283(4 52-4).

395. Matapurkar A, Lazebnik Y. Requirement of cytochrome c for apoptosis in human cells. Cell Death and Differentiation. 2006;13(12):2062-7.

396. Giotakis J, Gomatos IP, Alevizos L, Georgiou AN, Leandros E, Konstadoulakis MM, et al. Bax, cytochrome c, and caspase-8 staining in parotid cancer patients: Markers of susceptibility in radiotherapy? Otolaryngology - Head and Neck Surgery. 2010;142(4):605-11.

397. Wyllie AH. Glucocorticoid-induced thymocyte apoptosis is associated with endogenous endonuclease activation. Nature. 1980;284(5756):555-6.

398. Olins DEOaAL. The Nucleus. 2009 [14 November 2009]; Available from: http://users.rcn.com/jkimball.ma.ultranet/BiologyPages/N/Nucleus.html.

399. Leon SA, Shapiro B, Sklaroff DM, Yaros MJ. Free DNA in the serum of cancer patients and the effect of therapy. Cancer Res. 1977;37(3):646-50.

400. Jahr S, Hentze H, Englisch S, Hardt D, Fackelmayer FO, Hesch RD, et al. DNA fragments in the blood plasma of cancer patients: Quantitations and evidence for their origin from apoptotic and necrotic cells. Cancer Res. 2001;61(4):1659-65.

401. Chen Z, Fadiel A, Naftolin F, Eichenbaum KD, Xia Y. Circulation DNA: Biological implications for cancer metastasis and immunology. Med Hypotheses. 2005;65(5):956-61.

402. Van Der Auwera I, Elst HJ, Van Laere SJ, Maes H, Huget P, Van Dam P, et al. The presence of circulating total DNA and methylated genes is associated with circulating tumour cells in blood from breast cancer patients. Brit J Cancer. 2009;100(8):1277-86.

403. Thorgeirsson UP, Turpeenniemi-Hujanen T, Williams JE. NIH/3T3 cells transfected with human tumor DNA containing activated ras oncogenes express the metastatic phenotype in nude mice. Molecular and Cellular Biology. 1985;5(1):259-62.

404. Bennett RM, Gabor GT, Merritt MM. DNA binding to human leukocytes. Evidence for a receptor-mediated association, internalization, and degradation of DNA. Journal of Clinical Investigation. 1985;76(6):2182-90.

405. Bennett RM, Kotzin BL, Merritt MJ. DNA receptor dysfunction in systemic lupus erythematosus and kindred disorders. Induction by anti-DNA antibodies, antihistone antibodies, and antireceptor antibodies. Journal of Experimental Medicine. 1987;166(4):850-63.

406. Eberle F, Sirin M, Binder M, Dalpke AH. Bacterial RNA is recognized by different sets of immunoreceptors. European Journal of Immunology. 2009;39(9):2537-47.

407. Chelobanov BP, Laktionov PP, Kharkova MV, Rykova EY, Vlassov VV. 2004. p. 239-43.

408. Holdenrieder S, Stieber P, Von Pawel J, Raith H, Nagel D, Feldmann K, et al. Circulating nucleosomes predict the response to chemotherapy in patients with advanced non-small cell lung cancer. Clin Cancer Res. 2004;10(18 I):5981-7.